

AD-A266 217

1720

AERO & ASTRO ENG

002



988

AFOSR/NA

AERO & ASTRO ENG

003

REPORT DOCUMENTATION PAGE

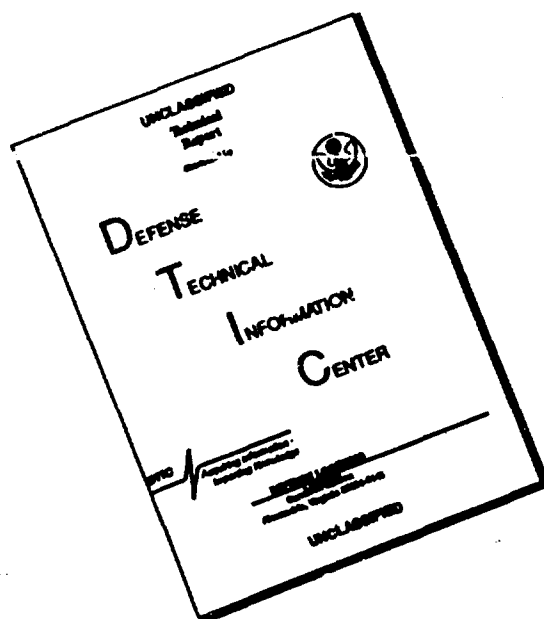
Form Approved

OMB No. 0704-0188

Public reporting burden for this collection of information is estimated to average 1 hour per response, including the time for reviewing instructions, searching existing data sources, gathering and maintaining the data needed, and completing and reviewing the collection of information. Send comments regarding this burden estimate or any other aspect of this collection of information, including suggestions for reducing this burden, to Washington Headquarters Office of Management and Budget, Paperwork Reduction Project (0704-0188), Washington, DC 20503.

1. AGENCY USE ONLY (Leave blank)		2. REPORT DATE May 27, 1993		3. REPORT TYPE AND DATES COVERED annual report 11/15/91 - 11/14/92	
4. TITLE AND SUBTITLE Nonlinear Analysis of Mechanical Systems Under Combined Harmonic and Stochastic Excitation				5. FUNDING NUMBERS G-AFOSR-91-0041	
6. AUTHOR(S) N. Sri Namachchivaya					
7. PERFORMING ORGANIZATION NAME(S) AND ADDRESS(ES) University of Illinois at Urbana-Champaign AAE Dept., 306 Talbot Laboratory 104 S. Wright Street Urbana, IL 61801 - 2935				8. PERFORMING ORGANIZATION REPORT NUMBER AFOSR-TR-92-0144	
9. SPONSORING/MONITORING AGENCY NAME(S) AND ADDRESS(ES) AFOSR / NA 110 Duncan Avenue, Suite B-115 Bolling AFB, DC 20352 - 0001				10. SPONSORING/MONITORING AGENCY REPORT NUMBER	
11. SUPPLEMENTARY NOTES					
12a. DISTRIBUTION/AVAILABILITY STATEMENT Approved for public release; distribution is unlimited				12b. DISTRIBUTION CODE	
13. ABSTRACT (Maximum 200 words) In the AFOSR grant, the complex interaction between noise, stability and nonlinear dynamics inherent in mechanical systems was examined and a consistent method for analyzing stochastic nonlinear systems was developed. The specific objective of the current work is to examine, both theoretically and experimentally, the nonlinear response of gyroscopic systems under stochastic and harmonic excitation. This study will include the following: examination of the combined effects of mass imbalance, asymmetry and realistic boundary conditions on the nonlinear response of rotating systems; development of a general nonlinear control technique designed to suppress unwanted vibrations and chaotic motions in gyroscopic systems; experimental verification of the theories developed.					
14. SUBJECT TERMS Nonlinear gyroscopic systems, nonlinear stochastic systems, nonlinear control, chaotic motions, experimental verification				15. NUMBER OF PAGES 16	
17. SECURITY CLASSIFICATION OF REPORT Unclassified				18. SECURITY CLASSIFICATION OF THIS PAGE Unclassified	
19. SECURITY CLASSIFICATION OF ABSTRACT Unclassified				20. LIMITATION OF ABSTRACT 117	

DISCLAIMER NOTICE



**THIS DOCUMENT IS BEST
QUALITY AVAILABLE. THE COPY
FURNISHED TO DTIC CONTAINED
A SIGNIFICANT NUMBER OF
PAGES WHICH DO NOT
REPRODUCE LEGIBLY.**

Progress Report

**Nonlinear Analysis of Mechanical Systems Under Combined
Harmonic and Stochastic Excitation**

Contract AFOSR 91-0041

Prepared for

**Dr. Spencer Wu
Program Manager, Structural Mechanics Division
Air Force Office of Scientific Research
Bolling Air Force Base, Washington, D.C.**

Prepared by

**Dr. N. Sri Namachchivaya, Principal Investigator
Nonlinear Systems Group
Department of Aeronautical and Astronautical Engineering
University of Illinois at Urbana-Champaign
104 South Mathews Avenue
Urbana, IL 61801**

93 6 29 05 5

93-14803



Progress Report

**Nonlinear Analysis of Mechanical Systems Under Combined
Harmonic and Stochastic Excitation**

Contract AFOSR 91-0041

DTIC QUALITY INSPECTED 8

Prepared for

**Dr. Spencer Wu
Program Manager, Structural Mechanics Division
Air Force Office of Scientific Research
Bolling Air Force Base, Washington, D.C.**

Prepared by

**Dr. N. Sri Namachchivaya, Principal Investigator
Nonlinear Systems Group
Department of Aeronautical and Astronautical Engineering
University of Illinois at Urbana-Champaign
104 South Mathews Avenue
Urbana, IL 61801**

Accession For	
NTIS CRA&I	
DTIC TAB	
Unannounced	
Justification	
By	
Distribution /	
Availability Codes	
Dist	Avail and/or Special
A-1	

Table of Contents

1.	Progress of Theoretical Work	3
1.1	Nonlinear Deterministic Systems	3
1.2.	Nonlinear Stochastic Systems	4
2.	Progress of Experimental Work	5
2.1	Mechanical Problem	5
2.2	Proposed Experimental Investigation of the Rotating Shaft	6
2.2.1	Design of Shaft and Test Rig	6
2.2.2	Integration of Motor and Shaker	8
2.2.3	Data Acquisition and Time Series Analysis	9
3.	Current Research	10
3.1	Specific Objectives	10
3.2	Scope of the Current Theoretical Work	11
3.3	Scope of the Current Experimental Work	12
4.	References (AFOSR Prior Support)	13
5.	Publications and Presentations	15
5.1	Journal Publications	15
5.2	Meetings and Conferences	16
6.	Personnel Supported by the AFOSR Grant	16

1. Progress of Theoretical Work

In the AFOSR grant, the complex interaction between noise, stability and nonlinear dynamics inherent in mechanical systems was examined and a consistent method for analyzing stochastic nonlinear systems was developed. This has led to a new qualitative understanding of the physical phenomena encountered in nonlinear mechanical and structural systems under harmonic and stochastic excitations. The mathematical techniques developed under the current AFOSR grant will allow engineers and scientists to predict possible motion instabilities in such systems as rotor blade dynamics in forward flight in a region of high atmospheric turbulence as well as rotating shafts subjected to harmonic, stochastic and combined harmonic and stochastic excitations.

1.1 Nonlinear Deterministic Systems

Recently, considerable effort has been directed toward obtaining a better understanding of nonlinear behavior and instability mechanisms of rotating shafts, a fundamental component of many mechanical systems. Toward this end, an analytical method based on both Hamiltonian and non-Hamiltonian frameworks is being developed by the PI and one of his graduate students. The case in which a harmonic axial excitation is applied has been studied in detail by the PI and his graduate student [1]. It was shown that in addition to the simple and Hopf bifurcations in the presence of subharmonic and combination resonances, respectively, such systems can exhibit a generalized Hopf bifurcation with 1:1 resonance when the damping is very small. In connection to this, the effects of periodic parametric excitations on systems exhibiting Hopf bifurcations with 1:1 resonance are also being investigated [2, 3]. Both semisimple and non-semisimple cases are of interest, and the normal forms are calculated when the forcing frequency is near twice the natural frequency. Furthermore, since symmetric properties are fundamental features of many engineering systems, the PI is currently studying global bifurcations with rotational and reflective symmetries, as well as the effects of imperfections that destroy this symmetry.

The techniques developed under the current AFOSR grant can be applied to a wide variety of realistic problems in nonlinear structural dynamics. As mentioned above, the results have already been applied to study the stability and bifurcation behavior of gyroscopic systems (i.e. the rotating shaft) under combined harmonic and stochastic excitations and the dynamics of rotor blades in forward flight. Further applications include the analysis of propellant lines conveying pulsating (possibly turbulent) fluid flow. The PI has introduced novel mathematical and computational methods to study the nonlinear behavior of both gyroscopic and nonconservative deterministic systems [4, 5]. Over the next few years, the PI will develop both local and global techniques to investigate various co-dimension two and three bifurcations under time periodic perturbations. Special emphasis will be given to the study of global chaotic phenomena in these systems.

1.2. Nonlinear Stochastic Systems

In many situations, parametric or external excitations cannot always be adequately modelled by deterministic time functions alone. They fluctuate randomly over a wide band of frequencies and have to be considered as stochastic functions of time defined only in probabilistic terms. Since the effects of stochastic perturbations are of greatest importance near bifurcation points in any dynamical system, a portion of this research focuses on noise induced transitions near such points. The results obtained have great impact on such engineering problems as aircraft at high angles of attack [6], panels under gas flow with both turbulent boundary layers and random axial loads [7,8], rotating systems under pulsating axial loads [9] and propellant lines conveying turbulent fluid flow [10].

The PI has developed a method called "stochastic normal forms" which replaces the original nonlinear system by an "equivalent" (in the stochastic sense) system of lower dimension [11,12]. A consistent method for analyzing stochastic nonlinear systems has been developed through this investigation. These new techniques [13, 14, 15, 16], based on the concept of Lyapunov exponents and multiplicative ergodic theory, provide insight into the effects of harmonic and stochastic excitations on the response of

nonlinear dynamical systems. Stability boundaries and bifurcation scenarios are then determined for such systems as helicopter rotor blades in forward flight [17, 18] and rotating shafts subjected to combined harmonic and stochastic excitations [9]. Results obtained in this study explain how small amplitude periodic or stochastic fluctuations in the parameters of a system or its environment can have a marked effect on the dynamics of physically realistic nonlinear systems. The current research has led to fundamental contributions in understanding co-dimension two stochastic bifurcations such as the interaction of Hopf and pitchfork bifurcations under stochastic excitations [19, 20].

In the prior AFOSR support, the results were obtained for white or nearly white noise cases. These assumptions, however, are idealistic. The PI is currently examining the the cases of realistic colored noise and simultaneous harmonic and stochastic excitations which are often encountered in nonlinear mechanical and structural systems.

2. Progress of Experimental Work

The objective of the experimental research is the development of laboratory facilities to conduct a series of tests designed to verify the analytical results obtained by the PI under his current AFOSR grant and other previous support.

2.1 Mechanical Problem

One of the most fundamental components of a mechanical system is a rotating shaft. It is, therefore, not surprising that through the years considerable effort has been directed toward obtaining a better understanding of such mechanisms. The dynamics and response of rotating and gyroscopic systems have been studied extensively in the literature. The equations describing the transverse motion of a continuous uniform elastic shaft of asymmetrical cross-section mounted in a rigid bearing and rotating with angular velocity $\Omega(t)$ about the horizontal center line of the bearings are

$$EI_u \frac{\partial^4 u}{\partial z^4} + P(t) \frac{\partial^2 u}{\partial z^2} + m \frac{\partial^2 u}{\partial t^2} + D \frac{\partial u}{\partial t} - 2m\Omega(t) \frac{\partial v}{\partial t} - m\Omega(t)^2 u = f_1(u, v)$$

$$EI_v \frac{\partial^4 v}{\partial z^4} + P(t) \frac{\partial^2 v}{\partial z^2} + m \frac{\partial^2 v}{\partial t^2} + D \frac{\partial v}{\partial t} - 2m\Omega(t) \frac{\partial u}{\partial t} - m\Omega(t)^2 v = f_2(u, v)$$

where $P(t)$ may be harmonic, stochastic or a combination of both. The shaft is of length L , mass per unit length m , and flexural rigidities EI_u and EI_v parallel to directions Ou and Ov , respectively. The terms $f_i(u, v)$, $i=1,2$, consist of all nonlinearities due to nonlinear strain-displacement relations and the nonlinear damping model. In addition, $f_i(u, v)$ may also contain the effects of mass imbalance and bearing forces, including impacts.

2.2 Proposed Experimental Investigation of the Rotating Shaft

One of the main objectives of the proposed research is to conduct a series of experiments on a rotating shaft. An important application of this work is the study of aircraft gas turbine engines. Both rotor imbalance and impact due to bearing clearance are inherent in such systems. Thus, the experimental set-up will consist of an elastic shaft supported by bearings with clearance to depict realistic operating conditions in a turbine engine. This clearance is modelled by a bilinear spring. It is intended to measure the time response of a rotating shaft under two separate operating conditions. Specifically, the transverse vibrations will be monitored as the shaft is subjected to (1) time varying axial thrust at various constant rotation rates and (2) various static axial loads with time-dependent angular velocity.

The experimental problem can be divided into three categories: design and construction of the shaft and test rig, integration of the shaker (external excitation) and motor (rotation), and implementation of sensors and time series analysis. Detailed descriptions of each of these components are given in the following four subsections.

2.2.1 Design of Shaft and Test Rig

The shaft to be studied will be constructed from hard naval brass. The published material properties of hardened yellow brass are shown in

Table 1 along with the shaft characteristics of interest. The shaft has a clamped length of $L = 25.1$ in. and a diameter of $d = 0.25$ in.

As shown in Table 1, the critical static buckling load of the shaft is $P_{cr} = 190$ lbf and the natural angular frequency is $f_n = 50$ Hz. Assuming a safety factor of 1.5 ($\sigma_{max} = \sigma_{yield}/1.5$), the maximum allowable strain will be $\epsilon_{max} = 2500$ $\mu\text{in/in}$ which corresponds to a centerline deflection of $\alpha = 0.3$ in.

Table I: Physical Characteristics of Shaft	
Shaft Property	Characteristic Value
Material	hard naval brass
E	15.9×10^6 psi
μ	7.92×10^{-4} lbf-s ² /in ⁴
S_y	60 ksi
L	25.1 in
d	0.25 in
f_n	50 Hz
P_{cr}	191 lbf
α_{max}	0.3 in
ϵ_{max}	2500 $\mu\text{in/in}$
$(\Delta x)_{max}$	0.018 in

The bearing assemblies are designed to closely approximate clamped-clamped boundary conditions. With the use of super-precision bearings, the maximum angular deflection of the shaft at the bearings is calculated to be 0.013 degrees. Thus, for the first 0.013 degrees of deflection at the bearings, the model behaves as if it is a pinned-pinned shaft. Assuming pinned-pinned boundary conditions, the maximum center line deflection corresponding to this angular deflection at the ends can be calculated to be 0.002 inches. This deflection corresponds to a strain gage reading of approximately 1.9 $\mu\text{in/in}$ which is negligible. Thus, we can assume clamped-clamped boundary conditions throughout.

The brass shaft is held in the motor end bearing hub using a slit clamp and bolts and four set screws. The large steel bearing blocks and

large thrust bearing take the full load transmitted by the shaft. The bearing hub has eight port holes tapped through it to allow for passage of the strain gage leads from the shaft to the slip ring, which is mounted on the bearing hub. The bearing hub is then passed through a radial bearing and coupled to the flywheel and drive motor. Also mounted on the bearing hub is a timing belt pulley used to drive the auxiliary shaft. The auxiliary shaft and timing belts are used to synchronize the rotation rate of the shaker end bearing hub with that of the shaft to minimize torque in the experimental model. Therefore, the shaft will experience only axial movement with respect to the linear/rotary bearings, insuring that they do not bind.

The shaker-end bearing hub is mounted in two bearings, one of which is a thrust bearing used to provide increased axial rigidity. Three 0.375 inch linear/rotary bearings are mounted inside the bearing hub to allow axial movement of the shaft. The hardened stainless steel sleeve on which the linear/rotary bearings act is attached to the shaft using a shrink fit. The sleeve acts as the inner race for the ball bearings and also increases the stiffness of the shaft through the bearing.

A small thrust bearing is used to transmit the axial loading to the rotating shaft. A load cell is mounted on the thrust bearing to measure the static and dynamic axial loads which are to be applied. Mounted directly above the load cell is a cross bar which transmits the static and dynamic axial loading to the shaft. The static load is applied using two small pneumatic air cylinders which are pressurized with a one gallon air tank. An air tank pressure of 100 psia will apply a static load of 260 lbf. The dynamic axial load is applied to the shaft using a 100 lbf shaker, which acts through the center of the cross bar.

2.2.2 Integration of Motor and Shaker

The motor currently under consideration for these experiments is the MTS 1000-Watt pulse-width modulated servo motor and controller. This motor/controller system provides high performance, high accuracy operation necessary for the proposed experimental project. In the case of a constant rotation rate, i.e. $\Omega(t)=\Omega_0$, such a high torque motor is not necessary. However, in the second phase of the proposed experimental program, the parametric excitation is given in the form of a time dependent

rotation rate, i.e. $\Omega(t) = \Omega_0 + \Omega_1(t)$. The high torque required to insure precise control of the time-varying component of this excitation necessitates a high performance motor.

The dynamic axial loading applied to the shaft is generated by a Bruel & Kjaer 445 N (100 lbf) shaker mounted as shown in Figures 3 and 5. The shaker is used to apply only the dynamic load since use of this system to apply static loads may cause the shaker to overheat. The Bruel & Kjaer shaker system was chosen since it provides the most precise frequency command following which is essential in these experiments. The command signal is generated by a Tektronix 2630 FFT Analyzer/Signal Generator. This signal generator is capable of producing dc, periodic, random or any combination of these waveforms.

The amplitude of the static load and the amplitude and frequency of the dynamic load will be measured by a 200 lbf S-type load cell mounted on the thrust bearing at the shaker end of the shaft. The signal from the load cell is passed through a Wagner model #460 Signal Conditioner/Amplifier. Currently, the shaker system is run open-loop; the signal from the amplifier is input to the Tektronix 2630 analyzer where it can be compared to the reference input. In this configuration, no corrective action is taken if the excitation amplitude does not correspond exactly to the desired waveform (for periodic inputs) or to the desired spectrum (for random inputs).

2.2.3 Data Acquisition and Time Series Analysis

A schematic diagram of the experimental set-up is given in Figure 9. The deflection of the shaft in the principle directions, i.e. the rotating u- and v-coordinates, will be measured by strain gages. A total of four foil gages are mounted on the shaft, one every 90°, and arranged in two half-bridge configurations. The strain gage signals are passed through the Fabricast model #1401001 slip ring to a Measurements Group #2311 Signal Conditioning Amplifier. The conditioned signals are then input to the Tektronix analyzer. The analyzer, run from a Gateway 486 PC, implements the following standard signal analysis functions:

- ♦ time domain waveform and orbit (x - y) plots;
- ♦ averaged power spectral density and cross spectral density functions;
- ♦ transfer (frequency response) function and FFT;
- ♦ coherence function;
- ♦ waveform averaging;
- ♦ auto- and cross-correlation;
- ♦ impulse response function;

These standard functions are indeed the most frequently applied techniques for understanding experimental data. Such analysis is useful for obtaining the frequency components and power distribution as a function of frequency. However, in order to gain a detailed description of the nonlinear dynamics, it is imperative to utilize nonstandard time series analysis. Lyapunov exponents, wavelet transforms and fractal dimensions are examples of such nonstandard techniques.

3. Current Research

3.1 Specific Objectives

The specific objective of the current work is to examine, both theoretically and experimentally, the nonlinear response of gyroscopic systems under stochastic and harmonic excitation. This study will include the following:

- ♦ examination of the combined effects of mass imbalance, asymmetry and realistic boundary conditions on the nonlinear response of rotating systems;
- ♦ development of a nonlinear control technique designed to suppress unwanted vibrations and chaotic motions in gyroscopic systems;
- ♦ experimental verification of the theories developed.

The current research will investigate the effects of both parametric and internal resonances on the local and global dynamics of realistic gyroscopic systems. In most realistic cases, the mechanical system is subject to stochastic as well as deterministic excitations. The stability boundaries for such cases must also be obtained. Toward this end, the PI

and his graduate students are extending the techniques developed in the study of stochastic dynamical systems by removing some of the restrictive conditions. The goal of this effort is the development of a systematic approach to nonlinear stochastic problems. The results obtained will identify the mechanisms which give rise to instability and unwanted vibrations under complex loading conditions. In addition to understanding the mechanisms of instability, it is beneficial to be able to suppress unwanted component oscillations. A general approximate nonlinear control methodology designed to suppress undesired motions in mechanical system such as the rotating shaft is also under development as part of the current research. In the above-mentioned studies, benchmark experiments are necessary to validate the current theories for the limited classes of systems to which they apply and to guide the development of more general theories in the areas of nonlinear dynamics and control.

3.2 Scope of the Current Theoretical Work

The research in the previous AFOSR grant has produced important analytical results for lower dimensional systems. However, little analysis and few results are available for large realistic multidegree-of-freedom ($n > 4$) mechanical systems due to their complexity. Furthermore, it is imperative that experimental results be provided for comparison to the theoretical models. This project addresses both the analytical and experimental aspects of the PI's current and planned research.

In the course of the current study, several questions, which have hitherto not been studied *globally*, will be addressed:

- ♦ What are the effects of mass imbalance, asymmetry and motion constraints on the nonlinear response of gyroscopic systems?
- ♦ What are the mechanisms of global bifurcations in such systems?
- ♦ Why is noise beneficial in some nonlinear systems but harmful in others?
- ♦ What additional effects are caused by the presence of harmonic excitation?
- ♦ What is the effect of noise on the stable and unstable periodic motions?

Answers to these questions will deepen our understanding of the dynamics of mechanical systems in real life situations and will aid in the design of more efficient dynamical systems.

The PI's current research is also concerned with the development of a general control algorithm for nonlinear multidegree-of-freedom mechanical systems. A variety of power generating components become unstable due to parametric excitations which may lead to catastrophic failures. Thus, it is important to study the instability mechanisms in detail and to control undesirable component motions. This work will result in a systematic method of suppressing unwanted vibrations and chaotic motions in rotating shafts subjected to motion constraints. The nonlinear control designs will then be implemented in the laboratory.

3.3 Scope of the Current Experimental Work

At this stage of our investigation, it is imperative to verify the theoretical results of the ongoing AFOSR grant through a series of experiments. To this end, the PI will conduct experiments with models whose essential dynamics correspond to the class of systems for which the theory was developed. These experiments are intended to validate the new theories and/or to identify the essence of physical phenomena that must be modelled.

Unlike the area of deterministic dynamics, there are very few experimental studies on nonlinear stochastic dynamics available for comparison. Therefore, the current experimental work will be valuable in providing insight into the stochastic dynamics of actual mechanical systems and in bridging the gap between the existing theoretical analysis and physical observation.

The numerical and analytical results will be compared with the following estimated results obtained from the experiments:

- ♦ mean squares and power spectra of responses;
- ♦ auto- and cross-correlation of the response coordinates;
- ♦ probability density functions of the responses;
- ♦ Lyapunov exponents and fractal dimensions.

The experiments will, in turn, guide the developments and refinements of the theories developed to incorporate any new phenomena observed. In addition, there is a primary need to increase the experimental skills of dynamics and control graduate students and the current program will establish a modern dynamics and control laboratory at the graduate level.

4. References (AFOSR Prior Support)

1. M. M. Doyle, Nonlinear dynamics of a rotating shaft subjected to a periodic axial load, Masters Thesis, Department of Aeronautical and Astronautical Engineering, University of Illinois, 1991.
2. N. Sri Namachchivaya and N. Malhotra, Parametrically Excited Hopf Bifurcation with Non-semisimple 1:1 Resonance, *Nonlinear Vibrations*, ASME-AMD, Vol. 114, 1992.
3. N. Sri Namachchivaya, M. Doyle, W. F. Langford, and N. W. Evans, Normal Form For Generalized Hopf Bifurcation With Non-semisimple 1:1 Resonance, to appear in *Journal of Applied Mathematics and Physics*, *ZAMP*
4. N. Sri Namachchivaya and W.M. Tien, Bifurcation Behavior of Nonlinear Pipes Conveying Pulsating Flow, *Journal of Fluids and Structures*, Vol. 3(4), 1989, 81-102.
5. M. Doyle and N. Sri Namachchivaya, Nonlinear Dynamics of a Rotating Shaft Subjected to a Periodic Axial Load, [in preparation].
6. N. Sri Namachchivaya and H. J. Van Roessel, Unfolding of Bifurcations Associated with Double Zero Eigenvalue for Supersonic Flow Past a Pitching Wedge, *Journal of Guidance, Control and Dynamics*, Vol. 13(2), 1990, pp.343-347.
7. N. Sri Namachchivaya and W.M. Tien, Stochastically Excited Linear Nonconservative Systems, *Journal of Mechanics, Structures and Machines*, Vol 18(4), 1990, 459-482.
8. G.S.B. Leng and N. Sri Namachchivaya, Critical Mode Interaction in the Presence of External Random Excitation, *Journal of Guidance, Control and Dynamics*, Vol. 14(4), 1991, pp.770-777.
9. N. Sri Namachchivaya, Mean Square Stability of a Rotating Shaft Under Combined Harmonic and Stochastic Excitations, *Journal of Sound and Vibration*, Vol 132(2), 1989, 301-314.

- 10.N. Sri Namachchivaya and Harry H. Hilton, Stochastic Stability of Supported Pipes Conveying Pulsating Fluid, ASME, PVP Conference, Hawaii, July 1989.
- 11.N. Sri Namachchivaya and G.S.B. Leng, Equivalence of Stochastic Averaging and Stochastic Normal Forms, *Journal of Applied Mechanics*, (ASME), Vol. 57(4), 1990, 1011-1017.
- 12.N Sri Namachchivaya and Y.K. Lin, Method of Stochastic Normal Forms, *International Journal of Nonlinear Mechanics*, Vol.26(6), 1991, 931-943.
- 13.N. Sri Namachchivaya, Instability Theorem Based on the Nature of Boundary Behavior for One Dimensional Diffusion, *Solid Mechanics Archives* , Vol. 14(3-4), 1989, pp.131-141.
- 14.N. Sri Namachchivaya, Maximal Lyapunov Exponent for a Stochastically Perturbed Co-Dimension Two Bifurcation, *Computational Stochastic Mechanics*, eds. P. D. Spanos and C. A. Brebbia, Elsevier, 113-124, 1991.
- 15.N. Sri Namachchivaya, M. A. Pai and M. Doyle, Stochastic Approach to Small Disturbance Stability in Power Systems, *Lyapunov Exponents* [ed. L. Arnold and J. P. Eckmann], Springer-Verlag, 1991.
- 16.N. Sri Namachchivaya, H. J. Van Roessel and S. Talwar, Maximal Lyapunov Exponent For Coupled Two Degree of Freedom Stochastic Systems, [submitted to *Journal of Applied Mechanics* (ASME)].
- 17.N. Sri Namachchivaya, Almost-sure Stability of Dynamical Systems under Combined Harmonic and Stochastic Excitations, *Journal of Sound and Vibration*, Vol.151(1), 1991, 77-90.
- 18.N. Sri Namachchivaya and J.E. Prussing, Almost-sure Asymptotic Stability of Rotor Blade Flapping Motion in Forward Flight in Turbulent Flow, *Journal of Probabilistic Engineering Mechanics*, Vol. 6(1), 2-9, 1991.
- 19.G. Leng, N. Sri Namachchivaya and S. Talwar, Robustness of Nonlinear Systems Perturbed by External Random Excitation, *Journal of Applied Mechanics*, (ASME), Vol 59(4), 1015-1022, 1992.
- 20.N. Sri Namachchivaya, and S. Talwar, Maximal Lyapunov Exponent and Rotation numbers for Co-Dimension Two Stochastic Bifurcation, [to appear in *Journal of Sound and Vibration*]

5. Publications and Presentations

The starting date of this proposal was November 1, 1991. Below is a summary of the results of the grant which have been published or accepted for publication or presentation.

5.1 Journal Publications

Copies of these manuscripts are sent to you under separate cover and are listed below:

1. M. M. Doyle, Nonlinear dynamics of a rotating shaft subjected to a periodic axial load, Masters Thesis, Department of Aeronautical and Astronautical Engineering, University of Illinois, 1991.
2. N. Sri Namachchivaya and N. Malhotra, Parametrically Excited Hopf Bifurcation with Non-semisimple 1:1 Resonance, *Nonlinear Vibrations*, ASME-AMD, Vol. 114, 1992.
3. N. Sri Namachchivaya, M. Doyle, W. F. Langford, and N. W. Evans, Normal Form For Generalized Hopf Bifurcation With Non-semisimple 1:1 Resonance, to appear in *Journal of Applied Mathematics and Physics*, ZAMP
4. M. Doyle and N. Sri Namachchivaya, Nonlinear Dynamics of a Rotating Shaft Subjected to a Periodic Axial Load, [in preparation].
5. N. Sri Namachchivaya and H. J. Van Roessel, Maximal Lyapunov Exponent and Rotation Numbers for Two Coupled Oscillators Driven by Real Noise, *Journal of Statistical Physics*, Vol. 71(4), 1993.
6. N. Sri Namachchivaya, M. A. Pai and M. Doyle, Stochastic Approach to Small Disturbance Stability in Power Systems, *Lyapunov Exponents* [ed. L. Arnold and J. P. Eckmann], Springer-Verlag, 1991.
7. N. Sri Namachchivaya, H. J. Van Roessel and S. Talwar, Maximal Lyapunov Exponent For Coupled Two Degree of Freedom Stochastic Systems, to appear in *Journal of Applied Mechanics* (ASME).
8. N. Sri Namachchivaya, Almost-sure Stability of Dynamical Systems under Combined Harmonic and Stochastic Excitations, *Journal of Sound and Vibration*, Vol. 151(1), 1991, 77-90.

9. G. Leng, N. Sri Namachchivaya and S. Talwar, Robustness of Nonlinear Systems Perturbed by External Random Excitation, *Journal of Applied Mechanics*, (ASME), Vol 59(4), 1015-1022, 1992.
10. N. Sri Namachchivaya, and S. Talwar, Maximal Lyapunov Exponent and Rotation numbers for Co-Dimension Two Stochastic Bifurcation, to appear in *Journal of Sound and Vibration*

5.2 Meetings and Conferences

The PI attended the ASME Winter Annual Meeting in 1992 and the Fields Institute for Research in Mathematical Sciences (also in 1992) at which the following results from the research in progress were presented:

- N. Sri Namachchivaya and N. Malhotra, Parametrically Excited Hopf Bifurcation with Non-semisimple 1:1 Resonance [presented at the *ASME Winter Annual Meeting*, Anaheim, California, November, 1992].
- N. Sri Namachchivaya and N. Malhotra, Homoclinic Chaos and Normal Forms: Application to Mechanical Systems [presented at the *Fields Institute for Research in Mathematical Sciences*, Canada, November, 1992].

6. Personnel Supported by the AFOSR Grant

1. Student Name: Win-Min Tien
Degree: Ph. D.
Thesis Title: Chaotic and Stochastic Dynamics of Nonlinear Structural Systems
Date of Completion: December, 1992
2. Student Name: Monica Doyle
Degree: Ph. D.
Thesis Title: Nonlinear Dynamics of Hamiltonian and Quasi-Hamiltonian Systems

Normal Form for Generalized Hopf Bifurcation with Non-semisimple 1:1 Resonance[†]

N. SRI NAMACHCHIVAYA AND MONICA M. DOYLE

*Department of Aeronautical and Astronautical Engineering
University of Illinois at Urbana-Champaign
Urbana, IL, 61810*

and

WILLIAM F. LANGFORD AND NOLAN W. EVANS

*Department of Mathematics and Statistics
University of Guelph
Guelph Ontario, Canada, N1G 2W1*

The primary result of this research is the derivation of an explicit formula for the Poincare-Birkhoff normal form of the generalized Hopf bifurcation with non-semisimple 1:1 resonance. The classical nonuniqueness of the normal form is resolved by the choice of complementary space which yields a unique equivariant normal form. The 4 leading complex constants in the normal form are calculated in terms of the original coefficients of both the quadratic and cubic nonlinearities by two different algorithms. In addition, the universal unfolding of the degenerate linear operator is explicitly determined. The dominant normal forms are then obtained by rescaling the variables. Finally, the methods of averaging and normal forms are compared. It is shown that the dominant terms of the equivariant normal form are, indeed, the same as those of the averaged equations with a particular choice for the constant of integration.

[†] Partially supported by NSF through grant MSS 90-57437, AFOSR through grant 91-0041 and NSERC of Canada.

Running Title:

Normal Form For Generalized Hopf Bifurcation

Corresponding Author:

N. SRI NAMACHCHIVAYA

*Department of Aeronautical and Astronautical Engineering
University of Illinois at Urbana-Champaign
306 Talbot Laboratory
104 S. Wright Street
Urbana, IL 61801*

I. INTRODUCTION

When a multidegree-of-freedom dynamical system undergoes a bifurcation, it usually does so in only a few degrees of freedom. One simple example is the buckling of a column. If μ and μ_c represent the axial and Euler loads of a column, respectively, then, as μ is varied in the vicinity of μ_c , the temporal evolution of the motion is dominated by the critical mode which, in the first approximation, is governed by $\dot{x} = (\mu - \mu_c)x + ax^3$. A more complicated situation arises when several control parameters $\underline{\mu}$ are varied in such a way that several modes become marginally unstable simultaneously. In the latter case, the system is said to undergo a multiple bifurcation. The simplest and smallest number of equations which capture the essential dynamics of the original system in the vicinity of $\underline{\mu}_c$ are said to be in the normal form. The theory of normal forms is an important analytical tool for investigating the qualitative behavior of nonlinear dynamical systems.

The idea of normal forms for nonlinear systems dates back as far as Euler; however, Poincare [16] and Birkhoff [3] were the first to bring forth the theory in a more definite form. Poincare [16] considered the problem of reducing a system of nonlinear differential equations to a system of linear ones; namely,

$$\frac{dx}{dt} = Ax + f(x) \quad \text{to} \quad \frac{dy}{dt} = Ay, \quad x \in R^n, \quad y \in R^n. \quad (1)$$

The formal solution of this problem entails finding near-identity coordinate transformations, $x = y + \Phi(y)$, which eliminate the analytic expressions of the nonlinear terms. It has been shown that such a formal solution exists provided the above system is hyperbolic and the eigenvalues λ_j of the diagonalizable matrix A satisfy the nonresonance condition

$$\lambda_i \neq \sum m_l \lambda_l \quad \text{for } i = 1, 2, \dots, n, \quad |m| = \sum m_l \geq 2 \quad (2)$$

where m is a vector of integers $m = (m_1, m_2, \dots, m_n)$ with $m_i \geq 0$. Furthermore, it was proven that if, in addition to the above results, the eigenvalues lie strictly to one side of a line separating them from zero in the complex plane, then the formal series $\Phi(y)$ is convergent.

If the system is nonhyperbolic or condition (2) is violated, the analytic expressions of the nonlinear terms cannot be completely eliminated via a nonlinear change of coordinates. The remaining terms comprise the normal form of the system of equations given by (1). The normal form is dictated by the nature of the linear operator A . Thus, the nonlinear system in Eq. (1) can be reduced to

$$\frac{dy}{dt} = Ay + g(y), \quad y \in \mathbb{R}^n \quad (3)$$

where g is simpler than f . Such reductions have been widely used to study deterministic autonomous and nonautonomous systems (see Arnold [1]).

In bifurcation problems, the eigenvalues of the linear operator A are composed of two sets, one on the imaginary axis and the other with strictly negative real parts. The linear vector space E associated with A can also be divided accordingly as $E = E_c \oplus E_s$ such that $x_c \in E_c$ and $x_s \in E_s$ with $x = x_c + x_s$. There are two approaches to obtaining normal forms for deterministic systems. In the first, as shown in Guckenheimer and Holmes [12], one first computes the lower dimensional center manifold onto which the dynamics settle for large times. The dynamical system defined on the center manifold is then transformed to the normal form through a nonlinear change of coordinates. In the second method, one systematically expands the original vector field in powers of amplitudes of the critical modes to yield both the normal form and center manifold, simultaneously, as shown by Elphick et al. [7]. The approach adopted in this paper for the computation of the normal form assumes that the center manifold theorem has been applied to the original system and is based heavily on the work of Elphick et al. [7].

The aim of this paper is two-fold: first, to present an explicit formula for the normal form of a generalized Hopf bifurcation with non-semisimple 1:1 resonance and, second, to compare the results with those obtained via the method of averaging. The results for the corresponding semisimple case were obtained by Bajaj and Sethna [2] using center manifold theory and the method of integral averaging.

Recently, the normal form for a generalized Hopf bifurcation was expressed as a 4-dimensional real system by Cushman and Sanders [5] and as a 2-dimensional complex system by Elphick et al. [7] and Iooss and Adelmeyer [18]. Iooss et al. [19] employed the 2-dimensional normal form given in [7] to examine the steady bifurcating solutions in nonlinear hydrodynamic stability problems. However, there are no explicit formulas relating the coefficients of the original system to those of the normal form. This paper presents explicit formulas for the 4 leading constants in the complex normal form in terms of coefficients of the original nonlinear system with both *quadratic and cubic nonlinearities*. The complex normal form presented by Elphick et al. [7] has recently been analyzed by van Gils et al. [11]. It was shown that this co-dimension 3 bifurcation problem is more complicated than the closely related case of the non-resonant double Hopf bifurcation and contains three different types of co-dimension 1 singularities and 4 different types of co-dimension 2 singularities. Thus, with the help of the results presented in this paper, one can apply the analysis of van Gils et al. [11] to any physical problem exhibiting generalized Hopf bifurcation with non-semisimple 1:1 resonance. Furthermore, it has been shown by Hale [13] that, for systems with linear operators whose superdiagonal terms are equal to 1, an appropriate scaling can be used to obtain the averaged equations. In the final section, the averaged equations up to the second order approximation are obtained and compared with the normal form equations.

II. BACKGROUND AND NOTATIONS

The problem of interest in this paper is a 4-dimensional one. However, we shall keep the analysis as general as possible for the time being. Consider a dynamical system governed by autonomous differential equations in C^n ,

$$\dot{y} = A(\mu)y + f(y, \mu) \quad (4)$$

where $f: C^n \rightarrow C^n$ is a C^r vector field, $r \geq 2$, A is an $n \times n$ complex matrix, $x=0$ is the trivial solution of Eq. (4) for all values of μ (i.e., $f(0, \mu) = 0$) and the nonlinear vector function can be represented as

$$f(y, \mu) = f^2(y, \mu) + f^3(y, \mu) + \dots + f^k(y, \mu) + \dots \quad (5)$$

Here, we have expressed the nonlinear terms as a formal power series of homogeneous terms with degree denoted by the superscripts. We define H_n^k to be the linear space of homogeneous vector polynomials of degree k in n variables with range C^n . Let (e_1, e_2, \dots, e_n) denote the basis of C^n and $y = (y_1, y_2, \dots, y_n)$ be the coordinates with respect to this basis. Thus, an element $f^k(y, \mu)$ of H_n^k can be represented in the form of vector-valued monomials as

$$\begin{aligned} f^k(y, \mu) &= \sum_s^n f_s^k(y, \mu) e_s = \sum_{s, m} f_{s, m}^k(\mu) y^m e_s, \quad |m| = k \\ &= \sum_s \sum_{|m|=k} f_{s, m_1, m_2, \dots, m_n}^k (y_1^{m_1} y_2^{m_2} \dots y_n^{m_n}) e_s \end{aligned} \quad (6)$$

with $\dim \{f_i^k(y, \mu)\} = (n+k-1)! / [(n-1)! k!]$ and $\dim \{H_n^k\} = n \cdot \dim \{f_i^k(y, \mu)\}$. Now that a formal set-up for representing Eq. (4) has been obtained, we can consider the problem of reducing Eq. (4) to the normal form

$$\dot{x} = A(\mu)x + g(x, \mu), \quad g(x, \mu) = g^2(x, \mu) + g^3(x, \mu) + \dots + g^k(x, \mu) + \dots \quad (7)$$

which, as stated previously, is in a simpler form than Eq. (4) and has all the essential features of the flow near the equilibrium point of the original system. The formal solution of this problem consists of determining near identity coordinate transformations

$$y = x + h(x), \quad h(x) = h^2(x) + h^3(x) + \dots + h^k(x) \quad (8)$$

where $x \in \Omega$, and Ω is a neighborhood of the origin of C^n , such that the analytic expressions of $f(y, \mu)$ are simplified to yield $g(x, \mu)$. Once again, f^k , g^k and h^k are homogeneous vector polynomials of degree k and belong to H_n^k . Assuming the normal form reduction up to order $k-1$ has been performed, differentiating Eq. (8) gives

$$\dot{y} = [I + D_x h^k(x)] \dot{x}$$

and substituting in Eq. (4) yields

$$\dot{x} = [I + D_x h^k(x)]^{-1} [A(x + h^k(x)) + f(x + h^k(x))].$$

Making use of the fact that, for $x \in \Omega$,

$$[I + D_x h^k(x)]^{-1} = I - D_x h^k(x) + O(|x|^{2k-1})$$

results in

$$\begin{aligned} \dot{x} = & Ax + f^2(x) + f^3(x) + \dots + f^{k-1}(x) \\ & + \{f^k(x) + [Ah^k(x) - D_x h^k(x) Ax]\} + O(|x|^{k+1}). \end{aligned} \quad (9)$$

It is worth noting that the transformation of degree k does not affect the normal form of order $(k-1)$ but does affect the terms of order k and higher. The task now is to select $h^k(x)$ so that the terms of degree k in the brackets are as simple as possible. Examining the terms of degree k in Eq. (9) and comparing with those of Eq. (8) yields

$$Ah^k(x) - D_x h^k(x) Ax + f^k(x) = g^k(x) \quad (10)$$

and $f^j(x) = g^j(x)$ for $j = 2, 3, \dots, k-1$. Introducing a linear operator L_A defined by

$$L_A h^k = [h^k, Ax] = Ah^k(x) - D_x h^k(x) Ax.$$

Eq. 10 can be rewritten as

$$-L_A h^k(x) = f^k(x) - g^k(x) = \eta^k(x). \quad (11)$$

The above equation is called a homological equation. $L_A : H_n^k \rightarrow H_n^k$ is called the homological operator and is linear in the space of homogeneous vector polynomials of degree k . Equation (11) is to be solved for $h^k(x)$.

Let us denote R_n^k as the range of L_A and let W_n^k be any complementary subspace to R_n^k in H_n^k . H_n^k can be decomposed as follows

$$H_n^k = R_n^k \oplus W_n^k, \quad k \geq 2. \quad (12)$$

Thus, for each $f^k(x) \in H_n^k$ there exists $\eta^k(x) \in R_n^k$ and $g^k(x) \in W_n^k$ such that any given homogeneous polynomial of degree k can be written as

$$f^k(x) = g^k(x) + \eta^k(x)$$

and the suitable transformation $h^k(x)$ is obtained from

$$-L_A h^k(x) = \eta^k(x). \quad (13)$$

Since the choice of complementary space W_n^k is not unique, neither is the transformation $h^k(x)$ or the normal form $g^k(x)$. This nonuniqueness was resolved by Elphick et al. [7] through a particular choice of inner product. As in [7] (refer also to Helgason [14]), we can introduce an inner product in H_n^k . To this end, we introduce a differential operator associated with an arbitrary $f_1^k(x) \in H_n^k$ as

$$f_i^k(\partial) e_i = \sum_{|m|=k} f_{im}^k \left(\frac{\partial}{\partial x} \right)^m e_i, \quad \left(\frac{\partial}{\partial x} \right)^m = \frac{\partial^{m_1}}{\partial x_1^{m_1}} \cdot \frac{\partial^{m_2}}{\partial x_2^{m_2}} \cdots \frac{\partial^{m_n}}{\partial x_n^{m_n}}.$$

Then, for $f_i^k(x), g_j^k(x)$ in H_n^k , the scalar product is given by

$$\langle f_i^k(x), g_j^k(x) \rangle = f_i^k(\partial) \bar{g}_j^k(x) \Big|_{x=0} \delta_{ij} = \sum_{|\alpha|=k} \sum_{|\beta|=k} f_{i\alpha}^k \bar{g}_{j\beta}^k \cdot \frac{\partial^\alpha (x^\beta)}{\partial x^\alpha} \Big|_{x=0} \delta_{ij}.$$

It is clear that the only terms that will survive are those for which α and β coincide, i.e.

$$\langle f_i^k(x), g_j^k(x) \rangle = \sum_{m=k} f_{im}^k \bar{g}_{jm}^k m! \delta_{ij}, \quad m! = m_1! m_2! \cdots m_n!.$$

Thus, the inner product in H_n^k is defined as

$$\langle f^k(x), g^k(x) \rangle_{H_n^k} = \sum_{i=1}^n \sum_{|m|=k} f_{im}^k \bar{g}_{im}^k m!. \quad (14)$$

Using this inner product, we can define the adjoint operator $(L_A)^*$ as

$$\langle L_A h^k(x), f^k(x) \rangle_{H_n^k} = \langle h^k(x), L_A^* f^k(x) \rangle_{H_n^k}$$

and making use of the fact

$$\langle h^k(Ax), f^k(x) \rangle_{H_n^k} = \langle h^k(x), f^k(A^*x) \rangle_{H_n^k}$$

Elphick et al. [7] has shown that

$$\ker(L_A^*) = \ker(L_A)^*. \quad (15)$$

Since H_n^k is a finite dimensional space, $\ker(L_A)^*$ is an orthogonal complement of R_n^k the elements of which we are free to choose. Equation (12) may then be written as

$$H_n^k = R_n^k \oplus \ker(L_A^*). \quad (16)$$

Now, considering the linear equations in H_n^k , we have

$$-L_A h^k(x) = \eta^k(x), \quad L_A^* g^k(x) = 0 \quad (17)$$

and the solvability condition

$$\langle \eta^k(x), g^k(x) \rangle_{H_n^k} = 0. \quad (18)$$

The normal form and explicit formulas for the coefficients can then be calculated using Eqs. (17) and (18). It is important to note that this normal form depends on the matrix A and the choice of complementary space W_n^k . Once the functions $f^k(x)$ are known, the above method can be applied to calculate both $h^k(x)$ and $g^k(x)$. A recursive algorithm, similar to that of Chow and Hale [4], can also be employed to compute the k^{th} order nonlinearities $f^k(x)$ given all transformations $h(x)$ and normal forms $g(x)$ up to order $k-1$. Both methods have been employed independently herein to calculate the normal form coefficients which are given explicitly in the Appendix.

III. NORMAL FORM FOR NON-SEMISIMPLE CASE

For the non-semisimple case, the normal form calculations are not as easy as in the case of a diagonalizable linear operator. However, the calculations can be simplified using certain well known results in Lie algebra. These will be introduced as we proceed through the calculations of the normal form for the generalized Hopf bifurcation.

Given a finite dimensional vector space V over the complex numbers C and a space L of linear transformations of V onto itself, one can define the Lie bracket by the formula

$$[P, Q] = (P \circ Q - Q \circ P) \in L \text{ for } P, Q \in L. \quad (19)$$

Then L becomes a Lie algebra and we say P commutes with Q iff $[P, Q] = 0$. The result that is of importance to us is the Jordan decomposition theorem which states that for any $A \in L$ there exist S and N such that

$$A = S + N \quad \text{and} \quad [S, N] = 0 \quad (20)$$

where S is semisimple (diagonalizable) and N is nilpotent. Moreover, these decompositions are unique and

$$\ker A = \ker S \cap \ker N. \quad (21)$$

In the calculation of normal forms for generalized Hopf bifurcation with non-semisimple 1:1 resonance, the linear operator of interest takes the form

$$A = \begin{bmatrix} i\omega & 1 & 0 \\ 0 & i\omega & 0 \\ 0 & -i\omega & 1 \\ 0 & 0 & -i\omega \end{bmatrix} = \begin{bmatrix} i\omega & 0 & 0 \\ 0 & i\omega & 0 \\ 0 & -i\omega & 0 \\ 0 & 0 & -i\omega \end{bmatrix} + \begin{bmatrix} 0 & 1 & 0 \\ 0 & 0 & 0 \\ 0 & 0 & 1 \\ 0 & 0 & 0 \end{bmatrix} = S + N \quad (22)$$

and $[S, N] = 0$. In addition, the homological operator for any two matrices A and B also satisfies the relation $[L_A, L_B] = L_{[A, B]}$. This implies that the Lie brackets of L_S , L_N and L_{S^*} , L_{N^*} also commute. Thus, the $\ker(L_{A^*})$, which is needed for the calculation of the normal form, is given by

$$\ker (L_{A^*}) = \ker L_{S^*} \cap \ker L_{N^*}.$$

It is worth pointing out that the above results can also be obtained using the arguments given in Meyer [15]. Furthermore, the normal form $g(z)$, given in Eq. (17), commutes with elements of the Lie groups

$$G = \{e^{sA^*} | s \in \mathbb{R}\} \quad \text{and} \quad S^1 = \{e^{sS} | s \in \mathbb{R}\}$$

and the normal form is said to have G - equivariance and a simpler S^1 -equivariance, respectively. Since the proofs of these results are similar, only that of S^1 -equivariance, i.e.

$$g(e^{sS}\xi) = e^{sS}g(\xi)$$

will be given here. To this end, consider $z = e^{sS}\xi$ and $g(z) = g(e^{sS}\xi)$. Taking the total differential of $g(z)$ w.r.t. the variable s yields

$$\frac{dg(z)}{ds} = D_z g(z) Sz.$$

Now, using the fact that the normal form is such that $g \in \ker(L_{A^*}) = \ker(L_{S^*}) \cap \ker(L_{N^*})$ and $S^* = -S$, we have

$$D_z g(z) Sz - Sg(z) = 0.$$

Combining the above two equations yields an O.D.E for $g(z)$

$$\frac{dg(z)}{ds} = Sg(z), \quad s \in \mathbb{R}$$

whose solution can be written as

$$g(z) = e^{sS}g(z; s=0) = e^{sS}g(\xi). \quad (23)$$

This proves the S^1 - equivariance. The G - equivariance can be proven similarly by replacing S by A^* in the above steps.

1. Linear Algebraic Calculation of the Normal Form Coefficients

Now we calculate the normal form and appropriate expressions for the coefficients of this normal form. To this end, consider the homological equation

$$-L_A h^k(x) = f^k(x).$$

It is easy to show that for the semisimple S with eigenvalues $\lambda_i, i = 1, 2 \dots n$, $L_A h^k(x)$ reduces to

$$L_S h^k(x) = \sum_{s, |m| = k} h_{s,m}^k [\langle m, \lambda \rangle - \lambda_s] x^m e_s$$

and

$$\langle m, \lambda \rangle - \lambda_s = 0; s = 1, 2, \dots, n; |m| \geq 2$$

is called the resonance condition. The $\ker(L_S^*)$ is determined by the appropriate combination of m 's which satisfy the above condition. The resonance condition for the problem under consideration can be expressed as

$$i\omega(m_1 + m_2 - m_3 - m_4 - 1) = 0, \quad m_1 + m_2 + m_3 + m_4 = k \quad \text{for } s = 1, 2$$

and

$$-i\omega(m_3 + m_4 - m_1 - m_2 - 1) = 0, \quad m_1 + m_2 + m_3 + m_4 = k \quad \text{for } s = 3, 4.$$

Since $m_i \geq 0$ and integer, it is obvious that k is always odd and the above conditions yield

$$(m_1 + m_2) = \frac{k+1}{2}, \quad (m_3 + m_4) = \frac{k-1}{2} \quad \text{for } s = 1, 2$$

and

$$(m_1 + m_2) = \frac{k-1}{2}, \quad (m_3 + m_4) = \frac{k+1}{2} \quad \text{for } s = 3, 4.$$

Thus, the non-zero nonlinear normal form exists only for $k = 3, 5, \dots$. However, the original quadratic nonlinear terms can contribute to the cubic terms as a result of the nonlinear transformation as will be seen in the subsequent section. Calculation of the coefficients of the leading order normal form ($k=3$) is of concern in this paper. Thus, in an 80 dimensional basis, only 24 vectors lie in the $\ker(L_S^*)$ and can be written as

$$\begin{aligned} & (x_1^2 x_3) e_s, (x_1 x_2 x_3) e_s, (x_2^2 x_3) e_s, (x_1^2 x_4) e_s, (x_1 x_2 x_4) e_s, (x_2^2 x_4) e_s \quad \text{for } s = 1, 2 \\ & (x_3^2 x_1) e_s, (x_3 x_4 x_1) e_s, (x_4^2 x_1) e_s, (x_3^2 x_2) e_s, (x_3 x_4 x_2) e_s, (x_4^2 x_2) e_s \quad \text{for } s = 3, 4. \end{aligned}$$

The action of L_{N^*} on these bases can be represented by a 24×24 matrix of the form

$$\begin{bmatrix} C & 0 & 0 & 0 \\ -I & C & 0 & 0 \\ 0 & 0 & C & 0 \\ 0 & 0 & -I & C \end{bmatrix} \text{ where } C = \begin{bmatrix} 0 & 1 & 0 & 1 & 1 & 0 \\ 0 & 0 & 2 & 0 & 1 & 0 \\ 0 & 0 & 0 & 0 & 0 & 0 \\ 0 & 0 & 0 & 0 & 1 & 0 \\ 0 & 0 & 0 & 0 & 0 & 2 \\ 0 & 0 & 0 & 0 & 0 & 0 \end{bmatrix}$$

where I and 0 are 6×6 identity and zero matrices. The 8-dimensional null space of the above matrix can be easily computed. Making use of this, the basis of $\ker(L_{A^*})$ can be written as

$$\begin{pmatrix} x_1(x_1x_4 - x_2x_3) \\ x_2(x_1x_4 - x_2x_3) \\ 0 \\ 0 \end{pmatrix}, \begin{pmatrix} x_1^2x_3 \\ x_1^2x_4 \\ 0 \\ 0 \end{pmatrix}, \begin{pmatrix} x_1^2x_3 \\ x_1x_2x_3 \\ 0 \\ 0 \end{pmatrix}, \begin{pmatrix} 0 \\ x_1^2x_3 \\ 0 \\ 0 \end{pmatrix}$$

$$\begin{pmatrix} 0 \\ 0 \\ x_3(x_2x_3 - x_1x_4) \\ x_4(x_2x_3 - x_1x_4) \end{pmatrix}, \begin{pmatrix} 0 \\ 0 \\ x_3^2x_1 \\ x_3^2x_2 \end{pmatrix}, \begin{pmatrix} 0 \\ 0 \\ x_3^2x_1 \\ x_3x_4x_1 \end{pmatrix}, \begin{pmatrix} 0 \\ 0 \\ 0 \\ x_3^2x_1 \end{pmatrix}.$$

It is worth noting that the first 4 basis vectors are complex conjugates of the last 4, as expected. Since any linear combination of these vectors spans the null space, we can manipulate the given basis such that the resulting normal form is as simple as possible. This manipulation is performed as follows: the second basis element is replaced by the vector obtained by subtracting the third basis element from the second and the sixth basis element is replaced by the vector obtained by subtracting the seventh basis element from the sixth. This procedure yields the new 2nd and 6th bases as

$$\begin{pmatrix} 0 \\ \mathbf{x}_1(\mathbf{x}_1\mathbf{x}_4 - \mathbf{x}_2\mathbf{x}_3) \\ 0 \\ 0 \end{pmatrix} \quad \text{and} \quad \begin{pmatrix} 0 \\ 0 \\ 0 \\ \mathbf{x}_3(\mathbf{x}_2\mathbf{x}_3 - \mathbf{x}_1\mathbf{x}_4) \end{pmatrix}.$$

Thus, the normal form for the generalized Hopf bifurcation with 1:1 resonance can be written as

$$\begin{pmatrix} \dot{z}_1 \\ \dot{z}_2 \end{pmatrix} = \begin{pmatrix} i\omega & 1 \\ 0 & i\omega \end{pmatrix} \begin{pmatrix} z_1 \\ z_2 \end{pmatrix} + \{a_1(z_1\bar{z}_1) + a_2(z_1\bar{z}_2 - \bar{z}_1z_2)\} \begin{pmatrix} z_1 \\ z_2 \end{pmatrix} + \{b_1(z_1\bar{z}_1) + b_2(z_1\bar{z}_2 - \bar{z}_1z_2)\} \begin{pmatrix} 0 \\ z_1 \end{pmatrix} \quad (24)$$

where $a_j = c_j + id_j$, $b_j = e_j + if_j$, $j = 1, 2$. In the above equation, we have replaced $(\mathbf{x}_1, \mathbf{x}_2, \mathbf{x}_3, \mathbf{x}_4)$ by $(z_1, z_2, \bar{z}_1, \bar{z}_2)$. Thus, the second and third equations can be obtained by conjugating the above equations.

While calculating the coefficients, we shall assume that the original system contains both quadratic and cubic nonlinearities. Thus, for the problem under consideration in this paper

$$f^2(y) = \sum_{s=1}^4 \sum_{|m|=2} f_{s,m_1,m_2,m_3,m_4}^2 (y_1^{m_1} y_2^{m_2} y_3^{m_3} y_4^{m_4}) e_s, \quad \dim(H_4^2) = 4C \quad (25a)$$

$$f^3(y) = \sum_{s=1}^4 \sum_{|m|=3} f_{s,m_1,m_2,m_3,m_4}^3 (y_1^{m_1} y_2^{m_2} y_3^{m_3} y_4^{m_4}) e_s, \quad \dim(H_4^3) = 80. \quad (25b)$$

We have shown in the previous section that $\ker(L_{A^*}) = \{\emptyset\}$ for $k = 2$ since $\ker(L_{S^*}) = \{\emptyset\}$. Thus, all the quadratic terms given by expression (25a) can be eliminated and the transformation which performs this reduction, obtained by the matrix representation of $\ker(L_{A^*})$, is given by

$$\begin{bmatrix} B & I & 0 & 0 \\ 0 & B & 0 & 0 \\ 0 & 0 & \bar{B} & I \\ 0 & 0 & 0 & \bar{B} \end{bmatrix} \begin{bmatrix} h_{1,m}^2 \\ h_{2,m}^2 \\ h_{3,m}^2 \\ h_{4,m}^2 \end{bmatrix} = \begin{bmatrix} f_{1,m}^2 \\ f_{2,m}^2 \\ f_{3,m}^2 \\ f_{4,m}^2 \end{bmatrix}$$

where

$$B = \begin{bmatrix} -i\omega & 0 & 0 & 0 & 0 & 0 & 0 & 0 & 0 & 0 \\ -2 & -i\omega & 0 & 0 & 0 & 0 & 0 & 0 & 0 & 0 \\ 0 & -1 & -i\omega & 0 & 0 & 0 & 0 & 0 & 0 & 0 \\ 0 & 0 & 0 & i\omega & 0 & 0 & 0 & 0 & 0 & 0 \\ 0 & 0 & 0 & -1 & i\omega & 0 & 0 & 0 & 0 & 0 \\ 0 & 0 & 0 & 0 & 0 & 3i\omega & 0 & 0 & 0 & 0 \\ 0 & 0 & 0 & -1 & 0 & 0 & i\omega & 0 & 0 & 0 \\ 0 & 0 & 0 & 0 & -1 & 0 & -1 & i\omega & 0 & 0 \\ 0 & 0 & 0 & 0 & 0 & -2 & 0 & 0 & 3i\omega & 0 \\ 0 & 0 & 0 & 0 & 0 & 0 & 0 & 0 & -1 & 3i\omega \end{bmatrix}$$

and $h_{i,m}^2$ and $f_{i,m}^2$ are vectors of dimension 10. Since B is nonsingular, it is easy to calculate

$$h_{2,m}^2 = B^{-1} f_{2,m}^2, \quad h_{1,m}^2 = B^{-1} (f_{1,m}^2 - h_{2,m}^2)$$

and $h_{3,m}^2$ and $h_{4,m}^2$ are the conjugates of $h_{1,m}^2$ and $h_{2,m}^2$, respectively. The complete expressions for $h_{1,m}^2$ and $h_{2,m}^2$, are given explicitly in the Appendix. As these transformations annihilate all of the quadratic nonlinearities in the given system, they alter the terms of order 3 and above. We denote the new coefficients of the cubic nonlinearities as

$$p_{s,m}^3 = f_{s,m}^3 + \tilde{f}_{s,m}^3 \quad \text{and} \quad \tilde{f}_{s,m}^3 = F(f_{1,m}^2, f_{2,m}^2, f_{3,m}^2, f_{4,m}^2)$$

where $f_{s,m}^3$ are the original coefficients of the cubic nonlinearities, and $\tilde{f}_{s,m}^3$ are the coefficients of the new cubic terms generated while eliminating the original quadratic nonlinearities. The coefficients are indeed functions of the coefficients of the original quadratic nonlinearities as one would expect. Now, the normal form for the leading nonlinearity is given by Eq. (23) and is defined in the space complementary to R_4^3 .

The coefficients a_1, a_2, b_1, b_2 and their conjugates are calculated using the solvability condition of Eq. (18). The first 4 coefficients are

$$a_1 = \frac{1}{4} (3 f_{1,2010}^3 + f_{2,1110}^3 + f_{2,2001}^3) + \tilde{a}_1$$

$$a_2 = \frac{1}{6} (2 f_{1,2001}^3 - 2 f_{2,0210}^3 - f_{1,1110}^3 + f_{2,1101}^3) + \tilde{a}_2$$

$$b_1 = f_{2,2010}^3 + \tilde{b}_1$$

$$b_2 = \frac{1}{4} (f_{1,2010}^3 - f_{2,1110}^3 + 3 f_{2,2001}^3) + \tilde{b}_2$$

where the expressions for $\tilde{a}_1, \tilde{a}_2, \tilde{b}_1$ and \tilde{b}_2 in terms of the coefficients of the quadratic nonlinearities are given in the Appendix. The remaining four coefficients are obtained by conjugation of the above expressions, i.e., $a_3 = \bar{a}_1, a_4 = \bar{a}_2, b_3 = \bar{b}_1$ and $b_4 = \bar{b}_2$.

2. Recursive Calculation of Normal Form Coefficients

This approach is based on a series of papers by Ponce, Gamero and Freire [8, 9, 10, 17] which are, in turn, implementations of a method of Chow and Hale [4, Chap. 12] which employs a technique developed by Deprit [6] using Lie transforms to determine the normal form.

In order to remain consistent with the literature, the following notation will be used: define $F^k, U^k, G^k \in H_n^k$ by

$$F^k = (k-1)! f^k(y), \quad U^k = (k-1)! h^k(x), \quad G^k = (k-1)! g^k(x).$$

The first step is a rescaling to isolate the homogeneous terms of degree k . Letting $x \rightarrow \epsilon x$ and $y \rightarrow \epsilon y$ for $\epsilon \in \mathbb{R}$, the original system of Eq. (4) becomes

$$\dot{y} = A y + \sum_{k \geq 2} \frac{\varepsilon^{k-1}}{(k-1)!} F^k(y) \quad (26)$$

the near identity transformation, (8), becomes

$$y = x + \sum_{k \geq 2} \frac{\varepsilon^{k-1}}{(k-1)!} U^k(x) \quad (27)$$

and the system in normal form, (7), becomes

$$\dot{x} = Ax + \sum_{k \geq 2} \frac{\varepsilon^{k-1}}{(k-1)!} G^k(x). \quad (28)$$

Following Chow and Hale [4], the sequence $\{F_l^k\}$ is defined by the recursion relation

$$F_l^k = F_{l-1}^k + \sum_{j=2}^{k-l+2} \binom{k-l}{j-2} F_{l-1}^{k-j+1} \times U^j, \quad l = 2, \dots, k, \quad k = 2, \dots \quad (29)$$

where $F_1^k = F^k$, $F_1^1 = Ax$ and

$$P \times Q = \frac{\partial P}{\partial x} Q - \frac{\partial Q}{\partial x} P.$$

It can be shown (see Chow and Hale [4]) that

$$F_k^k = G^k.$$

This recursion can be represented by a Lie triangle,

$$\begin{array}{ccccccc} [(F_1^1)] & & & & & & \\ (F_1^2) & [F_2^2] & & & & & \\ (F_1^3) & F_2^3 & [F_3^3] & & & & \\ (F_1^4) & F_2^4 & F_3^4 & [F_4^4] & & & \\ (F_1^5) & F_2^5 & F_3^5 & F_4^5 & [F_5^5] & & \\ (\vdots) & \vdots & \vdots & \vdots & \dots & [\vdots] & \end{array}$$

The terms in round brackets are from the original system and those in square brackets are the final normal form. Each term in the triangle depends on those immediately to the left and above. The indexing scheme used here is different from that in the above references; the superscript k refers to both the order of the monomials in the vector and the row in which it appears in the Lie triangle and the subscript refers to the column in which it appears in the Lie triangle.

The recursion operates across rows of the Lie triangle from left to right. As an example of what occurs during a recursion, consider the fifth row. F_1^5 is a vector containing the order 5 terms in the original system. To generate F_2^5 , F_1^5 is added to the sum of the terms in column 1 above F_1^5 combined with the appropriate U^j 's; $F_1^4 \times U^2, F_1^3 \times U^3, F_1^2 \times U^4, F_1^1 \times U^5$. To generate F_3^5 , F_2^5 is added to the sum of the terms in column 2 above F_2^5 combined with the appropriate U^j 's; $F_2^4 \times U^2, F_2^3 \times U^3, F_2^2 \times U^4$. This process is continued until F_5^5 is reached at which time the normal form has been obtained. What is happening as the recursion moves across the Lie triangle is the accumulation of the order 5 contributions of the near identity transformations of orders 2 to 5. In column 2, the contributions from substituting the transformations into the original equations are collected. In succeeding columns, the contributions from the interaction of new terms generated by the transformation and the subsequent transformations are collected until finally in column 5 one has the order 5 terms of the normal form. The coefficient $\binom{k-l}{j-2}$ which appears in the sum is a counting term analogous to the binomial coefficient in the binomial theorem.

Now rewrite Eq. (11) using the new notation

$$-L_A U^k = \tilde{F}^k - G^k$$

where \tilde{F}^k is a vector of the order k monomials resulting from the near identity transformations up to order $k-1$. If Eq. (11) is rewritten as

$$\tilde{F}^k = G^k - L_A U^k$$

then

$$\text{proj}_{k \in L_A} \tilde{F}^k = G^k \quad (30)$$

and

$$\text{proj}_{R_n} \tilde{F}^k = -L_A U^k. \quad (31)$$

However, if (11) is written as

$$G^k = \tilde{F}^k + L_A U^k$$

and it is noted that $F_1^1 \times U^k = (Ax) \times U^k = L_A U^k$, then

$$G^k = \tilde{F}^k + F_1^1 \times U^k.$$

Now consider the recursion (29). The only time U^k will appear is when $l = 2$, in which case (29) can be written

$$F_2^k = F_1^k + \sum_{j=2}^{k-1} \binom{k-2}{j-2} F_1^{k-j+1} \times U^j + F_1^1 \times U^k$$

or

$$F_2^k = \tilde{F}_2^k + F_1^1 \times U^k.$$

For $l = 3$, Eq. (29) can be written

$$F_3^k = \tilde{F}_2^k + F_1^1 \times U^k + \sum_{j=2}^{k-1} \binom{k-2}{j-2} F_2^{k-j+1} \times U^j$$

or

$$F_3^k = \tilde{F}_3^k + F_1^1 \times U^k.$$

So, for any l , $2 \leq l \leq k$,

$$F_l^k = \tilde{F}_l^k + F_1^1 \times U^k.$$

It is easy to see that the F_l^k obey the recursion relations

$$\tilde{F}_2^k = \tilde{F}_1^k + \sum_{j=2}^{k-1} \binom{k-2}{j-2} F_1^{k-j+1} \times U^j$$

$$\tilde{F}_l^k = \tilde{F}_{l-1}^k + \sum_{j=2}^{k-l+2} \binom{k-l}{j-2} F_{l-1}^{k-j+1} \times U^j, \quad l = 3, \dots, k.$$

This recursion is identical to Eq. (29) except for \tilde{F}_2^k , there the $F_1^1 \times U^k$ term was left out (and thus will not appear in any of the subsequent F_l^k). Thus

$$\tilde{F}_k^k = \tilde{F}^k = G^k - L_A U^k.$$

So Eq. (30) can be used to determine the order k normal form, and if Eq. (31) is written

$$U^k = -L_A^{-1} \text{proj}_{R_0^k} \tilde{F}^k$$

the order k near identity transformation can be obtained.

In order to continue on to higher order terms in the normal form, it is necessary to convert the \tilde{F}_l^k 's into F_l^k 's. This is accomplished using the following correction

$$F_l^k = \tilde{F}_l^k - \text{proj}_{R_0^k} \tilde{F}^k, \quad l = 2, \dots, k.$$

IV. DOMINANT NORMAL FORM

In order to study perturbations of a vector field with linear part given by the non-semisimple matrix A , we consider the universal unfolding of the linear vector field Ax used in van Gils et al. [11]

$$A(\lambda) = \begin{pmatrix} i + \alpha & 1 \\ \mu & i + \alpha \end{pmatrix}, \quad \lambda = (\alpha, \mu_1, \mu_2), \quad \alpha \in \mathbb{R}, \quad \mu = \mu_1 + i\mu_2 \in \mathbb{C} \quad (32)$$

This may be calculated explicitly using the homological equation (10) applied to first degree polynomials $h^1(x)$, in the same manner as (23) for cubic polynomials. The unfolding parameters λ are found in terms of the original linear coefficients to be

$$\alpha = \frac{1}{2} \left(f_{1,1000}^1 + f_{2,p100}^1 \right) \quad \text{and} \quad \mu = f_{2,1000}^1$$

The above unfolding of $A(\lambda)$ may also be found from the viewpoint of versal deformations of matrices, as in Arnold [1], allowing for rescaling of time.

Now, making the observation that $z_1 = 0$ implies $z_2 = 0$ and the normal form commutes with S , we choose a transformation as in van Gils et al. [11]

$$z_1 = r e^{i\Phi}, \quad z_2 = r e^{i\Phi} w, \quad w = u + iv, \quad \Phi = \omega t + \theta$$

which yields three real equations independent of the phase variable θ

$$\dot{r} = r [\alpha + u + r^2 (c_1 + 2d_2 v)]$$

$$\dot{u} = \mu_1 - u^2 + v^2 + r^2 (e_1 + 2f_2 v)$$

$$\dot{v} = \mu_2 - 2uv + r^2 (f_1 - 2e_2 v)$$

$$\text{and} \quad \dot{\theta} = v + r^2 (d_1 - 2c_2 v).$$

In order to "blow up" the dominant terms, we rescale the above variables as $r = \varepsilon \hat{r}$, $u = \varepsilon \hat{u}$, $v = \varepsilon \hat{v}$, $\varepsilon t = \hat{t}$, $\alpha = \varepsilon \hat{\alpha}$, $\mu_1 = \varepsilon^2 \hat{\mu}_1$, $\mu_2 = \varepsilon^2 \hat{\mu}_2$. Introducing $\hat{r}^2 = \hat{\rho}$ and dropping the hats, we have, in new time,

$$\begin{aligned} \rho' &= 2\rho (\alpha + u) + \varepsilon 2c_1 \rho^2 + O(\varepsilon^2) \\ u' &= \mu_1 - u^2 + v^2 + e_1 \rho + \varepsilon 2f_2 \rho v + O(\varepsilon^2) \end{aligned} \tag{33}$$

$$v' = \mu_2 - 2uv + f_1 \rho - \varepsilon 2e_2 \rho v + O(\varepsilon^2)$$

$$\text{and} \quad \theta' = v + \varepsilon d_1 \rho + O(\varepsilon^2)$$

where

$$c_1 = \text{Re}(a_1), \quad e_1 = \text{Re}(b_1), \quad e_2 = \text{Re}(b_2)$$

$$d_1 = \text{Im}(a_1), \quad f_1 = \text{Im}(b_1), \quad f_2 = \text{Im}(b_2).$$

V. AVERAGED EQUATIONS

In this section, we shall demonstrate the relationship between second order averaging and normal forms for the nilpotent case under consideration. To this end, we make use of the scaling suggested by Hale [13] for linear operators whose superdiagonals are equal to 1. In order to make the calculations less cumbersome, we only consider cubic nonlinearities and the nonlinear system can be written as

$$\dot{y} = A(\mu)y + F^0(y_1, y_3) + F^1(y) + F^2(y) + F^3(y_2, y_4) \quad (34)$$

where A is as given in Eq. (22) and the nonlinearities of degree 3 can be written in terms of the original notation as

$$F^0 = \sum_{s=1}^4 \left\{ f_{s,3000}^3 y_1^3 + f_{s,2010}^3 y_1^2 y_3 + f_{s,1020}^3 y_1 y_3^2 + f_{s,0030}^3 y_3^3 \right\} e_s$$

$$F^1 = \sum_{s=1}^4 \left\{ f_{s,2100}^3 y_1^2 y_2 + f_{s,2001}^3 y_1^2 y_4 + f_{s,1110}^3 y_1 y_2 y_3 + f_{s,1011}^3 y_1 y_3 y_4 \right. \\ \left. + f_{s,0120}^3 y_2 y_3^2 + f_{s,0021}^3 y_3^2 y_4 \right\} e_s$$

$$F^2 = \sum_{s=1}^4 \left\{ f_{s,1200}^3 y_1 y_2^2 + f_{s,1002}^3 y_1 y_4^2 + f_{s,1101}^3 y_1 y_2 y_4 + f_{s,0111}^3 y_2 y_3 y_4 \right. \\ \left. + f_{s,0210}^3 y_2^2 y_3 + f_{s,0012}^3 y_3 y_4^2 \right\} e_s$$

$$F^3 = \sum_{s=1}^4 \left\{ f_{s,0300}^3 y_2^3 + f_{s,0201}^3 y_2^2 y_4 + f_{s,0102}^3 y_2 y_4^2 + f_{s,0003}^3 y_4^3 \right\} e_s$$

In order to bring the above equations into "standard form", we make use of the scaling suggested by Hale [13], which is in line with that of van Gils et al. [11],

$$y_1 = \varepsilon x_1, \quad y_2 = \varepsilon^2 x_2, \quad y_3 = \varepsilon x_3; \quad y_4 = \varepsilon^2 x_4$$

and transform Eq. (34) to new variables z by means of the transformation

$$x_j = z_j e^{i\omega t}, \quad x_{j+2} = \bar{z}_j e^{-i\omega t}, \quad j = 1, 2.$$

This procedure yields a set of equations in standard form to $O(\epsilon^2)$ as

$$\dot{z} = \epsilon X^0(z, \bar{z}, t) + \epsilon^2 X^1(z, \bar{z}, t), \quad z = (z_1, z_2) \quad (35)$$

where

$$X^0 = \begin{bmatrix} z_2 \\ e^{-i\omega t} F_2^0(z_1, \bar{z}_1, t) \end{bmatrix}, \quad X^1 = \begin{bmatrix} e^{-i\omega t} F_1^0(z_1, \bar{z}_1, t) \\ e^{-i\omega t} F_2^1(z, \bar{z}, t) \end{bmatrix} \quad (36)$$

and the \bar{z} equations are obtained by conjugating Eq. (35). Now, applying the averaging procedure up to the second order yields

$$\dot{z} = \epsilon M_t \{X^0(z, \bar{z}, t)\} + \epsilon^2 M_t \left\{ \frac{\partial X^0}{\partial z} W + \frac{\partial X^0}{\partial \bar{z}} \bar{W} - \frac{\partial W}{\partial z} \tilde{X}^0 - \frac{\partial W}{\partial \bar{z}} \tilde{\bar{X}}^0 + X^1(z, \bar{z}, t) \right\} \quad (37)$$

where M_t is the averaging operator defined as

$$M_t(\cdot) = \lim_{T \rightarrow \infty} \frac{1}{T} \int_0^T (\cdot) dt$$

and

$$W(z, \bar{z}, t) = \int_0^t \tilde{X}^0 dt + c(z, \bar{z}), \quad \tilde{X}^0(z, \bar{z}, t) = X^0(z, \bar{z}, t) - M_t \{X^0(z, \bar{z}, t)\}$$

i. e.

$$W_1(z, \bar{z}, t) = c_1(z, \bar{z}) \quad \text{and} \quad W_2(z, \bar{z}, t) = k(z, \bar{z}, t) + c_2(z, \bar{z})$$

with $k(z, \bar{z}, t)$ defined as

$$k(z, \bar{z}, t) = \frac{1}{2i\omega} f_{23000}^3 z_1^3 e^{2i\omega t} - \frac{1}{2i\omega} f_{21020}^3 z_1 \bar{z}_1^2 e^{-2i\omega t} - \frac{1}{4i\omega} f_{20030}^3 \bar{z}_1^3 e^{-4i\omega t}$$

where c is an arbitrary vector function of z and \bar{z} . The choice of c is made such that the normal form coincides with the resulting second order averaged equations. We have made two observations concerning the product terms within the second curly bracket of Eq. (37). Note, in Eq. (36), that X_2^0 is only a function of z_1 and \bar{z}_1 and

$\tilde{X}_1^0 = 0, \tilde{\bar{X}}_1^0 = 0$. Thus, the second order contribution from $k(z, \bar{z}, t)$ is identically zero.

The second order contributions to the averaged equations are

$$\varepsilon^2 M_t \left\{ c_2 - L(c_1) + X_1^1(z, \bar{z}, t) \right\}$$

$$\varepsilon^2 M_t \left\{ 2 f_{22010}^3 c_1 z_1 \bar{z}_1 + f_{22010}^3 \bar{c}_1 z_1^2 - L(c_2) + X_2^1(z, \bar{z}, t) \right\}$$

where $L(.) = \frac{\partial(.)}{\partial z_1} z_2 + \frac{\partial(.)}{\partial z_2} f_{22010}^3 z_1^2 \bar{z}_1 - \frac{\partial(.)}{\partial \bar{z}_1} \bar{z}_2 - \frac{\partial(.)}{\partial \bar{z}_2} f_{41020}^3 z_1 \bar{z}_1^2$.

Comparing terms of like order in the averaged and normal form equations, the appropriate choice of the vector c is given by

$$c_1(z, \bar{z}) = \alpha_1 z_2, \quad c_2(z, \bar{z}) = \alpha_2 z_1^2 \bar{z}_1.$$

Equating coefficients yields

$$\alpha_1 f_{22010}^3 - \alpha_2 = \frac{1}{4} [f_{12010}^3 - f_{22001}^3 - f_{2,1110}^3], \quad \bar{\alpha}_1 f_{22010}^3 - \alpha_2 = \frac{1}{4} [f_{12010}^3 - f_{22001}^3 - f_{2,1110}^3].$$

It is obvious that α_1 must be real. Choosing α_1 to be identically zero, α_2 is obtained as

$$\alpha_2 = -\frac{1}{4} [f_{12010}^3 - f_{22001}^3 - f_{2,1110}^3].$$

Thus, the averaged equations are

$$\dot{z}_1 = \varepsilon z_2 + \varepsilon^2 a_1(z_1 \bar{z}_1) z_1 + O(\varepsilon^3)$$

$$\dot{z}_2 = \varepsilon b_1(z_1 \bar{z}_1) z_1 + \varepsilon^2 [b_2(z_1 \bar{z}_2) + (a_1 - b_2)(\bar{z}_1 z_2)] z_1 + O(\varepsilon^3). \quad (38)$$

The second pair of equations are obtained by conjugating Eq. (38). As before, we introduce the universal unfolding defined by matrix $A(\lambda)$ (see Eq. (32)) into Eq. (38), use the transformation

$$z_1 = r e^{i\theta}, \quad z_2 = r e^{i\theta} w, \quad w = u + iv \quad (39)$$

and rescale the variables as

$$\epsilon t = \hat{t}, \quad \mu_1 = \epsilon^2 \hat{\mu}_1, \quad \mu_2 = \epsilon^2 \hat{\mu}_2, \quad \alpha = \epsilon \hat{\alpha}. \quad (40)$$

After substituting Eqs. (39) and (40) into Eq. (38) and dropping the hats, we have the averaged equations in terms of $\rho = r^2$ as expressed in Eq. (33). Thus, one can conclude that the dominant terms of the scaled normal form equations (33) agree completely with those of the averaged equations.

ACKNOWLEDGEMENTS

This research was partially supported by the National Science Foundation through Grant MSS 90-57437-PYI, the Air Force Office of Scientific Research under grant 91-0041, and the National Science and Research Council of Canada. The first author would like to thank Prof. S. T. Ariaratnam of the University of Waterloo for pointing out the scaling given in Hale [13] and Prof. Ranga Rao of the University of Illinois for his valuable discussions.

REFERENCES

1. V. I. ARNOLD, "Geometric Methods in the Theory of Ordinary Differential Equations," Springer-Verlag, New York, 1983.
2. A. K. BAJAJ AND P. R. SETHNA, Flow induced bifurcations to three-dimensional oscillatory motions in continuous tubes, *SIAM J. Appl. Math.* **44**(2) (1984), 270-286.
3. G. D. BIRKHOFF, "Dynamical Systems," AMS Publications, Providence, 1927.
4. S. N. CHOW AND J. K. HALE, "Methods of Bifurcation Theory," Springer-Verlag, New York, 1982.
5. R. CUSHMAN AND J. A. SANDERS, Nilpotent normal forms and representation theory of $sl(2, \mathbb{R})$, "Multiparameter Bifurcation Theory," ed. M. GOLUBITSKI and J. GUCKENHEIMER, *Contemp. Math.* **56**, AMS Publications, Providence (1986), 31-51.
6. A. DEPRIT, Canonical transformations depending on a small parameter, *Celest. Mech.* **1** (1969), 12-32.
7. C. ELPHICK, E. TIRAPEQUI, M. E. BRACHET, P. COULLET AND G. IOOSS, A simple global characterization for normal forms of singular vector fields, *Physica* **29D** (1987), 95-127.
8. E. FREIRE, E. GAMERO AND E. PONCE, An algorithm for symbolic computation of Hopf bifurcation, *Computers and Mathematics*, eds. E. Kaltofen and S. M. Watt, Springer-Verlag, New York (1989), 109-118.
9. E. FREIRE, E. GAMERO, E. PONCE AND L. G. FRANQUELO, An algorithm for symbolic computation of centre manifolds, *Symbolic and Algebraic Computation*, ed. P. Gianni, *Lecture Notes in Computer Science* **358**, Springer-Verlag, New York (1989), 218-230.
10. E. GAMERO, E. FREIRE AND E. PONCE, Normal forms for planar systems with nilpotent linear part, *Int. Series of Num. Math.* **97** (1991), 123-127.

11. S. A. VAN GILS, M. KRUPA AND W. F. LANGFORD, Hopf Bifurcation with non-semisimple 1:1 resonance, *Nonlinearity* **3** (1990), 825-850.
12. J. GUCKENHEIMER AND P. HOLMES, "Dynamical Systems and Bifurcations of Vector Fields," Springer-Verlag, New York, 1983.
13. J. K. HALE, "Oscillations in Nonlinear Systems," McGraw-Hill, New York, 1963.
14. S. HELGASON, "Groups and Geometric Analysis," Academic Press, Inc., New York, 1984.
15. K. R. MEYER, Normal forms for the general equilibrium, *Funkcialaj Ekvacioj* **27** (1984), 261-271.
16. H. POINCARÉ, Memoire sur les courbes definis par une equation differentielle IV, *J. Math. Pures Appl.* **1** (1885), 167-244.
17. E. J. PONCE-NUNEZ AND E. GAMERO, Generating Hopf bifurcation formulae with MAPLE, *Int. Series of Num. Math.* **97** (1991), 295-299.
18. G. IOOSS AND M. ADELMEYER, "Topics in Bifurcation Theory and Applications," World Scientific, Singapore, 1992.
19. G. IOOSS, A. MIELKE AND Y. DEMAY, Theory of steady Ginsburg-Landau equation, in hydrodynamic stability problems, *Eur. J. Mech., B/Fluids.* **8**(3) (1989), 229-268.

APPENDIX

The transformations h_{im}^2 , $i = 1, 2$, which eliminate the quadratic terms are:

$$h_{1;2000}^2 = \frac{1}{\omega^2} (f_{2;2000}^2 + i \omega f_{1;2000}^2)$$

$$h_{1;1100}^2 = \frac{1}{\omega^3} \left[\omega (-2f_{1;2000}^2 + f_{2;1100}^2) + i (4f_{2;2000}^2 + \omega^2 f_{1;1100}^2) \right]$$

$$h_{1;0200}^2 = \frac{1}{\omega^4} \left[-6f_{2;2000}^2 + \omega^2 (-f_{1;1100}^2 + f_{2;0200}^2) + i \omega (-2f_{1;2000}^2 + 2f_{2;1100}^2 + \omega^2 f_{1;0200}^2) \right]$$

$$h_{1;1010}^2 = \frac{1}{\omega^2} (f_{2;1010}^2 - i \omega f_{1;1010}^2)$$

$$h_{1;0110}^2 = \frac{1}{\omega^3} \left[\omega (-f_{1;1010}^2 + f_{2;0110}^2) + i (-2f_{2;1010}^2 - \omega^2 f_{1;0110}^2) \right]$$

$$h_{1;0020}^2 = \frac{1}{3\omega^2} \left(\frac{1}{3} f_{2;0020}^2 - i \omega f_{1;0020}^2 \right)$$

$$h_{1;1001}^2 = \frac{1}{\omega^3} \left[\omega (-f_{1;1010}^2 + f_{2;1001}^2) + i (-2f_{2;1010}^2 - \omega^2 f_{1;1001}^2) \right]$$

$$h_{1;0101}^2 = \frac{1}{\omega^4} \left[-6f_{2;1010}^2 + \omega^2 (-f_{1;0110}^2 - f_{1;1001}^2 + f_{2;0101}^2) + i \omega (2f_{1;1010}^2 - \omega^2 f_{1;0101}^2) \right]$$

$$h_{1;0011}^2 = \frac{1}{3\omega^3} \left[\frac{1}{3} \omega (-2f_{1;0020}^2 + f_{2;0011}^2) + i \left(-\frac{4}{9} f_{2;0020}^2 - \omega^2 f_{1;0011}^2 \right) \right]$$

$$h_{1;0002}^2 = \frac{1}{3\omega^4} \left[-\frac{2}{9} f_{2;0020}^2 + \frac{1}{3} (-f_{1;0011}^2 + f_{2;0002}^2) + i \omega \left(\frac{2}{9} f_{1;0020}^2 - \omega^2 f_{1;0002}^2 \right) \right]$$

$$h_{2;2000}^2 = \frac{1}{\omega} f_{2;2000}^2$$

$$h_{2;1100}^2 = \frac{1}{\omega^2} (-2f_{2;2000}^2 + i \omega f_{2;1100}^2)$$

$$h_{2,0200}^2 = \frac{1}{\omega^3} \left[-\omega f_{2,1100}^2 + i \left(-2f_{2,2000}^2 + \omega^2 f_{2,0200}^2 \right) \right]$$

$$h_{2,1010}^2 = \frac{-i}{\omega} f_{2,1010}^2$$

$$h_{2,0110}^2 = \frac{-1}{\omega^2} \left(f_{2,1010}^2 + i f_{2,0110}^2 \right)$$

$$h_{2,0020}^2 = \frac{-i}{3\omega} f_{2,0020}^2$$

$$h_{2,1001}^2 = \frac{-1}{\omega^2} \left(f_{2,1010}^2 + i\omega f_{2,1001}^2 \right)$$

$$h_{2,0101}^2 = \frac{1}{\omega^3} \left[-\omega \left(f_{2,0110}^2 + f_{2,1001}^2 \right) + i \left(2f_{2,1010}^2 - \omega^2 f_{2,0101}^2 \right) \right]$$

$$h_{2,0011}^2 = \frac{-1}{3\omega^3} \left(2 f_{2,0020}^2 + i\omega f_{2,0011}^2 \right)$$

$$h_{2,0002}^2 = \frac{1}{3\omega^3} \left[-\frac{1}{3} f_{2,0011}^2 + i \left(\frac{2}{9} f_{2,0020}^2 - \omega^2 f_{2,0002}^2 \right) \right]$$

The contributions from the quadratic non-linearities to the normal form are given by the coefficients \tilde{a}_1 , \tilde{a}_2 , \tilde{b}_1 and \tilde{b}_2 and are expressed as follows:

$$\begin{aligned} \tilde{a}_1 = & \frac{1}{\omega^2} \left\{ \frac{1}{4} f_{1,1010}^2 f_{2,2000}^2 - f_{1,2000}^2 f_{2,1010}^2 - \frac{3}{4} f_{2,1001}^2 f_{2,2000}^2 + \frac{1}{2} f_{2,1010}^2 f_{3,1010}^2 \right. \\ & + \frac{1}{9} f_{2,0020}^2 f_{3,2000}^2 - \frac{1}{4} f_{2,1010}^2 f_{4,0110}^2 - \frac{1}{4} f_{2,1010}^2 f_{4,1001}^2 - \frac{3}{4} f_{1,1010}^2 f_{4,1010}^2 \\ & \left. - \frac{1}{4} f_{2,0110}^2 f_{4,1010}^2 + \frac{1}{2} f_{2,1001}^2 f_{4,1010}^2 - \frac{1}{18} f_{2,0020}^2 f_{4,1100}^2 - \frac{1}{6} f_{1,0020}^2 f_{4,2000}^2 \right\} \end{aligned}$$

$$\begin{aligned}
& + \frac{1}{36} f_{2,0011}^2 f_{4,2000}^2 \Big\} \\
& + \frac{i}{\omega^3} \left\{ f_{2,1010}^2 f_{2,2000}^2 - f_{2,1010}^2 f_{4,1010}^2 - \frac{2}{27} f_{2,0020}^2 f_{4,2000}^2 \right. \\
& + \omega^2 \left[\frac{3}{4} f_{1,1010}^2 f_{1,2000}^2 - \frac{1}{4} f_{1,2000}^2 f_{2,1001}^2 + \frac{1}{2} f_{1,1100}^2 f_{2,1010}^2 + \frac{1}{2} f_{2,0200}^2 f_{2,1010}^2 \right. \\
& + \frac{1}{4} f_{1,1010}^2 f_{2,1100}^2 + \frac{1}{4} f_{2,1001}^2 f_{2,1100}^2 - \frac{1}{4} f_{1,0110}^2 f_{2,2000}^2 + \frac{1}{2} f_{1,1001}^2 f_{2,2000}^2 \\
& - \frac{1}{4} f_{2,0101}^2 f_{2,2000}^2 - \frac{1}{4} f_{2,1010}^2 f_{3,0110}^2 - \frac{1}{4} f_{2,1010}^2 f_{3,1001}^2 - \frac{3}{4} f_{1,1010}^2 f_{3,1010}^2 \\
& - \frac{1}{4} f_{2,0110}^2 f_{3,1010}^2 - \frac{1}{6} f_{2,0020}^2 f_{3,1100}^2 - \frac{1}{2} f_{1,0020}^2 f_{3,2000}^2 - \frac{1}{12} f_{2,0011}^2 f_{3,2000}^2 \\
& - \frac{1}{4} f_{2,1001}^2 f_{4,0110}^2 - \frac{1}{4} f_{2,1001}^2 f_{4,1001}^2 - \frac{3}{4} f_{1,1001}^2 f_{4,1010}^2 - \frac{1}{4} f_{2,0101}^2 f_{4,1010}^2 \\
& \left. \left. - \frac{1}{12} f_{2,0011}^2 f_{4,1100}^2 - \frac{1}{4} f_{1,0011}^2 f_{4,2000}^2 - \frac{1}{6} f_{2,0002}^2 f_{4,2000}^2 \right] \right\}
\end{aligned}$$

$$\begin{aligned}
\tilde{a}_2 = \frac{1}{\omega^4} & \left\{ f_{2,1010}^2 f_{4,1010}^2 - \frac{4}{81} f_{2,0020}^2 f_{4,2000}^2 + \omega^2 \left[\frac{1}{3} f_{1,2000}^2 f_{2,0110}^2 - \frac{1}{3} f_{1,2000}^2 f_{2,1001}^2 \right. \right. \\
& + \frac{1}{6} f_{2,0110}^2 f_{2,1100}^2 - \frac{1}{6} f_{2,1001}^2 f_{2,1100}^2 + \frac{1}{6} f_{2,1010}^2 f_{3,0110}^2 + \frac{1}{6} f_{2,1010}^2 f_{3,1001}^2 \\
& + \frac{1}{6} f_{1,1010}^2 f_{3,1010}^2 - \frac{1}{6} f_{2,0110}^2 f_{3,1010}^2 - \frac{2}{27} f_{2,0020}^2 f_{3,1100}^2 - \frac{2}{27} f_{1,0020}^2 f_{3,2000}^2 \\
& + \frac{1}{27} f_{2,0011}^2 f_{3,2000}^2 - \frac{1}{6} f_{2,1010}^2 f_{4,0101}^2 + \frac{1}{6} f_{1,1010}^2 f_{4,0110}^2 + \frac{1}{3} f_{2,0110}^2 f_{4,0110}^2 \\
& \left. \left. + \frac{1}{6} f_{2,1001}^2 f_{4,0110}^2 + \frac{2}{27} f_{2,0020}^2 f_{4,0200}^2 - \frac{1}{3} f_{1,1010}^2 f_{4,1001}^2 - \frac{1}{6} f_{2,0110}^2 f_{4,1001}^2 \right] \right\}
\end{aligned}$$

$$\begin{aligned}
& + \frac{1}{6} f_{2,1001}^2 f_{4,1001}^2 + \frac{1}{6} f_{1,0110}^2 f_{4,1010}^2 + \frac{1}{6} f_{1,1001}^2 f_{4,1010}^2 - \frac{1}{6} f_{2,0101}^2 f_{4,1010}^2 \\
& + \frac{1}{27} f_{1,0020}^2 f_{4,1100}^2 - \frac{1}{18} f_{2,0011}^2 f_{4,1100}^2 - \frac{2}{27} f_{1,0011}^2 f_{4,2000}^2 + \frac{2}{27} f_{2,0002}^2 f_{4,2000}^2 \Big] \\
& + \frac{i}{\omega^3} \left\{ \frac{1}{3} f_{2,1010}^2 f_{3,1010}^2 - \frac{4}{81} f_{2,0020}^2 f_{3,2000}^2 - \frac{1}{3} f_{2,1010}^2 f_{4,0110}^2 - \frac{1}{3} f_{2,1010}^2 f_{4,1001}^2 \right. \\
& - \frac{1}{3} f_{1,1010}^2 f_{4,1010}^2 + \frac{1}{3} f_{2,0110}^2 f_{4,1010}^2 + \frac{1}{3} f_{2,1001}^2 f_{4,1010}^2 + \frac{4}{81} f_{2,0020}^2 f_{4,1100}^2 \\
& + \frac{4}{81} f_{1,0020}^2 f_{4,2000}^2 - \frac{4}{81} f_{2,0011}^2 f_{4,2000}^2 + \omega^2 \left[\frac{1}{3} f_{1,1001}^2 f_{1,2000}^2 - \frac{1}{3} f_{1,0110}^2 f_{1,2000}^2 \right. \\
& - \frac{1}{6} f_{1,1100}^2 f_{2,0110}^2 - \frac{1}{3} f_{2,0110}^2 f_{2,0200}^2 + \frac{1}{6} f_{1,1100}^2 f_{2,1001}^2 + \frac{1}{3} f_{2,0200}^2 f_{2,1001}^2 \\
& - \frac{1}{6} f_{1,0110}^2 f_{2,1100}^2 + \frac{1}{6} f_{1,1001}^2 f_{2,1100}^2 - \frac{1}{6} f_{2,1010}^2 f_{3,0101}^2 + \frac{1}{6} f_{1,1010}^2 f_{3,0110}^2 \\
& + \frac{1}{3} f_{2,0110}^2 f_{3,0110}^2 + \frac{2}{9} f_{2,0020}^2 f_{3,0200}^2 - \frac{1}{3} f_{1,1010}^2 f_{3,1001}^2 - \frac{1}{6} f_{2,0110}^2 f_{3,1001}^2 \\
& + \frac{1}{6} f_{1,0110}^2 f_{3,1010}^2 + \frac{1}{9} f_{1,0020}^2 f_{3,1100}^2 - \frac{1}{18} f_{2,0011}^2 f_{3,1100}^2 - \frac{1}{9} f_{1,0011}^2 f_{3,2000}^2 \\
& - \frac{1}{6} f_{2,1001}^2 f_{4,0101}^2 + \frac{1}{6} f_{1,1001}^2 f_{4,0110}^2 + \frac{1}{3} f_{2,0101}^2 f_{4,0110}^2 + \frac{1}{9} f_{2,0011}^2 f_{4,0200}^2 \\
& - \frac{1}{3} f_{1,1001}^2 f_{4,1001}^2 - \frac{1}{6} f_{2,0101}^2 f_{4,1001}^2 + \frac{1}{6} f_{1,0101}^2 f_{4,1010}^2 + \frac{1}{18} f_{1,0011}^2 f_{4,1100}^2 \\
& \left. - \frac{1}{9} f_{2,0002}^2 f_{4,1100}^2 - \frac{2}{9} f_{1,0002}^2 f_{4,2000}^2 \right] \Big\}
\end{aligned}$$

$$\tilde{b}_1 = -\frac{1}{\omega^2} \left\{ 3f_{2,1010}^2 f_{2,2000}^2 + f_{2,1010}^2 f_{4,1010}^2 + \frac{2}{9} f_{2,0020}^2 f_{4,2000}^2 \right\}$$

$$\begin{aligned}
& + \frac{i}{\omega} \left\{ f_{2,1010}^2 f_{2,1100}^2 - f_{1,2000}^2 f_{2,1010}^2 + 2 f_{1,1010}^2 f_{2,2000}^2 - f_{2,0110}^2 f_{2,2000}^2 \right. \\
& \quad \left. - f_{2,1010}^2 f_{3,1010}^2 - \frac{2}{3} f_{2,0020}^2 f_{3,2000}^2 - f_{2,1001}^2 f_{4,1010}^2 - \frac{1}{3} f_{2,0011}^2 f_{4,2000}^2 \right\} \\
\tilde{b}_2 = & + \frac{1}{\omega^2} \left\{ f_{2,1010}^2 f_{2,1100}^2 - f_{1,2000}^2 f_{2,1010}^2 + \frac{3}{4} f_{1,1010}^2 f_{2,2000}^2 - \frac{9}{4} f_{2,1001}^2 f_{2,2000}^2 \right. \\
& + \frac{1}{2} f_{2,1010}^2 f_{3,1010}^2 - \frac{1}{9} f_{2,0020}^2 f_{3,2000}^2 + \frac{1}{4} f_{2,1010}^2 f_{4,0110}^2 - \frac{3}{4} f_{2,1010}^2 f_{4,1001}^2 \\
& - \frac{1}{4} f_{1,1010}^2 f_{4,1010}^2 + \frac{1}{4} f_{2,0110}^2 f_{4,1010}^2 + \frac{1}{2} f_{2,1001}^2 f_{4,1010}^2 + \frac{1}{18} f_{2,0020}^2 f_{4,1100}^2 \\
& \quad \left. - \frac{1}{18} f_{1,0020}^2 f_{4,2000}^2 - \frac{5}{36} f_{2,0011}^2 f_{4,2000}^2 \right\} \\
& + \frac{i}{\omega^3} \left\{ 3 f_{2,1010}^2 f_{2,2000}^2 - f_{2,1010}^2 f_{4,1010}^2 + \frac{2}{27} f_{2,0020}^2 f_{4,2000}^2 \right. \\
& + \omega^2 \left[\frac{1}{4} f_{1,1010}^2 f_{1,2000}^2 - \frac{3}{4} f_{1,2000}^2 f_{2,1001}^2 + \frac{1}{2} f_{1,1100}^2 f_{2,1010}^2 - \frac{1}{2} f_{2,0200}^2 f_{2,1010}^2 \right. \\
& - \frac{1}{4} f_{1,1010}^2 f_{2,1100}^2 + \frac{3}{4} f_{2,1001}^2 f_{2,1100}^2 - \frac{3}{4} f_{1,0110}^2 f_{2,2000}^2 + \frac{3}{2} f_{1,1001}^2 f_{2,2000}^2 \\
& - \frac{3}{4} f_{2,0101}^2 f_{2,2000}^2 + \frac{1}{4} f_{2,1010}^2 f_{3,0110}^2 - \frac{3}{4} f_{2,1010}^2 f_{3,1001}^2 - \frac{1}{4} f_{1,1010}^2 f_{3,1010}^2 \\
& + \frac{1}{4} f_{2,0110}^2 f_{3,1010}^2 + \frac{1}{6} f_{2,0020}^2 f_{3,1100}^2 - \frac{1}{6} f_{1,0020}^2 f_{3,2000}^2 - \frac{1}{4} f_{2,0011}^2 f_{3,2000}^2 \\
& + \frac{1}{4} f_{2,1001}^2 f_{4,0110}^2 - \frac{3}{4} f_{2,1001}^2 f_{4,1001}^2 - \frac{1}{4} f_{1,1001}^2 f_{4,1010}^2 + \frac{1}{4} f_{2,0101}^2 f_{4,1010}^2 \\
& \quad \left. + \frac{1}{12} f_{2,0011}^2 f_{4,1100}^2 - \frac{1}{12} f_{1,0011}^2 f_{4,2000}^2 - \frac{1}{2} f_{2,0002}^2 f_{4,2000}^2 \right] \Big\}.
\end{aligned}$$

PARAMETRICALLY EXCITED HOPF BIFURCATION WITH NON-SEMISIMPLE 1:1 RESONANCE

N. Sri Namachchivaya and Naresh Malhotra
Department of Aeronautical and Astronautical Engineering
University of Illinois, Urbana-Champaign
Urbana, Illinois

ABSTRACT

A generalized four dimensional, nonlinear and non-autonomous system is studied. The effect of periodic parametric excitations is examined on systems that exhibit Hopf bifurcation with one to one resonance along with subharmonic external resonance. The linear operator is assumed to have a generic nonsemisimple structure. In this case, the dimensionality of the system can not be reduced despite the presence of an S^1 symmetry. However, the system is simplified considerably by reducing it to the corresponding four dimensional normal form equations. The local behavior of the equilibrium solutions is studied along with their stability properties. Several codimension 1, 2 and 3 bifurcation varieties are observed. Some of the global bifurcations that are present, can be associated with the Bogdanov Takens and $(0, +i, -i)$ bifurcation varieties. The numerical results, obtained by using AUTO and CHAOS, indicate the existence of homoclinic orbits along with the period doubling behavior which leads to chaos.

1. INTRODUCTION

The objective of this study is to investigate the effect of periodic parametric excitations on systems that exhibit Hopf bifurcation with 1:1 resonance. For this purpose we consider a generalized four dimensional, nonlinear, non-autonomous system. It is assumed that, at some critical parameter values, the linear operator contains two coincidental purely imaginary eigenvalues which generically lead to a non-semisimple structure. Under these conditions, the system defined on a four dimensional center manifold is described by a

5-parameter family of normal form equations.

One to one resonant Hopf bifurcation has been studied by several authors in the past (Caprino et al. (1984); Meyer (1984); Krupa (1986)) and recently by van Gils et al. (1990), who considered 3-parameter unfolding of the vector field singularity. The work of van Gils et al. considered a system similar to one presented in this paper but without parametric excitation, and the associated normal form was reduced to three dimensional first order equations. Here, several codimension 1 and codimension 2 bifurcation varieties, in addition to some interesting periodic behavior, were examined. Furthermore, it was shown that the normal form of the fourth order autonomous system has an S^1 symmetry, and hence it is possible to reduce the dimension by one, bringing the system to a set of three equations in an appropriate co-ordinate frame. In this paper, we consider the corresponding nonautonomous generic system. As in van Gils et al. the structure of the equations in the present case, can be simplified considerably by bringing them into their normal-form or by using the method of averaging. Here, a modified version of the normal form of Namachchivaya et al. (1992) is considered which takes into consideration the subharmonic resonance with respect to the forcing frequency, in addition to the 1:1 internal resonance. However the disadvantage in such a system with parametric harmonic excitations is that the dimensionality of the system can not be reduced. Moreover, in addition to the traditional 3 unfolding

parameters for the autonomous system, one has to introduce 2 more parameters, namely the amplitude of the forcing and a detuning parameter which represents the deviation of the excitation frequency from twice the natural frequency. One expects very rich local dynamics in such a system due to the presence of 5 parameters. For the problem under consideration, there is an S^1 symmetry and the normal form equations can be further simplified. The equilibrium points of this simplified fourth order system extend to the periodic orbits that are the relative equilibria of the original four dimensional normal form.

The system of equations discussed here arises in a variety of physical problems which have 1:1 internal resonance under parametric periodic excitation. The problems of parametric excitation of nonlinear dynamical systems are of importance in several branches of engineering such as vibrations of beam structures under dynamic loads, flow induced vibrations and control systems. The major part of this analysis deals with the local behavior of the equilibrium solutions and their stability properties. We also study the global bifurcation set associated with Bogdanov-Takens and $(0, +i, -i)$ bifurcation varieties. In addition, we observe period doubling bifurcation which leads to chaos. Due to the complicated nature of the computations involved, we have used symbolic computations extensively. The analytical solutions have been compared with those obtained numerically using AUTO [Doedel (1986)], a general purpose software package for the bifurcation analysis of differential equations and the maps. We have also used CHAOS [Aronson (1991)], which is a SUN-based software program for numerically simulating the nonlinear systems. The analysis of the complete global behavior is in progress and we anticipate presentation of these results in the near future [Namachchivaya and Malhotra (1992)].

2. STATEMENT OF THE PROBLEM

We consider the following system on a four dimensional center manifold:

$$\dot{x} = f(x, t) \quad (2.1)$$

where $x \in \mathbb{R}^4$, is the state vector and $f: \mathbb{R}^4 \rightarrow \mathbb{R}^4$, is the non-autonomous vector field which is analytic in its arguments. We assume that the system (2.1) has both

quadratic and cubic nonlinearities, and the linear operator $A = D_x f(0)$ has two equal purely imaginary nonzero eigenvalues along with their conjugates. Furthermore, the double eigenvalues are assumed to be non-semisimple, and the time dependency on $f(x, t)$ is given explicitly in terms of parametric harmonic excitation. Under these conditions, the system (2.1) can be expressed as:

$$\dot{y} = A y + \mu_f B y \cos(\omega_f t) + f(y, \bar{y}) \quad (2.2)$$

where $y \in \mathbb{C}^4$, $y_{1,3} = x_1 \pm i x_2$, $y_{2,4} = x_3 \pm i x_4$, μ_f and ω_f are the amplitude and the frequency of the parametric excitation and B is a constant 4×4 matrix. $f(y, \bar{y})$ is the nonlinear term. The linear operator, A , has the following non-semisimple form:

$$A = \begin{bmatrix} i\omega & 1 & 0 & 0 \\ 0 & i\omega & 0 & 0 \\ 0 & 0 & -i\omega & 1 \\ 0 & 0 & 0 & -i\omega \end{bmatrix} \quad (2.3)$$

where $i\omega$ is the pure imaginary eigenvalue. In the subsequent sections we study the stability and the bifurcation behavior of the system described by Eq. (2.2).

3. TRANSFORMATION TO STANDARD FORM

In order to study the dynamic behavior, it is desirable to reduce the system under consideration (2.2) to its normal form. The normal form of the nonautonomous (periodic) linear part of Eq. (2.2) is obtained via a periodic transformation $y = v + H(t)v$ (See Namachchivaya and Malhotra (1992)), as:

$$\dot{v} = Av + \frac{\mu_f}{2} \begin{bmatrix} b_{13} \bar{v}_1 e^{i\omega_f t} \\ b_{23} \bar{v}_1 e^{i\omega_f t} + b_{13} \bar{v}_2 e^{i\omega_f t} \\ b_{31} v_1 e^{-i\omega_f t} \\ b_{41} v_1 e^{-i\omega_f t} + b_{31} v_2 e^{-i\omega_f t} \end{bmatrix} + \text{h.o.t.} \quad (3.1)$$

We define a new time τ such that $\tau = \omega_f t$, where $\omega_f = \omega_0 (1 - \epsilon \lambda)$, and λ is the detuning parameter. In addition to the internal 1:1 resonance, we consider the case of subharmonic parametric resonance ($k = \omega/\omega_0 = 1/2$). Without loss of generality, letting $\omega_0 = 1$, and using

the new time derivative with respect to τ , Eq. (3.1) takes the following form:

$$\begin{aligned} \dot{v}_1 &= \left[\frac{i v_1}{2} + v_2 + \frac{\mu_f}{2} b_{13} \bar{v}_1 e^{i\tau} \right] + \\ &\quad \varepsilon \left[\frac{i \lambda v_1}{2} + \lambda v_2 + \frac{\mu_f}{2} \lambda b_{13} \bar{v}_1 e^{i\tau} \right] + \text{h.o.t.} \\ \dot{v}_2 &= \left[\frac{i v_2}{2} + \frac{\mu_f}{2} (b_{23} \bar{v}_1 e^{i\tau} + b_{13} \bar{v}_2 e^{i\tau}) \right] + \\ &\quad \varepsilon \left[\frac{i \lambda v_2}{2} + \frac{\mu_f}{2} (\lambda b_{23} \bar{v}_1 e^{i\tau} + \lambda b_{13} \bar{v}_2 e^{i\tau}) \right] + \text{h.o.t.} \end{aligned} \quad (3.2)$$

The prime denotes differentiation with respect to τ , and the other two equations can be written as complex conjugates of these equations.

The next step is to include the normal form of the nonlinear terms in Eqs (3.2). For a detailed discussion of the calculation of the nonlinear normal form with a four dimensional non-semisimple linear operator, one is referred to Namachchivaya et al. (1992). Following this procedure yields the complete normal form of the original system of Eq. (2.2) and is expressed as following:

$$\begin{aligned} \dot{v}_1 &= \left[\frac{i v_1}{2} + v_2 + \frac{\mu_f}{2} b_{13} \bar{v}_1 e^{i\tau} + a_1 v_1^2 \bar{v}_1 + a_2 v_1^2 \bar{v}_2 \right. \\ &\quad \left. - a_2 v_1 v_2 \bar{v}_1 \right] + \varepsilon \lambda \left[\frac{i v_1}{2} + v_2 + \frac{\mu_f}{2} b_{13} \bar{v}_1 e^{i\tau} \right. \\ &\quad \left. + a_1 v_1^2 \bar{v}_1 + a_2 v_1^2 \bar{v}_2 - a_2 v_1 v_2 \bar{v}_1 \right] + \text{h.o.t.} \\ \dot{v}_2 &= \left[\frac{i v_2}{2} + \frac{\mu_f}{2} (b_{23} \bar{v}_1 e^{i\tau} + b_{13} \bar{v}_2 e^{i\tau}) + a_1 v_1 v_2 \bar{v}_1 \right. \\ &\quad \left. - b_2 v_1 v_2 \bar{v}_1 + b_1 v_1^2 \bar{v}_1 + a_2 v_1 v_2 \bar{v}_2 - a_2 \bar{v}_1 v_2^2 \right. \\ &\quad \left. + b_2 v_1^2 \bar{v}_2 \right] + \varepsilon \lambda \left[\frac{i v_2}{2} + \frac{\mu_f}{2} (b_{23} \bar{v}_1 e^{i\tau} \right. \\ &\quad \left. + b_{13} \bar{v}_2 e^{i\tau}) + (a_1 - b_2) v_1 v_2 \bar{v}_1 + b_1 v_1^2 \bar{v}_1 \right. \\ &\quad \left. + a_2 v_1 v_2 \bar{v}_2 - a_2 \bar{v}_1 v_2^2 + b_2 v_1^2 \bar{v}_2 \right] + \text{h.o.t.} \end{aligned} \quad (3.3)$$

Now consider the universal unfolding of the linear operator A as given by (2.3). The two dimensional analog of A can be written as:

$$A = \begin{bmatrix} i\omega & 1 \\ 0 & i\omega \end{bmatrix} \quad (3.4)$$

The universal unfolding of A , obtained from a four parameter versal deformation given by Arnold (1983), is expressed as:

$$A(\sigma) = \begin{bmatrix} (i\omega + \alpha) & 1 \\ \mu & (i\omega + \alpha) \end{bmatrix} \quad (3.5)$$

where $\sigma = (\alpha, \mu)$ and $\mu = (\mu_1 + i \mu_2)$. van Gils et al. (1990) interpret α as a real crossing parameter and μ is interpreted as a complex splitting parameter for the eigenvalues of the linear operator of A . In order to get rid of the time dependent terms in Eqs (3.3), we make the following transformation,

$$v_{1,2} = u_{1,2} e^{(i v_2)} \quad v_{3,4} = u_{3,4} e^{(-i v_2)} \quad (3.6)$$

The nonlinear terms remain invariant under this transformation due to S^1 symmetry and, in order to distinguish the dominant terms in Eqs (3.3), we introduce the following scaling:

$$\begin{aligned} u_{1,3} &= \varepsilon z_{1,3}, \quad u_{2,4} = \varepsilon^2 z_{2,4}, \quad \mu_f = \varepsilon^2 h, \text{ and} \\ \alpha &= \varepsilon \beta, \quad \mu = \varepsilon^2 v \end{aligned} \quad (3.7)$$

On applying the universal unfolding given by (3.5), the transformation given by (3.6) and the scaling given by (3.7), the normal form Eqs (3.3) become

$$\begin{aligned} \dot{z}_1 &= \varepsilon \left[\beta z_1 + z_2 + \frac{i \lambda z_1}{2} \right] + \\ &\quad \varepsilon^2 [g b_{13} \bar{z}_1 + \lambda z_2 + a_1 z_1^2 \bar{z}_1] + O(\varepsilon^3) \\ \dot{z}_2 &= \varepsilon \left[v z_1 + \beta z_2 + g b_{23} \bar{z}_1 + \frac{i \lambda z_2}{2} + b_1 z_1^2 \bar{z}_1 \right] + \\ &\quad \varepsilon^2 [g b_{13} \bar{z}_2 + g b_{23} \lambda \bar{z}_1 + a_1 z_1 \bar{z}_1 z_2 + b_2 z_1^2 \bar{z}_2 - \\ &\quad b_2 z_1 \bar{z}_1 z_2 + b_1 \lambda z_1^2 \bar{z}_1] + O(\varepsilon^3) \end{aligned} \quad (3.8)$$

where a_1, b_1, a_2, b_2 can be expressed in terms of the original nonlinear coefficients of Eq. (2.2). It is worth mentioning that these equations up to $O(\varepsilon^3)$ terms, have also been obtained by using the method of averaging, as shown in Namachchivaya et al. (1992). The above mentioned reduced system has 5 parameters. The three unfolding parameters (β, v, v_2) control the behavior of

the eigenvalues of the linear operator A , while g and λ control the extent of the forcing in terms of its amplitude and the deviation from the subharmonic excitation frequency. With the help of these parameters, it is possible to explore the local dynamics of the system in the neighboring regions. In order to explore the dominant dynamics, the time τ is rescaled as $\tau = \hat{\tau}/\epsilon$ so that in the slow time Eqs (3.8) take the following form:

$$\begin{aligned}\dot{z}_1 &= \beta z_1 + z_2 + \frac{i\lambda z_1}{2} + O(\epsilon) \\ \dot{z}_2 &= v z_1 + \beta z_2 + gb \bar{z}_1 + \frac{i\lambda z_2}{2} + b_1 z_1^2 \bar{z}_1 + O(\epsilon)\end{aligned}\quad (3.9)$$

where $gb = g b_{23}$, and the dot denotes differentiation with respect to the slow time.

4. STABILITY OF THE TRIVIAL SOLUTION

It is clear that $z = 0, \bar{z} = 0$ is the trivial solution of the normal form equations, and as a first step we consider their stability. Transforming Eqs (3.9) to real variables (x_1, y_1, x_2, y_2) by means of the usual transformations

$$\begin{aligned}x_1 &= (z_1 + \bar{z}_1)/2, \quad y_1 = (z_1 - \bar{z}_1)/(2i) \quad \text{and} \\ x_2 &= (z_2 + \bar{z}_2)/2, \quad y_2 = (z_2 - \bar{z}_2)/(2i),\end{aligned}$$

yields the following set of equations:

$$\begin{bmatrix} \dot{x}_1 \\ \dot{y}_1 \\ \dot{x}_2 \\ \dot{y}_2 \end{bmatrix} = L \begin{bmatrix} x_1 \\ y_1 \\ x_2 \\ y_2 \end{bmatrix} + \begin{bmatrix} 0 \\ 0 \\ c_2(x_1^3 + x_1 y_1^2) - d_2(x_1^2 y_1 + y_1^3) \\ c_2(x_1^2 y_1 + y_1^3) + d_2(x_1^3 + x_1 y_1^2) \end{bmatrix} \quad (4.1)$$

where

$$L = \begin{bmatrix} \beta & -\lambda/2 & 1 & 0 \\ \lambda/2 & \beta & 0 & 1 \\ (v_1 + gb) & -v_2 & \beta & -\lambda/2 \\ v_2 & (v_1 - gb) & \lambda/2 & \beta \end{bmatrix} \quad (4.2)$$

and v_1 and v_2 are the real and imaginary parts of the scaled complex splitting parameter v , and c_2 and d_2 are the real and imaginary parts of the nonlinear coefficient b_1 in Eqs 3.9. For the linear operator L , the non

redundant stability conditions are expressed as:

$$\begin{aligned}T1: & \quad \beta < 0 \\ T2: & \quad (v_1 + v_{10})^2 + (v_2 + v_{20})^2 > gb^2 \\ T3: & \quad v_2^2 < -v_{30}v_1 + v_{40}\end{aligned} \quad (4.3)$$

where,

$$v_{10} = \frac{1}{2} \left(\frac{\lambda^2}{2} - 2\beta^2 \right), \quad v_{20} = -\beta\lambda, \quad v_{30} = 4\beta^2$$

and

$$v_{40} = \frac{4\beta^2(4\beta^4 + \beta^2\lambda^2 + gb^2)}{(4\beta^2 + \lambda^2)} \quad (4.4)$$

Thus T2 and T3 completely determine the stability of the linear operator L once T1 is ensured. The typical stability region for the trivial solution of (4.2) is shown in Fig. (1) in (v_1, v_2) parameter space, where T2 represents the region outside the circle centered at $(-v_{10}, -v_{20})$ with radius gb , while T3 represents the region on the left side of the parabola described by $v_2^2 + v_{30}v_1 = v_{40}$.

5. EXISTENCE OF NON-TRIVIAL SOLUTION

In order to examine the existence of the non-trivial equilibrium solutions, we need to transform Eqs 3.9 into a convenient coordinate system. The structure of these equations suggest the coordinate transformation of (z_1, z_2) to the new coordinates (r, θ, u, v) by using:

$$z_1 = r e^{i\theta} \quad z_2 = r e^{i\theta} (u + iv) \quad (5.1)$$

where $(r, u, v) \in \mathbb{R}^3$, and θ is the phase variable. This leads to the following set of four coupled equations.

$$\begin{aligned}\dot{\rho} &= 2\rho(\beta + u) + O(\epsilon) \\ \dot{u} &= v_1 + (v^2 - u^2) + c_2\rho + gb \cos 2\theta + O(\epsilon) \\ \dot{v} &= v_2 - 2uv + d_2\rho - gb \sin 2\theta + O(\epsilon) \\ \dot{\theta} &= v + \frac{\lambda}{2} + O(\epsilon)\end{aligned} \quad (5.2)$$

where $\rho = r^2 > 0$. This coordinate transformation involves a singular change of the coordinates, which

restricts the applicability of Eqs (5.2) near $\rho = 0$, but this possibility has already been considered in the previous section. In the absence of parametric excitation (i.e., $gb = 0$ and $\lambda = 0$), Eqs (5.2) reduce to a set of three coupled equations (in ρ, u, v), independent of the phase variable θ and a fourth equation describing the evolution of θ , which is precisely the form studied by van Gils et al. (1990). The parametric excitation acts to couple the phase (θ) equation with the other three equations. The equilibrium points of Eqs (5.2) extend to the periodic orbits of the normal form of the original system. Thus the study of the non-trivial equilibrium solutions of the above system is vital to our analysis. The dominant part of Eqs (5.2) is

$$\begin{aligned}\dot{\rho} &= 2\rho(\beta + u) \\ \dot{u} &= v_1 + (v^2 - u^2) + c_2\rho + gb\cos 2\theta \\ \dot{v} &= v_2 - 2uv + d_2\rho - gb\sin 2\theta \\ \dot{\theta} &= v + \frac{\lambda}{2}\end{aligned}\quad (5.3)$$

The equilibrium solutions of Eqs (5.3) can be obtained by solving the following algebraic equations

$$\begin{aligned}\beta + u &= 0 \\ v_1 + (v^2 - u^2) + c_2\rho + gb\cos 2\theta &= 0 \\ v_2 - 2uv + d_2\rho - gb\sin 2\theta &= 0 \\ v + \lambda/2 &= 0\end{aligned}\quad (5.4)$$

Eqs (5.4) yield the following equilibrium points

$$\begin{aligned}\rho &= \frac{-b \pm \sqrt{b^2 - 4ac}}{2a} \\ u &= -\beta \\ v &= -\lambda/2 \\ \theta &= \frac{1}{2} \sin^{-1} \left[\frac{v^2 - 2uv + d_2\rho}{gb} \right]\end{aligned}\quad (5.5)$$

ρ satisfies the following quadratic equation:

$$a\rho^2 + b\rho + c = 0 \quad (5.6)$$

where

$$\begin{aligned}a &= (c_2^2 + d_2^2) \\ b &= 2[c_2(v_1 + v_{10}) + d_2(v_2 + v_{20})] \\ c &= (v_1 + v_{10})^2 + (v_2 + v_{20})^2 - gb^2\end{aligned}\quad (5.7)$$

and v_{10} and v_{20} are defined in Eqs (4.4). The non-trivial equilibrium solutions (5.5) are admissible only if ρ is real and positive.

According to Implicit Function Theorem, these equilibrium solutions (5.5) extend smoothly to the equilibrium solutions of (5.2) for small $\epsilon > 0$, if the Jacobian matrix (J_0) of (5.5) is nonsingular. The Jacobian matrix (J_0) is given by:

$$J_0 = \begin{bmatrix} 0 & 2\rho & 0 & 0 \\ c_2 & 2\beta & -\lambda & e_1 \\ d_2 & \lambda & 2\beta & e_2 \\ 0 & 0 & 1 & 0 \end{bmatrix} \quad (5.8)$$

where

$$e_1 = -2[v_2 + v_{20} + d_2\rho], \quad e_2 = 2[v_1 + v_{10} + c_2\rho]$$

$$\text{Det}[J_0] = 4\rho \left[\frac{b}{2} + a\rho \right], \quad (5.9)$$

a and b are given by Eqs (5.7). We observe that if the discriminant (D) of the quadratic equation (Eq. (5.6)) is nonzero, then the Jacobian J_0 (5.8) is nonsingular, i.e.,

$$D = (b^2 - 4ac) \geq 0 \quad \Rightarrow \quad \text{Det}[J_0] \neq 0 \text{ except where } D=0$$

This implies that the equilibrium solutions (5.5) extend locally in ϵ , to the equilibria of (5.2), except where D is zero. Throughout this investigation the nondegeneracy condition i.e., $(c_2^2 + d_2^2) > 0$ is assumed to be satisfied. Eq. (5.6) suggests that ρ may have 2, 1 or 0 equilibrium solutions that satisfy the requirements on ρ . Depending upon the values of the parameters we have the following scenarios.

Case A:

The following should be satisfied for two equilibrium solutions of ρ to exist, which would lead to real and positive values of ρ .

$$A.1: \quad c_2(v_1 + v_{10}) + d_2(v_2 + v_{20}) < 0$$

$$A.2: (v_1 + v_{10})^2 + (v_2 + v_{20})^2 - gb^2 > 0$$

$$A.3: |d_2(v_1 + v_{10}) - c_2(v_2 + v_{20})| < \sqrt{(c_2^2 + d_2^2)} \cdot gb$$

Case B:

If $a > 0$, and $c < 0$, Eq. (5.6) will have only 1 root that satisfies the requirement on ρ . In this case, the sign of the coefficient b does not affect the number of equilibrium solutions of ρ , but it determines the magnitude of the positive root of ρ . Thus, the following condition needs to be satisfied for only one root of ρ to exist.

$$B.1: (v_1 + v_{10})^2 + (v_2 + v_{20})^2 - gb^2 < 0$$

Elsewhere in the parameter space, ρ does not have a permissible solution. Figure (2) shows the typical regions where 2, 1 or 0 non-trivial equilibrium solutions of ρ exist for different values of the nonlinear coefficients. For both cases (Fig. 2a and b), there is one permissible root inside the circle, two such roots outside the circle between two tangent lines and no real and positive roots elsewhere. Furthermore, the second stability condition for the trivial solution T2, and the existence condition A.2 and B.1 are given by the same circle centered at $(-v_{10}, -v_{20})$. For the nondegenerate case ($a > 0$), various possibilities for the number of non-trivial equilibrium solutions are shown in Fig. (3), where $f(\rho)$ is plotted vs. ρ .

6. STABILITY OF THE NON-TRIVIAL SOLUTION

In this section we discuss the stability of the non-trivial equilibrium solutions obtained in the previous section. The Jacobian matrix (5.8) has a dependence on the equilibrium values of ρ , which in turn depend on the system parameters in a complex way as given by Eqs (5.5). Using the Routh-Hurwitz criteria, we arrive at the following stability conditions that must be satisfied for the non-trivial equilibrium solution (if it exists):

$$N1: \beta < 0$$

$$N2: (v_1 + v_{10}) < 2\left(\beta^2 + \frac{\lambda^2}{4}\right) - 2c_2\rho$$

$$N3: \{2\beta(v_1 + v_{10}) + \lambda(v_2 + v_{20}) + 2(2\beta c_2 + \lambda d_2)\rho\} > 0$$

$$N4: \left(\frac{b}{2} + a\rho\right) > 0 \quad (6.1)$$

$$N5: \left[80\beta^6 + 24\beta^4\lambda^2 + \beta^2\lambda^4 - 96\beta^4v_1 - 8\beta^2\lambda^2v_1 + 16\beta^2v_1^2 - 32\beta^3\lambda v_2 - 4\lambda^2v_2^2 - 128\beta^4c_2\rho - 32\beta^2\lambda^2c_2\rho - 64\beta^2v_2d_2\rho - 16\lambda^2v_2d_2\rho - 64\beta^2d_2^2\rho^2 - 16\lambda^2d_2^2\rho^2\right] > 0$$

where ρ is given by (5.5). Due to the complex nature of these conditions, it is difficult to comment on the nature of the stability of the non-trivial equilibrium solution. Figure (4) indicates the several solution branches of ρ , which are given by:

$$\rho^- = -\frac{b}{2a} - \frac{\sqrt{b^2 - 4ac}}{2a} \quad (6.2)$$

$$\rho^+ = \left(-\frac{b}{2a} + \frac{\sqrt{b^2 - 4ac}}{2a}\right) | b < 0, c > 0 \quad (6.3)$$

$$\rho^{+1} = \left(-\frac{b}{2a} + \frac{\sqrt{b^2 - 4ac}}{2a}\right) | b < 0, c < 0 \quad (6.4)$$

$$\rho^{+2} = \left(-\frac{b}{2a} + \frac{\sqrt{b^2 - 4ac}}{2a}\right) | b > 0, c < 0 \quad (6.5)$$

Clearly, the lower branch (ρ^-) violates N4, which requires:

$$\rho > -\frac{b}{2a}$$

Thus ρ^- is an unstable branch of the non-trivial equilibrium solution. It can be shown that ρ^+ and ρ^{+1} branches are unstable since they violate the sufficiency condition (N5). Numerically it can easily be checked that part of ρ^{+2} equilibrium branch satisfies all five conditions of stability (N1 to N5). The complexity of the computations hinders the calculation of the stable part of ρ^{+2} equilibrium branch, analytically. Sometimes the fourth condition (N4) can provide important information about the stability of the non-trivial equilibrium solution branches.

7. BIFURCATION ANALYSIS

In this section we describe the bifurcation behavior associated with Eqs (4.1). The steady state solutions of (4.1) represent periodic solutions of the original system. In this system, several codimension 1 and codimension 2 bifurcation varieties are detected along with a codimension 3 singularity. One is referred to

Namachchivaya and Malhotra (1992) for a detailed description of the necessary conditions for the different bifurcation varieties to exist. Following is a brief description of each of these bifurcation varieties that are detected in our system (4.1):

7.1. Simple Bifurcation:

This bifurcation variety occurs when one of the eigenvalues of the linear operator L passes through zero. When this happens, the condition T2 is violated. Under these conditions, the trivial solution loses its stability and a non-trivial solution with $\rho > 0$ bifurcates from the trivial solution. For fixed values of β, λ and gb , condition T2 can be depicted as a circle (\mathbb{S}) in the parameter space (v_1, v_2) , as shown in Fig. (1). Along any generic path transverse to \mathbb{S} , the stable trivial solution would lose its stability (provided T1 and T3 are satisfied) through simple bifurcation, when the following condition is satisfied:

$$(v_1 + v_{10})^2 + (v_2 + v_{20})^2 = gb^2 \quad (7.1)$$

When the linear operator L has a zero eigenvalue, the system (4.1) can be reduced to its corresponding one dimensional center manifold. If we fix β, λ, gb and v_1 at $-0.5, 0.1, 0.5$ and 0.0 , respectively, the one dimensional manifold, in terms of the nonlinear coefficients (c_2 and d_2) and the perturbation parameter $\eta_2 = v_2 - v_{2cr}$, is given as:

at $v_{2cr} = -0.484446$,

$$w = w [2.13 \eta_2 - 19.98 \eta_2^2 + (c_2 + 1.76 d_2) w^2]$$

and,

at $v_{2cr} = 0.484446$,

$$w = w [-1.49 \eta_2 - 6.97 \eta_2^2 + (c_2 - 1.8 d_2) w^2]$$

It can be easily verified that the nature of the non-trivial equilibrium branches, as captured by these center manifold equations, agrees qualitatively with the numerical results (Fig. 7).

7.2. Hopf Bifurcation:

This bifurcation variety occurs when condition T3 is violated, i.e.:

$$v_2^2 = -v_{30} v_1 + v_{40} \quad (7.2)$$

provided T1 and T2 are satisfied. In this case, the linear operator L has a pair of pure imaginary eigenvalues with nonzero imaginary part at the critical value of the parameters. This bifurcation variety occurs along a generic path transverse to the curve \mathcal{H} , which is depicted as parabola in the parameter space (v_1, v_2) , as shown in Fig. (1), provided other stability conditions are satisfied. The dynamics of the system (4.1) can be studied on a two dimensional center manifold. Once again, for the same values of β, λ, gb and v_1 , the corresponding two dimensional center manifold can be expressed as:

A. at $v_{2cr} = -0.705354$,

$$\begin{aligned} \dot{r} &= r [(0.5 \eta_1 - 0.7 \eta_2) + (3.8 c_2 - 7.18 d_2) r^2 + \dots] \\ \dot{\theta} &= [0.426 + (-0.5 \eta_1 - 0.8 \eta_2) + (-4.2 c_2 - 8.45 d_2) r^2 + \dots] \end{aligned}$$

B. at $v_{2cr} = 0.705354$,

$$\begin{aligned} \dot{r} &= r [(0.5 \eta_1 + 0.7 \eta_2) + (2.86 c_2 + 4.8 d_2) r^2 + \dots] \\ \dot{\theta} &= [0.568 + (-0.5 \eta_1 + 0.6 \eta_2) + (-2.7 c_2 + 4.1 d_2) r^2 + \dots] \end{aligned}$$

where η_1 and η_2 are the perturbations in the critical values of v_1 and v_2 . One can easily observe that the periodic equilibrium branches, as described by these center manifold equations, have the same dynamical behavior as observed numerically, in the neighborhood of the critical value of the bifurcation parameter v_2 (Fig. 7).

7.3. Bogdanov-Takens Bifurcation:

Now we study the possibility of the intersections of two codimension 1 bifurcation varieties, the simple bifurcation \mathbb{S} and the Hopf bifurcation \mathcal{H} . At this intersection (\mathbb{C}_2) we have two eigenvalues of the linear operator L , becoming zero, where \mathbb{C}_2 is defined by:

$$4\beta v_1 + 2\lambda v_2 - \beta(4\beta^2 + \lambda^2) = 0 \quad (7.3a)$$

$$(v_1 + v_{10})^2 + (v_2 + v_{20})^2 = gb^2 \quad (7.3b)$$

These equations lead to the following two critical points in (v_1, v_2) parameter space.

$$\begin{aligned} v_{1cr} &= -v_{10} \pm \frac{gb\lambda}{\sqrt{(4\beta^2 + \lambda^2)}}, \\ v_{2cr} &= -v_{20} \pm \frac{2gb\beta}{\sqrt{(4\beta^2 + \lambda^2)}} \end{aligned} \quad (7.3c)$$

At each of these critical points the linear operator can be brought to the following form:

$$L_{cr} = \begin{bmatrix} 0 & 1 & 0 & 0 \\ 0 & 0 & 0 & 0 \\ 0 & 0 & \lambda_3 & 0 \\ 0 & 0 & 0 & \lambda_4 \end{bmatrix} \quad (7.3d)$$

where λ_3 and λ_4 represent the two stable eigenvalues of L at the critical points (7.3c). Dynamics near this nonhyperbolic fixed point can be studied by examining the equations defined on a two dimensional center manifold. The procedure to reduce the four dimensional system to the corresponding two dimensional center manifold is fairly systematic. Once the reduction to the two dimensional center manifold is achieved, we obtain the corresponding truncated normal form (Gamero et al. (1991)) Now we compare our system with a similar system studied by Takens (1974), which is as following:

$$\begin{aligned} \dot{w}_1 &= w_2 \\ \dot{w}_2 &= \alpha_1 w_1 + \alpha_2 w_2 + a_3 w_1^3 + b_3 w_1^2 w_2 \end{aligned}$$

where α_1 and α_2 are the unfolding parameters, w_1 and w_2 are the two dimensional center manifold, and a_3 and b_3 are the nonlinear coefficients. Considerable research has already been done on this bifurcation variety. Guckenheimer and Holmes (1983) discuss the details on the global bifurcation behavior associated with this class of bifurcation.

If we fix β , λ and gb at -0.5 , 0.1 and 0.5 respectively, the linear operator (4.3) has double zero eigenvalues at the following critical parameter values of v_1 and v_2 :

$$A. \quad v_{1cr} = 0.29725, \quad v_{2cr} = 0.44752$$

If η_1 and η_2 are the small perturbations in v_{1cr} and v_{2cr} , then the corresponding values of α_1 , α_2 , a_3 and b_3 are given in terms of η_1 and η_2 and the original nonlinear coefficients c_2 and d_2 , in the following manner:

$$\begin{aligned} \alpha_1 &= -0.11 \eta_1 - 1.09 \eta_2, & \alpha_2 &= 0.97 \eta_1 - 1.4 \eta_2 \\ a_3 &= -0.134 c_2 - 1.34 d_2, & b_3 &= 6.26 c_2 + 8.28 d_2 \end{aligned}$$

For $c_2 = 1$ and $d_2 = 1$, $a_3 < 0$ and $b_3 > 0$, the magnitude

of a_3 and b_3 can be scaled to unity by rescaling other variables. For positive values of v_2 , as v_2 is varied from zero for a fixed value of v_1 , we obtain the phase portraits 6, 7, 8, 9, 10 and 11 as indicated in Fig. (5), these show various local and global bifurcations and completely agree with the numerical results presented in the next section.

$$B. \quad v_{1cr} = 0.19775, \quad v_{2cr} = -0.54752$$

The corresponding values of α_1 , α_2 , a_3 and b_3 are given as following:

$$\begin{aligned} \alpha_1 &= 0.1 \eta_1 + 0.9 \eta_2, & \alpha_2 &= 0.8 \eta_1 - 1. \eta_2 \\ a_3 &= 0.1 c_2 + 0.7 d_2, & b_3 &= 2.6 c_2 - 4.15 d_2 \end{aligned}$$

For $c_2 = 1$ and $d_2 = 1$, $a_3 > 0$ and $b_3 < 0$, the magnitude of a_3 and b_3 can be scaled to unity as before by rescaling other variables. For the negative values of v_2 , once again as v_2 is varied from zero for a fixed value of v_1 , we obtain the phase portraits 5, 4, 3, 2 and 1 as shown in Fig. (5). Thus combining these two cases we can construct partially the bifurcation diagram for the original problem.

Depending upon the values of a_3 and b_3 , two distinct cases of unfolding (i.e., I: $a_3 > 0$, $b_3 < 0$ and II: $a_3 < 0$, $b_3 < 0$) are possible for this bifurcation variety. As mentioned before, these two cases are completely studied by Takens (1974) and Guckenheimer and Holmes (1983). The other two cases (Ic: $a_3 > 0$, $b_3 > 0$ and IIc: $a_3 < 0$, $b_3 > 0$) can be constructed from I and II by reversing the sign of w_2 , α_2 and time. Table 1 shows the possible cases of unfoldings that can occur for all possible combinations of c_2 and d_2 , near the two codimension 2 bifurcation points A and B.

Table 1

Case	Possible unfolding (A)	Possible unfolding (B)
$c_2 > 0, d_2 > 0$	II ^c	I, I ^c
$c_2 = 0, d_2 > 0$	II ^c	I
$c_2 > 0, d_2 < 0$	I, I ^c , II ^c	I ^c , II ^c
$c_2 = 0, d_2 < 0$	I	II ^c
$c_2 < 0, d_2 > 0$	I, II, II ^c	I, II
$c_2 > 0, d_2 = 0$	II ^c	I ^c
$c_2 < 0, d_2 < 0$	I	II, II ^c
$c_2 < 0, d_2 = 0$	I	II

7.4. Simple and Hopf Bifurcation Variety:

In this case, the linear operator has a simple zero eigenvalue along with a pair of pure imaginary eigenvalues for some critical value of the parameters. Following are the requirements for the simultaneous existence of simple and Hopf bifurcation varieties:

$$(v_1 + v_{10})^2 + (v_2 + v_{20})^2 = gb^2 \quad (7.4a)$$

$$4\beta v_1 - 2\lambda v_2 - \beta(20\beta^2 + \lambda^2) = 0 \quad (7.4b)$$

$$v_1 < \left(3\beta^2 + \frac{\lambda^2}{4}\right) \quad (7.4c)$$

These conditions lead to the following critical point in (v_1, v_2) parameter space:

$$v_{1cr} = \left(5\beta^2 - \frac{\lambda^2}{4}\right) + \beta\lambda \sqrt{\frac{gb^2}{\beta^2(4\beta^2 + \lambda^2)} - 4} \quad (7.4d)$$

$$v_{2cr} = -\beta\lambda + 2\beta^2 \sqrt{\frac{gb^2}{\beta^2(4\beta^2 + \lambda^2)} - 4}$$

At the critical point, the system can be reduced to its three dimensional center-manifold and the linear operator assumes the following form:

$$L_{cr} = \begin{bmatrix} 0 & -\omega & 0 \\ \omega & 0 & 0 \\ 0 & 0 & 0 \end{bmatrix} \quad (7.4e)$$

The structure of the linear operator completely determines the normal form for the linear and nonlinear parts of the three dimensional center-manifold equations. If we fix β, λ and gb at -0.1, 0.1 and 0.5 respectively then the resulting normal form, in cylindrical co-ordinates is given as:

$$\begin{aligned} \dot{r} &= r(\mu_1 + a_{11}r^2 + a_{12}z^2) + \text{h.o.t.} \\ \dot{z} &= z(\mu_2 + a_{21}r^2 + a_{22}z^2) + \text{h.o.t.} \\ \dot{\theta} &= \omega + \text{h.o.t.} \end{aligned} \quad (7.4f)$$

where,

$$\begin{aligned} \mu_1 &= 0.04\eta_1 + 0.95\eta_2 \\ \mu_2 &= 2.2\eta_1 - 5.6\eta_2 \\ a_{11} &= 0.58c_2 + 3.42d_2 \\ a_{12} &= -5.64c_2 + 68.15d_2 \end{aligned}$$

$$\begin{aligned} a_{21} &= 4.72c_2 - 42.66d_2 \\ a_{22} &= 55.84c_2 - 142.25d_2 \\ \omega &= 0.64 \end{aligned}$$

μ_1 and μ_2 are the unfolding parameters that are expressed in terms of η_1 and η_2 which represent the perturbations in the values of v_1 and v_2 from their critical values. i.e.,

$$\eta_1 = v_1 - v_{1cr}, \quad \eta_2 = v_2 - v_{2cr}$$

where $v_{1cr} = -0.175$, $v_{2cr} = 0.455$, and a_{ij} 's, the nonlinear coefficients of the the normal form, are given in terms of nonlinear coefficients c_2 and d_2 .

We notice that the θ equation is decoupled from the r and z equations, so we can study the planar system (r, z) independent of θ and later interpret the results for the full three dimensional system (r, θ, z) . A rescaling procedure can be applied to the first two equations of 7.4f to bring these to the form described in Guckenheimer and Holmes (1983). After rescaling, these equations up to third order are expressed as:

$$\begin{aligned} \dot{r} &= r(\mu_1 + r^2 + b z^2) \\ \dot{z} &= z(\mu_2 + c r^2 + d z^2) \end{aligned} \quad (7.4g)$$

where $d = \pm 1$, $b = \frac{a_{12}}{|a_{22}|}$ and $c = \frac{a_{21}}{|a_{11}|}$

This system has been studied by Takens(1974), Langford and Iooss (1980) and Holmes (1980). In this work, we use the same numbering scheme as given in Guckenheimer and Holmes (1983). They classify 12 different cases of distinct unfoldings. Table 2 shows the possible cases of unfoldings that can occur for all possible combinations of c_2 and d_2 , the nonlinear coefficients of our original normal form equations.

Table 2

Case	Possible unfoldings
$c_2 > 0, d_2 > 0$	Ia, Ib, II, III, V, VIa, VIb, VIIa, VIIb
$c_2 = 0, d_2 > 0$	II, VIa, VIb
$c_2 > 0, d_2 < 0$	III, VIIa, V
$c_2 = 0, d_2 < 0$	III, VIIa, VIIb
$c_2 < 0, d_2 > 0$	II, VIa, VIb
$c_2 > 0, d_2 = 0$	III, VIIa, VIIb
$c_2 < 0, d_2 < 0$	II, III, IVa, IVb, VIa, VIb, VIIa, VIIb, VIII
$c_2 < 0, d_2 = 0$	II, VIa, VIb

If we start with system (7.4g) and consider the case where

$c_2 = d_2 = 1.0$, one can easily notice that the resulting system corresponds to VIa class of unfolding. The bifurcation set and the associated phase portraits for this class of unfolding are discussed in the literature. When viewed for full three dimensional flow of Eq. (7.4f), these results qualitatively match with the phase portraits obtained by numerically integrating the original normal form equations (Eqs (4.1)) near the relevant parameter values.

7.5. Double Hopf Bifurcation Variety:

Now we consider the case where the linear operator L has two pairs of identical purely imaginary eigenvalues. The conditions for this codimension 2 bifurcation variety can be simplified to the following:

$$\lambda = 0, \beta = 0, v_1 < 0, v_2 = \pm gb \text{ and } v_1^2 + v_2^2 > gb^2 \quad (7.5a)$$

Under these conditions, the linear operator takes the following form:

$$L_H = \begin{bmatrix} 0 & 0 & 1 & 0 \\ 0 & 0 & 0 & 1 \\ (v_1 + gb) & -v_2 & 0 & 0 \\ v_2 & (v_1 - gb) & 0 & 0 \end{bmatrix} \quad (7.5b)$$

Whether L_H will have the semisimple structure or non-semisimple, depends upon the value of gb . For the stability of the trivial solution, we require $\beta < 0$, if $\beta = -\epsilon$, where $0 < \epsilon \ll 1$, the typical bifurcation diagram for this case is presented in Fig. (6). Along a path, transverse to \mathcal{H}_2 , the trivial solution loses its stability through double Hopf bifurcation as $\beta \rightarrow 0$. In fact $v_2 = \pm gb$ is the degenerate form of the \mathcal{H} curve as $\beta \rightarrow 0$ and $\lambda \rightarrow 0$.

$$\mathcal{H}: v_2^2 = -v_{30}v_1 + v_{40} \quad (7.5c)$$

As $\beta \rightarrow 0$ and $\lambda \rightarrow 0$, we have $v_{30} \rightarrow 0$ and $v_{40} \rightarrow gb^2$, thus $v_2 = \pm gb$.

7.6. Bogdanov-Takens and Hopf Bifurcation:

Along with the assortment of codimension 1 and codimension 2 bifurcation varieties, we may also have the case where the linear operator has a pair of zero eigenvalues along with a pair of pure imaginary eigenvalues. This codimension 3 bifurcation variety has not been studied in detail. The conditions for the linear operator L to go through this bifurcation variety are as following:

$$\beta < 0, \lambda = 0, v_1 = \beta^2 \text{ and } v_2 = \pm gb \quad (7.6)$$

This is also a degenerate bifurcation variety (\mathcal{C}_3). Along a path through \mathcal{C}_3 , the trivial solution may lose its stability through $(0, 0, \pm i)$ bifurcation variety.

The trivial solution may lose its stability in one of the many ways mentioned in this section, giving rise to a non-trivial steady state branch or a periodic equilibrium branch of solutions. The non-trivial equilibrium may also lose its stability through a secondary bifurcation. The secondary hopf bifurcation occurs when condition N5 is violated. In this case a secondary equilibrium branch of periodic solutions is generated. These periodic branches may lose their stability after going through a period doubling or homoclinic bifurcation, which may lead to chaotic behavior. The other bifurcation varieties (of higher codimension) are also possible, but those are not considered here.

8. NUMERICAL SIMULATIONS

Numerical computations were performed in order to verify the results obtained in the previous sections and to study in more detail the various bifurcation varieties and the structure of the periodic orbits. The numerical simulations were carried out using AUTO, a software package for continuation and bifurcation problems in ordinary differential equations. The structure of the periodic orbits was studied in detail using CHAOS, a versatile software for simulating nonlinear systems. These numerical simulations were very helpful in confirming the bifurcation behavior obtained through analysis and in providing a substantial clue for the new phenomena, which were global in nature and not detected through the theoretical analysis. The parameter regions where period doubling or chaos may occur, were located as a result of these simulations.

Figure (7) shows the 1-parameter bifurcation diagram for the normal form Eqs (4.2). In this diagram the coordinate y_1 is shown vs. v_2 , as v_2 is varied between -1.0 and 1.0, while β, v_1, λ and gb are fixed at -0.5, 0.0, 0.1 and 0.5, respectively. The nonlinear coefficients c_2 and d_2 are fixed at 1.0. By changing the sign of either c_2 or d_2 , the orientation and the nature of the stability of the non-trivial equilibrium and periodic branches change, but the bifurcation behavior remains qualitatively similar for codimension 1 bifurcation variety. In these diagrams the solid (dashed) curves represent the stable (unstable) branches.

(unstable) stationary solutions, solid (open) circles represent stable (unstable) periodic orbits and solid (open) squares represent Hopf (Simple) bifurcation varieties. As v_2 is increased from -1.0, the unstable trivial equilibrium branch first gains stability through a Hopf bifurcation (at label 2), which results in a equilibrium branch of stable periodic solutions. The trivial solution loses its stability through a simple bifurcation and results in an unstable non-trivial steady state equilibrium branch (at label 3). As v_2 is increased further, the trivial branch of equilibrium goes through a Simple and a Hopf bifurcation and results in a stable steady state branch (at label 4) and an unstable periodic branch of equilibrium solutions (at label 5). This non-trivial equilibrium branch loses its stability through a secondary Hopf bifurcation and gives rise to a secondary branch of stable periodic solutions. This matches identically with what has already been shown in Fig. 1, 2a and 4 of the previous section.

The periodic branch (through label 2) approaches the unstable non-trivial equilibrium branch and loses its stability by going through a homoclinic bifurcation. The transition from the stable periodic orbit to the homoclinic orbit is clearly visible in Fig. (8 a & b). The labels in this diagram (Fig. 8) correspond to the labels in Fig. (7). The unstable periodic branch (at label 5) rises up and tends to approach the unstable non-trivial equilibrium branch, but it merges with the secondary branch of stable periodic solutions (through label 11). A very interesting phenomenon is observed just before the merger. The unstable periodic branch (through label 5) goes through a cascade of period doubling bifurcation, which eventually leads to chaos (Fig. (9)). Precisely at the merging point a homoclinic orbit is observed (Fig. (8d)). This homoclinic bifurcation is due to the proximity of Bogdanov-Takens bifurcation point. The lower branch of the non-trivial equilibrium solution (through label 4) also loses its stability through a secondary bifurcation, which results in a symmetry breaking stable periodic branch, which rises up and goes through a period doubling bifurcation near the unstable trivial solution branch and ends with the period becoming very large.

To study the period doubling sequence and the possibility of chaos, computations were performed using CHAOS near the point where the change in stability occurs for the global periodic branch (from label 5). These computations were performed for the same values of parameters, except v_1 was set at 0.1 to get closer to the

region where the Bogdanov Takens bifurcation occurs. At $v_2 = 0.3589$, one stable periodic orbit is seen, which goes through a period doubling bifurcation at $v_2 = 0.35882$ (Fig. (9a & b)). These periodic branches go through a cascade of period doubling bifurcation sequences, and finally become chaotic at $v_2 = 0.35875$ (Fig. 9e & f). This chaotic behavior quickly changes into a regular two period orbit structure, which also goes through period doubling sequence and leads to another chaotic attractor (at $v_2 = 0.35855$).

Now, in order to study the bifurcation behavior near $(0, +i, -i)$ singularity, we fix β , v_1 , λ and gb at -0.1, -0.3, 0.1 and 0.5 respectively, while fixing c_2 and d_2 at 1.0. As noted in the previous section, this singularity occurs at $(v_{1cr} = -0.175, v_{2cr} = 0.455)$. In this case (Fig. (10)), the steady state bifurcation behavior is similar to what had been observed earlier, but the nature of the periodic solutions which result due to secondary hopf bifurcation, is different. Both the periodic branches (through labels 4 and 6) lose their stability after going through a period doubling bifurcation. Figure (11a-e) shows the phase portraits near the v_2 values where the period doubling sequence occurs, and finally the flow becomes chaotic at $v_2 = -0.352$.

To conclude, the numerical results confirm the rich variety of local bifurcation behavior observed analytically. Codimension 1 and codimension 2 bifurcation varieties are observed in numerical simulations. In addition the numerical simulation exhibits breaking of the homoclinic orbits, change in stabilities, rich periodic behavior and the period doubling cascade leading to chaos. These bifurcation diagrams give a clue to study the global bifurcation behavior that is associated with the Bogdanov-Takens and $(0, +i, -i)$ bifurcation varieties, which were described in the previous section.

9. CONCLUSIONS AND DIRECTIONS FOR FUTURE RESEARCH

In this study, we analyze the stability and bifurcation behavior of a parametrically excited, four dimensional nonlinear system under the combined conditions of one to one internal and subharmonic parametric resonance. The stability properties of the trivial and non-trivial solutions of the 5-parameter family of normal form equations were investigated and various codimension 1, 2 and 3 bifurcation varieties were

located. The reduced fourth order system may have 2, 1 or 0 non-trivial equilibrium solutions depending upon the parameter values. These steady state solutions extend to the periodic orbits which are the relative equilibria of the original four dimensional normal form. The global bifurcation behavior associated with double zero and $(0, +i, -i)$ eigenvalues is also investigated and it matches identically with the numerical results. The complete analysis of the global bifurcation behavior for this system is currently in progress. The numerical results indicate homoclinic bifurcation along with an interesting sequence of period doubling bifurcation which leads to chaotic behavior. These issues also need further investigation.

ACKNOWLEDGEMENTS

This research was partially supported by AFOSR through Grant 91-0041 and the National Science Foundation through Grant MSS 90-57437 PYL.

REFERENCES

1. Arnold, V. I., 1983, *Geometric Methods in the Theory of Ordinary Differential Equations*, Springer-Verlag, New York.
2. Aronson, J. W., 1991, CHAOS: A SUN based program for analyzing chaotic systems, *Programmers Guide*, College Park, Maryland.
3. Caprino, S., Maffei, C., and Negrini, P., 1984, "Hopf Bifurcation with 1:1 resonance," *Nonlin. Anal. Theor. Meth. Appl.*, Vol. 8, pp. 1011-1032.
4. Carr, J., 1981, *Applications of Center Manifold Theory*, Applied Mathematical Sciences, Vol. 35, Springer-Verlag, New York.
5. Chow, S. N., and Wang, D., 1986, "Normal Forms of Bifurcating Periodic Orbits," *Contemporary Mathematics*, Vol. 56, pp. 9-18.
6. Doedel, E. J., and Kernevez, J. P., 1986, AUTO: Software for Continuation and Bifurcation Problems in Ordinary Differential Equations, *AUTO 86 User Manual*, California.
7. Feng, Z. C., and Sethna, P. R., 1990, "Global Bifurcation and Chaos in parametrically forced Systems with one-one resonance," *Dynamics and Stability of Systems*, Vol. 5, pp. 201-225.
8. Gamero, E., Freire, E., and Ponce, E., 1991, "Normal Forms for Planner Systems with Nilpo Linear Part," *International Series of Numerical Mathematics*, Vol. 97, pp. 123-127.
9. Guckenheimer, J., and Holmes, P. J., 1983, *Dynamical Systems and Bifurcations of Vector Fields*, Springer-Verlag, New York.
10. Holmes, P. J., 1981, "Center manifolds, normal forms and bifurcations of vector fields with applications to coupling between periodic steady motions," *Physica 2D*, pp. 449-481.
11. Krupa, M., 1986, "On 1:1 Resonant Hopf Bifurcation," M. Sc. Thesis, University of Waterloo, Canada.
12. Langford, W. F., 1979, "Periodic and steady state mode interactions lead to tori," *SIAM J. A Math.*, Vol. 37, No. 1, pp. 22-48.
13. Langford, W. F., and Iooss, G., 1980, "Interact of hopf and pitchfork bifurcations," In *Bifurcation Problems and their Numerical Solution*, Herausgegeben von, H. D. Mittelmann and Weber, eds., Birkhauser Verlag Basel, pp. 103-117.
14. Meyer, K. R., 1984, "Normal Forms for the Generalized Hopf Bifurcation," *Funkcialaj Ekvacioj* 27, pp. 261-277.
15. Namachchivaya, N. Sri, and Ariratham, S., 1990, "Periodically Perturbed Hopf Bifurcation," *SIAM Journal of Applied Mathematics*, Vol. 47, pp. 15-27.
16. Namachchivaya, N. Sri, Doyle, M. M., Langford, W. F., and Evans, N., 1992, "Normal Form for Generalized Hopf Bifurcation With Non-semisimple 1:1 Resonance," (in preparation).
17. Namachchivaya, N. Sri, and Malhotra, N., 1991, "Parametrically Excited Hopf Bifurcation With Non-semisimple 1:1 Resonance: Local and Global Analysis," (in preparation).
18. Namachchivaya, N. Sri, and Tien, W. M., 1990, "Bifurcation Behavior of Nonlinear Pipes Conveying Pulsating Flow," *Journal of Fluids and Structures* 3, pp. 609-629.
19. Takens, F., 1974, "Forced Oscillations and Bifurcations," *Comm. Math. Inst., Rijksuniversiteit Utrecht*, 3, pp. 1-59.
20. van Gils, S. A., Krupa, M., and Langford, W. F., 1990, "Hopf Bifurcation with non-semisimple resonance," *Nonlinearity* 3, pp. 825-850.
21. Wiggins, S., 1990, *Introduction to Applied Nonlinear Dynamical Systems and Chaos*, Springer-Verlag, New York.

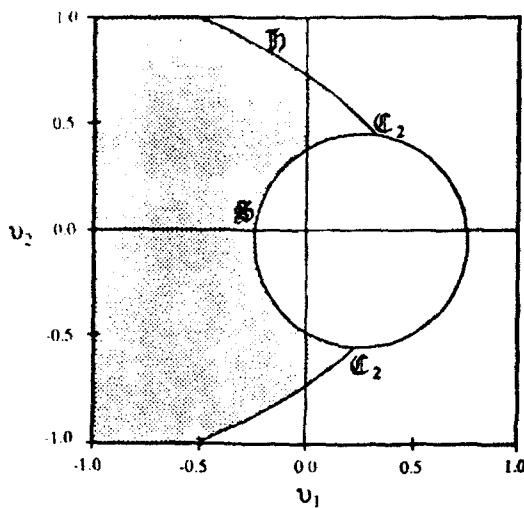


Fig. 1: Stability boundary for the trivial solution (for $\beta = -0.5$, $\lambda = 0.1$ and $gb = 0.5$). The shaded part indicates the stable region. S , H and C_2 indicate the simple, Hopf and Bogdanov-Takens bifurcation varieties respectively.

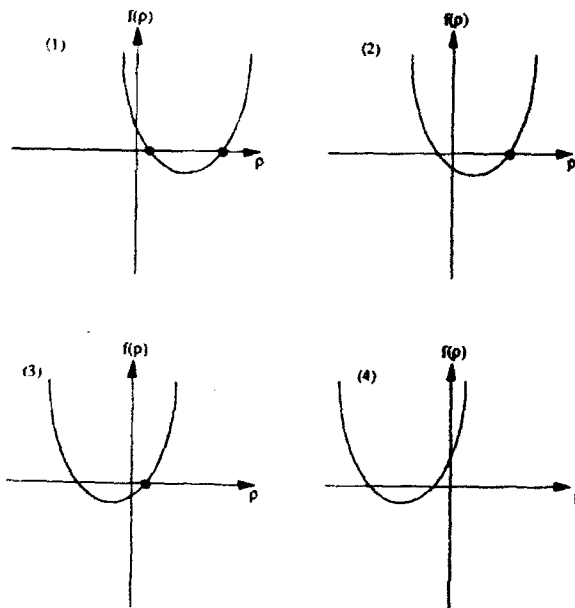


Fig. 3: Graph of $f(p)$ vs. p . Various possibilities are shown for the existence of non-trivial equilibrium solutions of r for the nondegenerate case (i.e., $a > 0$). (1). $b < 0$, $c > 0$, $D > 0$, (2). $b < 0$, $c < 0$, (3). $b > 0$, $c < 0$, (4). $b < 0$, $c > 0$, $D < 0$. (The dot indicates the possible non-trivial steady state solution.)

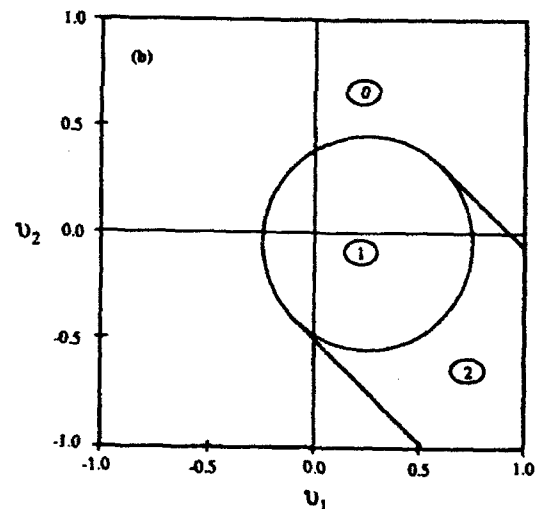
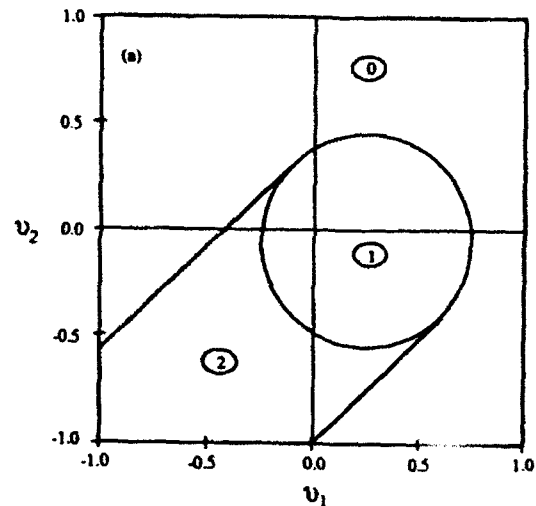


Fig. 2: Existence of the non-trivial steady state solutions for $\beta = -0.5$, $\lambda = 0.1$, $gb = 0.5$ and (a) $c_2 = 1$, $d_2 = 1$. (b) $c_2 = -1$, $d_2 = 1$. The number inside the small ellipse indicates the possible number of non-trivial equilibrium solutions that may exist in that region.

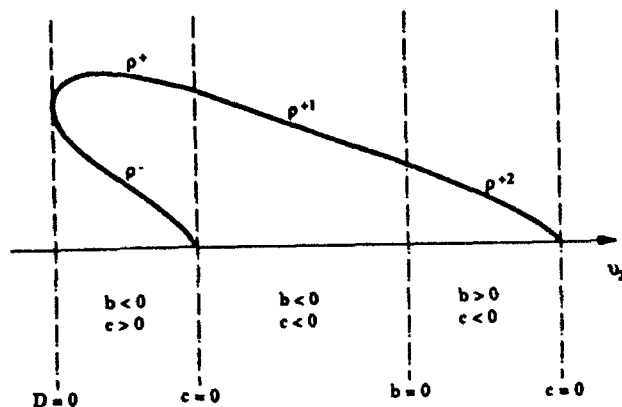


Fig. 4: Curve showing various branches of the non-trivial equilibrium solution for different combinations of b and c , as v_2 is varied from -1.0 to 1.0.

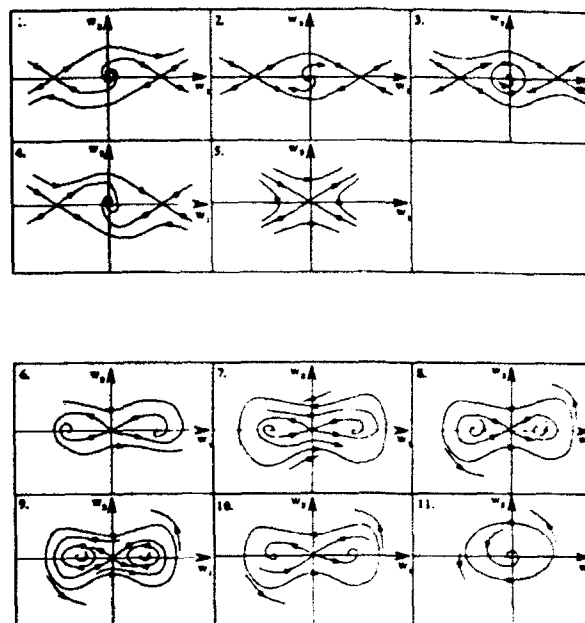


Fig. 5: Contd...

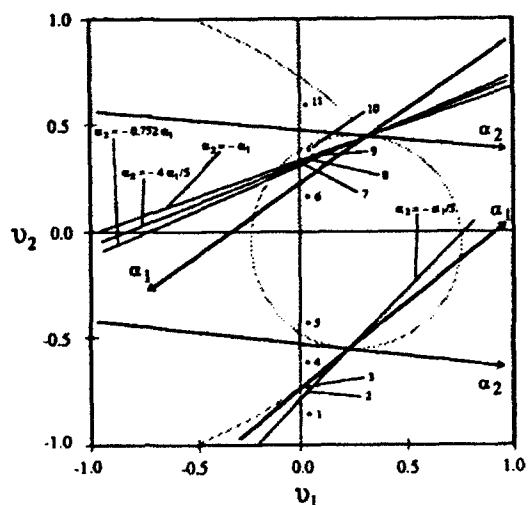


Fig. 5: Global bifurcation set corresponding to Bogdanov-Takens bifurcation variety.

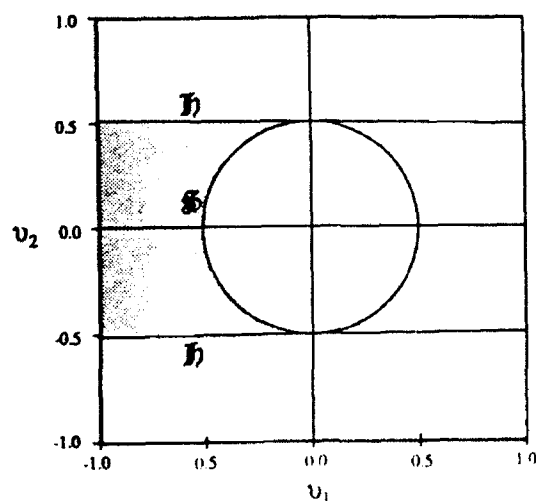


Fig. 6: Stability boundary for the trivial solution for $\beta = -0.005$, $\lambda = 0.0$ and $gb = 0.5$. The shaded part indicates the stable region. The Hopf variety (H_1) leads to the Double Hopf bifurcation variety (H_2) as $\beta \rightarrow 0$.

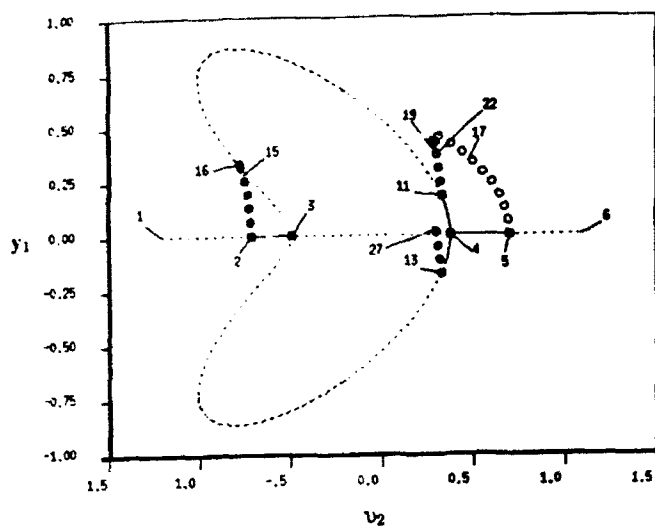


Fig. 7: Response y_1 as a function of v_2 ; $\beta = -0.5$, $\lambda = 0.1$, $gb = 0.5$, $v_1 = 0.0$.

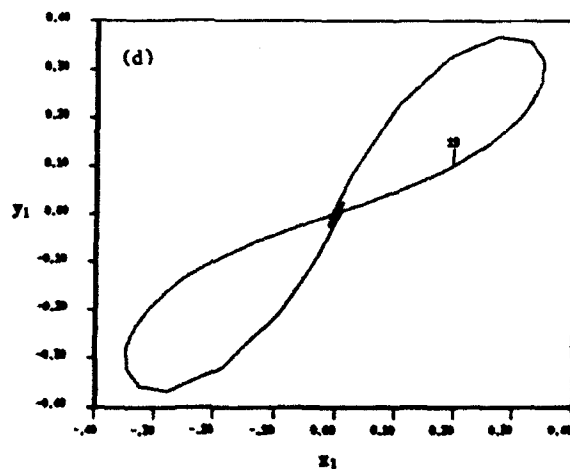
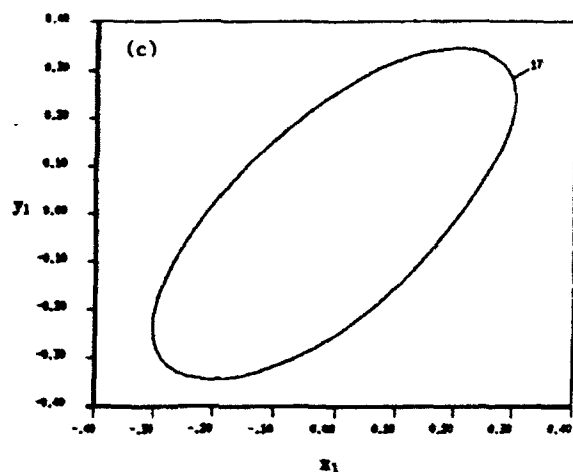
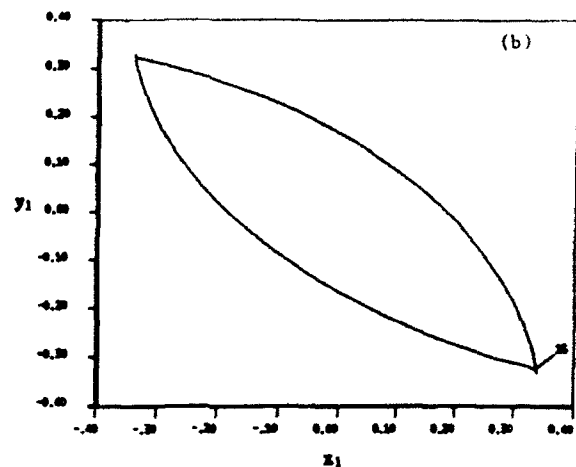
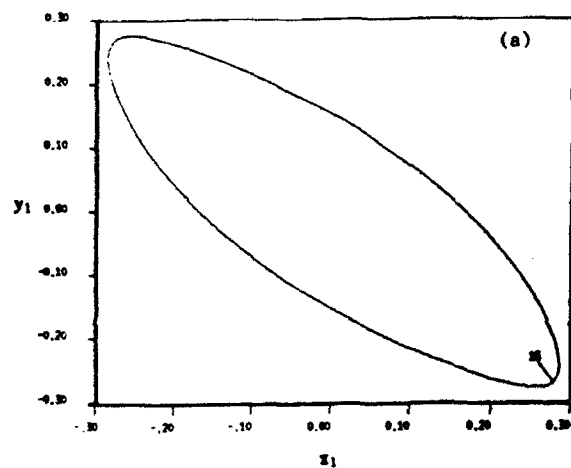


Fig. 8: Phase plane trajectories (x_1 - y_1) for the selected orbits of Fig. 6. The labels in this diagram correspond to their respective positions in the bifurcation diagram (Fig. 6).

Fig. 8: Contd...

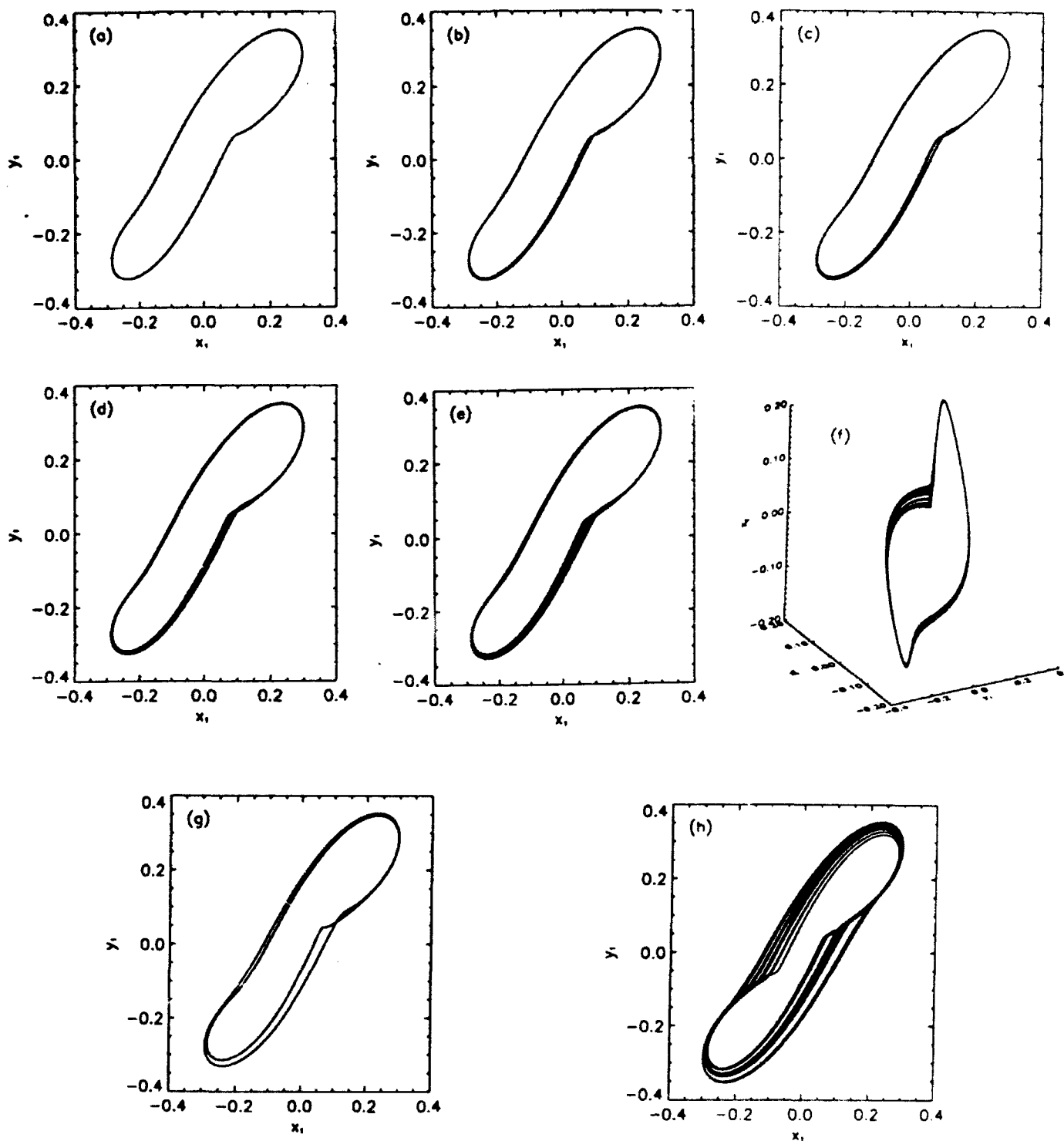


Fig. 9: Phase plane trajectories (x_1 - y_1) for various values of v_2 ; $\beta = -0.5$, $\lambda = 0.1$, $gb = 0.5$, $v_1 = 0.1$, (a) $v_2 = 0.3589$, (b) $v_2 = 0.35882$, (c) $v_2 = 0.3588$, (d) $v_2 = 0.358785$, (e) $v_2 = 0.35875$, (f) Same as (e) but in $(x_2$ - y_1 - y_2) plane, (g) $v_2 = 0.3586$, (h) $v_2 = 0.35855$

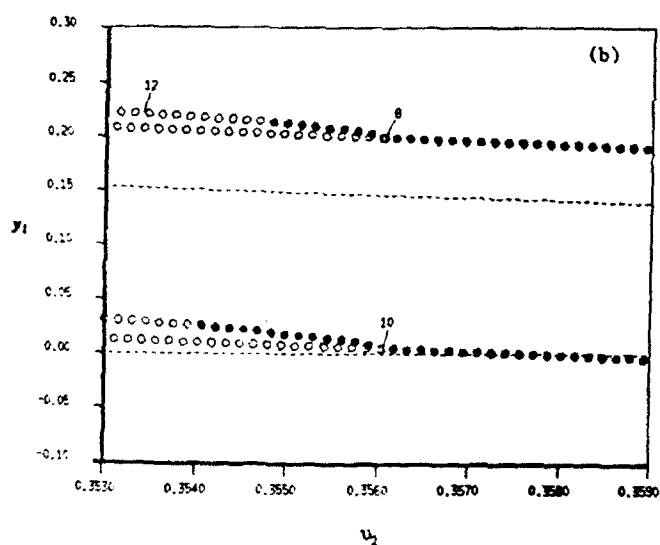
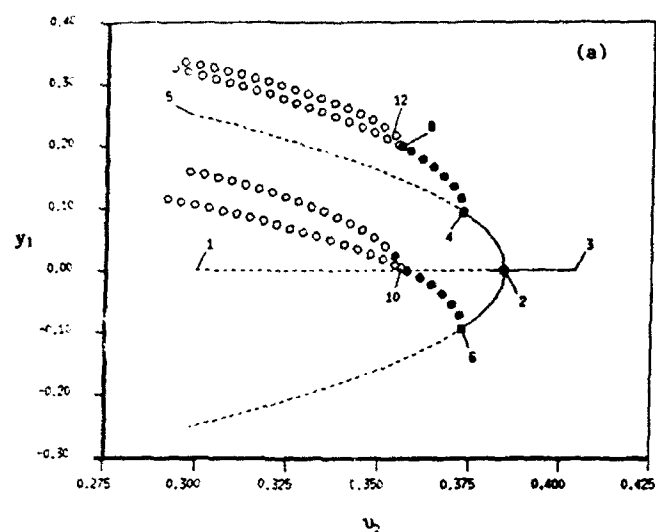


Fig. 10: (a). Response y_1 as a function of v_2 ; $\beta = -0.1$, $\lambda = 0.1$, $gb = 0.5$, $v_1 = -0.3$. (b) Same as (a) but near the parameter region where the period doubling occurs.

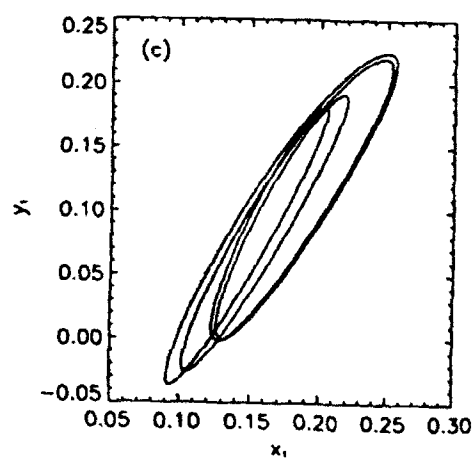
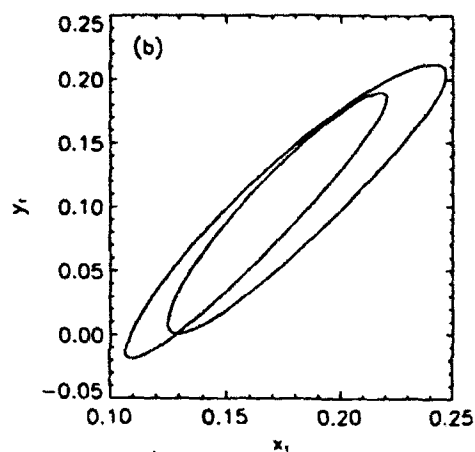
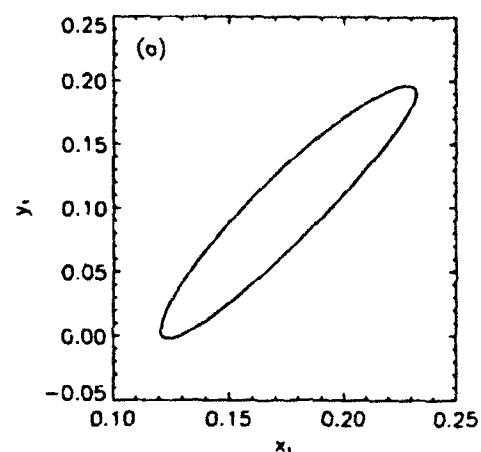


Fig. 11: Phase plane trajectories $(x_1 - y_1)$ for various values of v_2 for the upper periodic branch of Fig. 10. ($\beta = -0.1$, $\lambda = 0.1$, $gb = 0.5$, $v_1 = -0.3$), (a) $v_2 = 0.357$, (b) $v_2 = 0.355$, (c) $v_2 = 0.353$, (d) $v_2 = 0.352$, (e) Same as (d) but in $(y_1 - y_2 - x_2)$ plane.

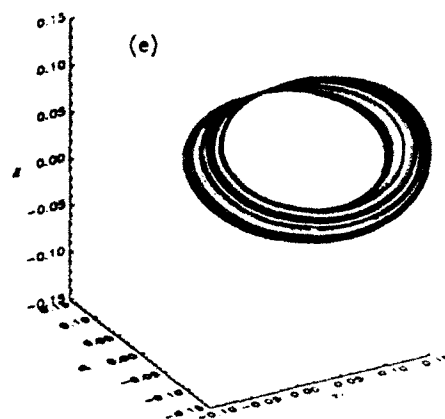
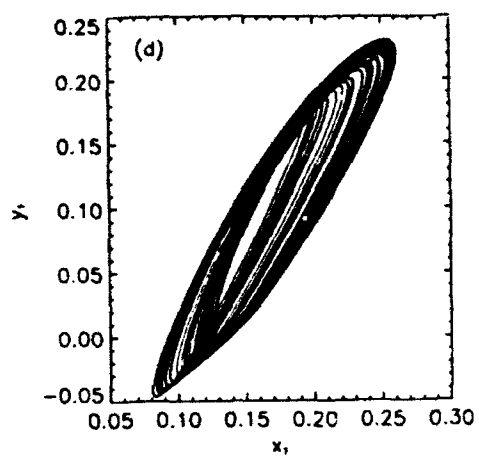


Fig. 11: Contd...

G. Leng

N. Sri Namachchivaya

Mem. ASME

S. Talwar

Department of Aeronautical and
Astronautical Engineering,
University of Illinois,
Urbana, IL 61801

Robustness of Nonlinear Systems Perturbed by External Random Excitation

The effect of external random excitation on nonlinear continuous time systems is examined using the concept of the Lyapunov exponent. The Lyapunov exponent may be regarded as the nonlinear/stochastic analog of the poles of a linear deterministic system. It is shown that while the stationary probability density function of the response undergoes qualitative changes (bifurcations) as system parameters are varied, these bifurcations are not reflected by changes in the sign of the Lyapunov exponent. This finding does not support recent proposals that the Lyapunov exponent be used as a basis for a rigorous theory of stochastic bifurcation.

Introduction

The design of practical control systems requires that the mathematical model used be sufficiently robust. This implies that qualitative properties should be preserved under the effect of all possible perturbations. Such systems were referred to by Andronov, Vitt, and Chaikin (1965) as "coarse systems" and formed the basis for the concept of structural stability in the mathematical theory of dynamical systems (Arnold, 1983). In the context of single-input single-output (SISO) linear control systems, robustness is characterized by the Nyquist plot and the concepts of phase and gain margins. The extension of these ideas to multiple-input multiple-output (MIMO) linear systems is documented by Dorato (1987). Currently, there are two major approaches to robustness analysis. The first assumes unstructured additive or multiplicative perturbations of the plant transfer function. Robustness is then measured by the singular values of the return difference matrix. This is a frequency domain technique which does not make explicit use of the nonlinearities present in the system. The second method is referred to as a structured or parametric approach. The precise values of system parameters are unknown but the uncertainty is assumed to be bounded. The degree of robustness, indicated by the system poles of the linearized system, is then determined in terms of these bounds using Kharitonov-type theorems (Barmish, 1988). These two techniques constitute a deterministic approach to the robustness analysis of linear systems. The possibility of random parametric or external excitation is not considered.

So far the robustness analysis of stochastic systems has received relatively limited attention. Wonham (1967) investigated the problem of a linear continuous time system with linear multiplicative white noise gain in terms of optimal stationary control using a state space formulation. A similar problem was studied by Willems and Blankenship (1971) in the frequency domain (see also Willems and Willems, 1983). In both instances, robustness was measured by a mean-square type criterion. Robustness measures of stable, linear discrete time systems were obtained by Yaz and Yildizbayrak (1985) and Yaz (1988). Their robustness measures are based on the sample stability of the perturbed system. The references mentioned above are mainly concerned with the effect of parametric fluctuations/uncertainties on linear systems. For nonlinear systems, as systems parameters are varied, qualitative changes (bifurcations) in the system response can occur. In this paper, the robustness of such bifurcations under the effect of random external excitation will be examined. In the following section, the problem is formulated in a general context and the idea of the Lyapunov exponent as a quantitative measure of robustness is introduced. Examples of systems undergoing codimension 1 and 2 bifurcations are then studied.

Problem Formulation

Consider the following system:

$$\frac{dX}{dt} = AX + f(X) + \sigma\eta(t) \quad (1)$$

where X is a vector in R^n and without loss of generality it is assumed that A is in canonical form, $f(X)$ are nonlinear terms, and $\eta(t)$ represents independent zero-mean white noise excitation of unit intensity. Since only additive noise is present, it does not matter whether the Itô or Stratonovich interpretation is used. Assuming that a stationary solution X_s exists, the problem of robustness is concerned with the sample stability of this stationary solution. As with deterministic systems, con-

Contributed by the Applied Mechanics Division of THE AMERICAN SOCIETY OF MECHANICAL ENGINEERS for presentation at the 1992 ASME Winter Annual Meeting, Anaheim, CA, Nov. 8-13, 1992.

Discussion on this paper should be addressed to Prof. Leon M. Keer, The Technological Institute, Northwestern University, Evanston, IL 60208, and will be accepted until four months after final publication of the paper itself in the ASME JOURNAL OF APPLIED MECHANICS.

Manuscript received by the ASME Applied Mechanics Division, June 4, 1990; final revision, Feb. 10, 1992. Associate Technical Editor: D. J. Inman.

Paper No. 92-WA/APM-3.

sider a small perturbation x , about this stationary solution. Then to first order in the perturbation, a linear system with stochastic coefficients is obtained:

$$\frac{dx}{dt} = \left[A + \frac{\partial f}{\partial X} \right] x = [A + F(t)]x. \quad (2)$$

Define a norm $\rho = (x^T x)^{1/2}$, the exponential growth rate of the perturbation is then given by

$$\frac{d(\log \rho)}{dt} = \frac{x^T [(A + F(t)) + (A + F(t))^T] x}{2\rho^2}. \quad (3)$$

The Lyapunov exponent, Λ , is simply the time-averaged exponential growth rate defined by

$$\Lambda = \lim_{t \rightarrow \infty} \frac{1}{t} \left(\log \left(\frac{\rho(t)}{\rho(0)} \right) \right), \quad (4)$$

where

$$\log \left(\frac{\rho(t)}{\rho(0)} \right) = \int_0^t \frac{x^T [(A + F(s)) + (A + F(s))^T] x}{2\rho^2} ds.$$

The stationary solution is sample stable if $\Lambda < 0$, and this is a necessary condition for a robust system. Assuming that the stationary state is also ergodic, the temporal average may be replaced by the ensemble average and a quantitative measure for robustness can then be computed, i.e.,

$$\Lambda = E \left[\frac{x^T [(A + F(t)) + (A + F(t))^T] x}{2\rho^2} \right]. \quad (5)$$

One may regard the Lyapunov exponent as the stochastic analog of the poles of a deterministic system. This concept of the Lyapunov exponent (Bylov et al., 1966) has been proposed by L. Arnold (1988) as a basis for a rigorous theory of stochastic bifurcation. A similar approach was also used by Caughey and Gray (1965), Infante (1968), Kozin and Wu (1973), and Ariaratnam and Xie (1988a) in their derivation of sufficient conditions for the sample stability of linear systems with stochastic coefficients.

One-Dimensional Systems

For one-dimensional systems, the computation of the Lyapunov exponent is fairly simple. Consider the general one-dimensional system written as

$$\frac{dX}{dt} = \lambda X + f(X) + \sigma \eta(t), \quad (6)$$

and the perturbed system is

$$\frac{dx}{dt} = \left[\lambda + \frac{df(X_s)}{dX} \right] x. \quad (7)$$

If the stationary state is ergodic, then the Lyapunov exponent is given by

$$\Lambda = \lambda + E \left[\frac{df(X_s)}{dX} \right] \quad (8)$$

and the stationary probability density function can be obtained by solving the Fokker-Planck equation (FPE) for the system

$$0 = -\frac{\partial}{\partial X} \left\{ [\lambda X + f(X)] p(X) - \frac{\sigma^2}{2} \frac{\partial p}{\partial X} \right\}. \quad (9)$$

The stationary probability density function (pdf) is given by

$$p_s(X) = N \exp \left(\frac{2}{\sigma^2} \left(\lambda \frac{X^2}{2} + \int^X f(z) dz \right) \right) \quad (10)$$

where N is an appropriate normalization constant. It is instructive to consider a simple example:

Example 1 (Simple Bifurcation—Soft Loss of Stability). For a symmetric system undergoing a soft loss of stability (i.e.,

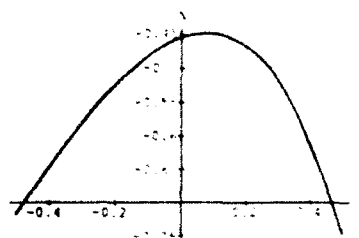


Fig. 1 Lyapunov exponent (soft loss of stability)

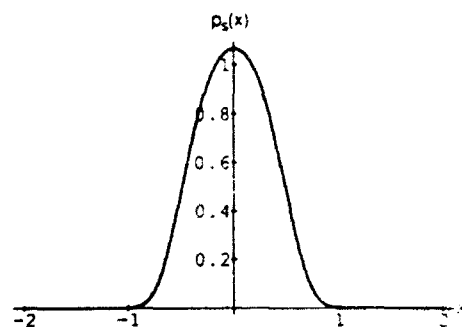


Fig. 2(a) Probability density function (soft loss of stability), $\lambda = -0.2$

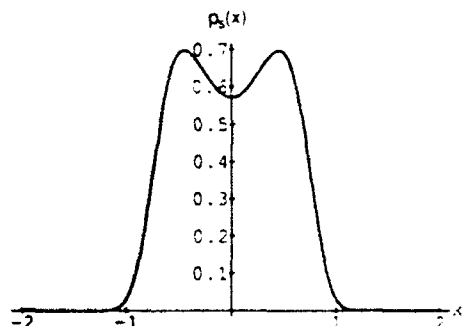


Fig. 2(b) Probability density function (soft loss of stability), $\lambda = 0.2$

a loss of stability to a nearby equilibrium, $f(X) = aX^3$ with $a < 0$) and the stationary probability density function is

$$p_s(X) = \exp \left(\frac{2}{\sigma^2} (\lambda X^2/2 + aX^4/4) \right) \int_{-\infty}^{\infty} \exp \left(\frac{2}{\sigma^2} (\lambda X^2/2 + aX^4/4) \right) dX. \quad (11)$$

Assuming that the stationary solution is ergodic, the Lyapunov exponent is then given by Eq. (8):

$$\Lambda = \lambda + 3aE[X^2]. \quad (12)$$

The Lyapunov exponent Λ is plotted against the eigenvalue λ for the deterministic system in Fig. 1 with $\sigma^2 = 0.1$ and $a = -1$. The deterministic system undergoes a bifurcation at $\lambda = 0$ and the probability density function changes from a unimodal density to a bimodal density (Fig. 2(a) and 2(b)). As evident from Fig. 1, the Lyapunov exponent Λ is negative which indicates that this is a robust feature, but the system is least robust at $\lambda = 0$. Physically, this implies that perturbations will take a much longer time to decay. It should be noted that the Lyapunov exponent does not indicate the qualitative change in the stationary pdf. This point was not adequately emphasized by L. Arnold (1988) in his theory of stochastic bifurcation based on the Lyapunov exponent.

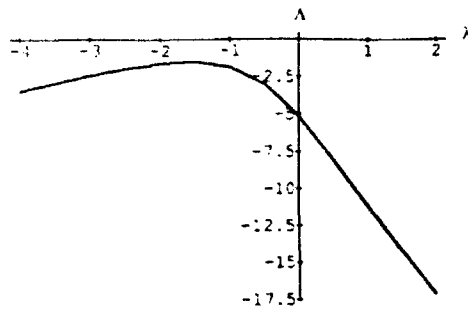


Fig. 3 Lyapunov exponent (hard loss of stability)

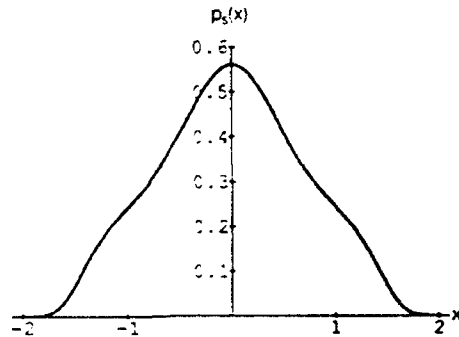


Fig. 4(a) Probability density function (hard loss of stability), $\lambda = -1.5$

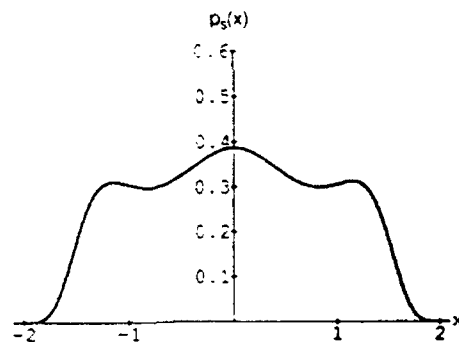


Fig. 4(b) Probability density function (hard loss of stability), $\lambda = -0.9$

Example 2 (Simple Bifurcation—Hard Loss of Stability). Now consider the one-dimensional system

$$\frac{dX}{dt} = \lambda X + C_3 X^3 + C_5 X^5 + \sigma \eta(t) \quad (13)$$

where $C_3 > 0$, $C_5 < 0$ for a hard loss of stability. The steady-state pdf is given by

$$p_s(X) = N \exp \left[\frac{2}{\sigma^2} \left(\lambda \frac{X^2}{2} + C_3 \frac{X^4}{4} + C_5 \frac{X^6}{6} \right) \right] \quad (14)$$

where the normalization constant N is defined by

$$N = \int_{-\infty}^{\infty} \exp \left[\frac{2}{\sigma^2} \left(\lambda \frac{X^2}{2} + C_3 \frac{X^4}{4} + C_5 \frac{X^6}{6} \right) \right] dX \quad (15)$$

and the Lyapunov exponent is (from Eq. (8))

$$\Lambda = \lambda + 3C_3 E[X^2] + 5C_5 E[X^4] \quad (16)$$

where the expectation is taken with respect to the steady-state pdf defined by Eq. (14). Numerical results for $C_3 = 2$, $C_5 = -1$ and $\sigma^2 = 1$ are shown as Fig. 3. In this case, the system is least robust just before the deterministic bifurcation point at $\lambda = 0$. It is interesting to compare this result with the

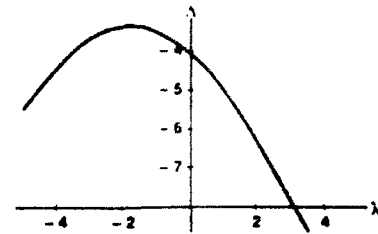


Fig. 5 Lyapunov exponent for $dX = (1 + \lambda X - X^3)dt + \sqrt{2}X \circ dW$

qualitative changes in the pdf as λ is varied (Fig. 4). It can be seen that the decrease in robustness coincides with the emergence of two additional peaks in the pdf. Once again, it should be noted that the Lyapunov exponent remains negative and cannot be used as a bifurcation parameter.

The results derived here for nonlinear systems under external random excitation is by no means typical. In fact, parametrically excited systems studied by previous researchers in stochastic bifurcation theory are extremely sensitive to errors in the reference input. Consider the nonlinear system with fluctuating gain:

$$dX = (\lambda X - X^3)dt + \sqrt{2}X \circ dW, \quad (17)$$

where " \circ " denotes that the Stratonovich interpretation is used. It is well known that the Lyapunov exponent is simply λ and the trivial solution $X = 0$ loses its stability at $\lambda = 0$ and this coincides with a qualitative change in the probability density function. Suppose now that a nonzero reference input is present, i.e.,

$$dX = (1 + \lambda X - X^3)dt + \sqrt{2}X \circ dW. \quad (18)$$

Since the drift term is not zero at $X = 0$, the system is ergodic and a steady-state solution exists and is defined by the steady-state pdf:

$$p_s(X) = \begin{cases} X^{\lambda-1} \exp[-(1/X + X^2/2)]/C & X > 0 \\ 0 & \text{else} \end{cases} \quad (19)$$

where

$$C = \int_0^{\infty} X^{\lambda-1} \exp[-(1/X + X^2/2)] dx,$$

Perturbing about this stationary (ergodic) solution leads to the following linear system with stochastic coefficients:

$$dx = [\lambda - 3(X_s)^2]xdt + \sqrt{2}x \circ dW. \quad (20)$$

The Lyapunov exponent is then given by

$$\Lambda = \lim_{t \rightarrow \infty} \frac{1}{t} \log \frac{|x(t)|}{|x(0)|} = \lambda - 3E[X_s^2] \quad (21)$$

since the Wiener process $W(t) \sim (t \log \log t)^{1/2}$ as $t \rightarrow \infty$ with probability one. The Lyapunov exponent Eq. (21) is plotted in Fig. 5 and is negative. The variation of the Lyapunov exponent with λ is not unlike that of a system perturbed by external random excitation. This "quasi-external excitation" effect of a nonzero reference input is apparent if the transformation $X = Y + C$ is made in Eq. (18) so that the nonzero reference input is eliminated. One sees that an additional external excitation term (CdW) is then generated from the multiplicative noise term $X \circ dW$.

Two-Dimensional Systems

Noting that the problem of robustness leads to a linear system with stochastic coefficients, it is convenient to first consider the general two-dimensional linear system with stochastic coefficients:

$$\begin{aligned}\frac{dx_1}{dt} &= F_{11}(t)x_1 + F_{12}(t)x_2 \\ \frac{dx_2}{dt} &= F_{21}(t)x_1 + F_{22}(t)x_2\end{aligned}\quad (22)$$

where the $F_{ij}(t)$ are colored noise sources generated from white noise. Making the transformation, $x_1 = r \cos \theta$, $x_2 = r \sin \theta$,

$$\begin{aligned}\frac{dr}{dt} &= \frac{1}{2} [(F_{11} + F_{22}) + (F_{12} + F_{21}) \sin 2\theta + (F_{11} - F_{22}) \cos 2\theta] r \\ \frac{d\theta}{dt} &= \frac{1}{2} [(F_{21} - F_{12}) + (F_{22} - F_{11}) \sin 2\theta + (F_{21} + F_{12}) \cos 2\theta]\end{aligned}\quad (23)$$

If the θ process and the $F_{ij}(t)$'s are ergodic then the Lyapunov exponent is given by

$$\Lambda = \frac{1}{2} E[(F_{11} + F_{22}) + \sqrt{(F_{12} + F_{21})^2 + (F_{11} - F_{22})^2} \sin(2\theta + \phi)] \quad (24)$$

where ϕ is a random phase angle defined by

$$\phi = \arctan \left(\frac{F_{11} - F_{22}}{F_{12} + F_{21}} \right) \quad (25)$$

Noting that $|\sin(2\theta + \phi)| \leq 1$, an upper bound for the Lyapunov exponent can be found and hence a sufficient condition for sample stability is:

$$E[(F_{11} + F_{22}) + \sqrt{(F_{12} + F_{21})^2 + (F_{11} - F_{22})^2}] < 0. \quad (26)$$

A necessary condition for sample stability requires that the joint moment of the stochastic coefficients and the phase process θ be computed. These ideas are applicable to the following system:

Example 3: Hopf Bifurcation (Dynamic Instability). Consider the nonlinear system perturbed by independent external white noise sources:

$$\frac{dX}{dt} = \mu X - \omega Y + (aX - bY)(X^2 + Y^2) + \sigma \eta_1(t)$$

$$\frac{dY}{dt} = \omega X + \mu Y + (aY + bX)(X^2 + Y^2) + \sigma \eta_2(t) \quad (27)$$

where the deterministic terms correspond to the normal form for the Hopf bifurcation. A stationary state exists for the case $a < 0$, and the pdf is given by

$$p_s(X, Y) = N \exp \left[\frac{2}{\sigma^2} \left(\mu \frac{(X^2 + Y^2)}{2} + a \frac{(X^2 + Y^2)^2}{4} \right) \right] \quad (28)$$

and

$$N^{-1} = \int_{-\infty}^{\infty} \int_{-\infty}^{\infty} \exp \left[\frac{2}{\sigma^2} \left(\mu \frac{(X^2 + Y^2)}{2} + a \frac{(X^2 + Y^2)^2}{4} \right) \right] dX dY. \quad (29)$$

Perturbing about this stationary state, the resulting linear system, Eq. (22), is defined by $x_1 = x$, $x_2 = y$ and

$$\begin{aligned}F_{11} &= \mu + a(3X^2 + Y^2) - 2bXY \\ F_{12} &= -\omega - b(X^2 + 3Y^2) + 2aXY \\ F_{21} &= \omega + b(3X^2 + Y^2) + 2aXY \\ F_{22} &= \mu + a(X^2 + 3Y^2) + 2bXY\end{aligned}\quad (30)$$

which leads to

$$\begin{aligned}\frac{dr}{dt} &= [\mu + 2a(X^2 + Y^2) \\ &\quad + \sqrt{a^2 + b^2}[(X^2 - Y^2) \sin \psi - 2XY \cos \psi]] r\end{aligned}\quad (31)$$

$$\frac{d\theta}{dt} = \omega + 2b(X^2 + Y^2) + \sqrt{a^2 + b^2}[(X^2 - Y^2) \cos \psi + 2XY \sin \psi]$$

where $\psi = 2\theta + \arctan(a/b)$. Since ω is nonzero and the X , Y processes are assumed to be ergodic, the Lyapunov exponent is then given by

$$\Lambda = E[\mu + 2a(X^2 + Y^2) + \sqrt{a^2 + b^2}[(X^2 - Y^2) \sin \psi - 2XY \cos \psi]] \quad (32)$$

where the expectation is taken with respect to the steady-state joint probability density function $p_s(X, Y, \theta)$. A perturbation expansion for this steady-state pdf may be constructed using a separation of time scales technique given in Blankenship and Papanicolaou (1978). Roughly, since the X , Y processes are assumed to be stationary to start with, these processes must have evolved sufficiently fast to reach a stationary state and should be scaled accordingly for consistency. The technique has also been applied by Horsthemke and Lefever (1984) and is explained in Appendix A. Then the Lyapunov exponent can be computed term-wise from such an expansion has been proven by Arnold et al. (1988). For simplicity, the technique will be applied for the case $b = 0$ and the angular frequency ω is large. The system defining the steady-state pdf is scaled as follows:

$$\frac{d\theta}{dt} = \frac{\omega}{\epsilon^2} - \frac{a}{\epsilon} [(X^2 - Y^2) \sin 2\theta - 2XY \cos 2\theta]$$

$$\frac{dX}{dt} = \frac{1}{\epsilon^2} [\mu X - \omega Y + aX(X^2 + Y^2)] + \frac{\sigma}{\epsilon} \eta_1(t)$$

$$\frac{dY}{dt} = \frac{1}{\epsilon^2} [\omega X + \mu Y + aY(X^2 + Y^2)] + \frac{\sigma}{\epsilon} \eta_2(t) \quad (33)$$

Let the steady-state pdf take the following form:

$$p_s(X, Y, \theta) = p_0(X, Y, \theta) + \epsilon p_1(X, Y, \theta) + \dots \quad (34)$$

The steady-state Fokker-Planck Equation for Eq. (33) may be written as

$$\frac{1}{\epsilon^2} L_0[p_s] + \frac{1}{\epsilon} L_1[p_s] = 0, \quad (35)$$

where the operators L_0 and L_1 are defined as follows:

$$\begin{aligned}L_0[p] &= -\frac{\partial}{\partial X} \left([\mu X - \omega Y + aX(X^2 + Y^2)] p - \frac{\sigma^2}{2} \frac{\partial p}{\partial X} \right) \\ &\quad - \frac{\partial}{\partial Y} \left([\omega X + \mu Y + aY(X^2 + Y^2)] p - \frac{\sigma^2}{2} \frac{\partial p}{\partial Y} \right) - \omega \frac{\partial p}{\partial \theta} \\ L_1[p] &= -a \frac{\partial}{\partial \theta} [(X^2 - Y^2) \sin 2\theta - 2XY \cos 2\theta] p.\end{aligned}\quad (36)$$

Substituting Eq. (34) for the pdf leads to the system of equations:

$$\begin{aligned}L_0[p_0] &= 0 \\ L_0[p_1] &= L_1[p_0] \\ &\dots \\ L_0[p_n] &= L_1[p_{n-1}].\end{aligned}\quad (37)$$

The solution to the lowest order equation is

$$p_n(X, Y, \theta) = p_n(X, Y)p_n(\theta) \\ = N \exp \left[\frac{2}{\sigma^2} \left(\mu \frac{(X^2 + Y^2)}{2} + a \frac{(X^2 + Y^2)^2}{4} \right) \right] \cdot \frac{1}{2\pi} \quad (38)$$

and an approximation to the Lyapunov exponent is then obtained from Eq. (32) by taking expectation with respect to Eq. (38),

$$\Lambda = \mu + 2aE[X^2 + Y^2]. \quad (39)$$

This is compared in Fig. 6 with the sufficient condition obtained from Eq. (26), which states that the system is robust if

$$\mu + (2a + |a|)E[X^2 + Y^2] < 0. \quad (40)$$

For $a = -0.5$ and $\sigma^2 = 1$, the sufficient condition Eq. (40) is satisfied. This indicates that the system is robust but as expected, it provides a more conservative robustness measure compared to Eq. (39).

One may also check if the polar representation of the Hopf bifurcation, Eq. (27), is robust to external excitation. Consider

$$\frac{dR}{dt} = \mu R + aR^3 + \sigma\eta_1(t), \quad a < 0, R \geq 0$$

$$\frac{d\theta}{dt} = \omega + bR^2 + \sigma\eta_2(t) \quad (41)$$

where the noise terms are included for the robustness analysis and, for purposes of comparison, b will be set to zero. Observing that the amplitude R is decoupled from the phase, the Lyapunov exponent is then given by

$$\Lambda = \mu + 3aE[R^2], \quad (42)$$

where the expectation is taken with respect to the probability density function

$$p_1(R, \theta) = N \exp \left(\frac{2}{\sigma^2} (\mu R^2/2 + aR^4/4) \right) \cdot \frac{1}{2\pi}$$

and

$$N^{-1} = \int_0^\infty \exp \left(\frac{2}{\sigma^2} (\mu R^2/2 + aR^4/4) \right) dR. \quad (43)$$

The Lyapunov exponent, Eq. (42), is also plotted against μ in Fig. 6 for the same parameters, i.e., $\sigma^2 = 1$ and $a = -0.5$. It is evident that the polar representation is less robust to external random excitation. Physically, in Eq. (41), the perturbations are aligned with the radial direction and hence the perturbations should have a greater effect on the amplitude.

Example 4 (Hopf-Pitchfork Interaction—Coupled Dynamic/Static Instability). Consider the deterministic normal form for the Hopf-pitchfork bifurcation perturbed by external independent white noise sources:

$$\frac{dR}{dt} = \mu R + c'R^3 + e'RZ^2 + \sigma_1\eta_1(t) \\ \frac{dZ}{dt} = \lambda Z + b'Z^3 + d'R^2Z + \sigma_2\eta_2(t), \quad (44)$$

where R represents the dynamic mode ($R > 0$), and Z , the static mode. Based on Example 3, the polar representation is used since from a robustness viewpoint, this corresponds to a "worst-case" situation. It is convenient to rescale the state variables by

$$R = \sqrt{2}R/\sigma_1, \quad Z = \sqrt{2}Z/\sigma_2,$$

resulting in

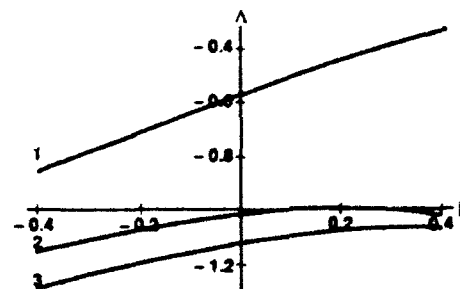


Fig. 8 Lyapunov exponent (Hopf bifurcation) (1) upper bound—non-radial excitation, (2) exact—radial excitation, (3) lowest-order approximation—nonradial excitation

$$\frac{dR}{dt} = \mu R + cR^3 + eRZ^2 + \sqrt{2}\eta_1(t)$$

$$\frac{dZ}{dt} = \lambda Z + bZ^3 + dR^2Z + \sqrt{2}\eta_2(t), \quad (45)$$

where the new system parameters are given by

$$b = b'(\sigma_2)^2/2, \quad c = c'(\sigma_1)^2/2, \quad d = d'(\sigma_1)^2/2, \quad e = e'(\sigma_2)^2/2.$$

An explicit normalizable solution to the steady-state FPE for Eq. (45) can be found for the case $d = e = k$, provided $b, c < 0$ and if $k > 0$, then $bc - k^2 > 0$ must also be satisfied. The steady-state probability density function is then

$$p_1(R, Z) = N \exp \left(\frac{1}{4} (2\mu + cR^2)R^2 + 2kR^2Z^2 + (2\lambda + bZ^2)Z^2 \right), \quad (46)$$

with N as a normalization constant. Perturbing about this stationary state and to first order in the perturbation,

$$\frac{dr}{dt} = (\mu + 3cR^2 + kZ^2)r + (2kRZ)z$$

$$\frac{dz}{dt} = (2kRZ)r + (\lambda + 3bZ^2 + kR^2)z. \quad (47)$$

Using the formula derived earlier, Eqs. (22)–(23), and letting $r = \rho \cos \theta$, $z = \rho \sin \theta$, the growth rate of the norm of the perturbation, ρ , is governed by

$$\frac{d\rho}{dt} = \frac{1}{2} [(\lambda + \mu) + (3c + k)R^2 + (3b + k)Z^2 + 4kRZ \sin 2\theta] \\ + ((\mu - \lambda) + (3c - k)R^2 + (k - 3b)Z^2) \cos 2\theta] \rho. \quad (48)$$

Scaling the θ, R, Z processes as in Appendix A yields

$$\frac{d\theta}{dt} = \frac{1}{2} (\lambda - \mu) \sin 2\theta + \frac{1}{2\epsilon} [4kRZ \cos 2\theta \\ + [(3b - k)Z^2 + (k - 3c)R^2] \sin 2\theta] \\ \frac{dR}{dt} = \frac{1}{\epsilon} (\mu R + cR^3 + kRZ^2) + \frac{1}{\epsilon} \sqrt{2} \eta_1(t) \\ \frac{dZ}{dt} = \frac{1}{\epsilon} (\lambda Z + bZ^3 + kR^2Z) + \frac{1}{\epsilon} \sqrt{2} \eta_2(t). \quad (49)$$

For simplicity, let $k = 3b = 3c$. The steady-state FPE is given by

$$\frac{1}{\epsilon} L_0[\rho] - \frac{1}{\epsilon} L_1[\rho] - L_2[\rho] = 0, \quad (50)$$

with L_0, L_1, L_2 defined by

$$L_0[p] = -\frac{\partial}{\partial R} \left\{ \left(\mu R + \frac{k}{3} R^3 + k R Z^2 \right) p - \frac{\partial p}{\partial R} \right\} - \frac{\partial p}{\partial Z} \left\{ \left(\lambda Z + \frac{k}{3} Z^3 + k Z R^2 \right) p - \frac{\partial p}{\partial Z} \right\}$$

$$L_1[p] = 2kRZ \frac{\partial}{\partial \theta} [p \cos 2\theta]$$

$$L_2[p] = \frac{(\lambda - \mu)}{2} \frac{\partial}{\partial \theta} [p \sin 2\theta].$$

Let the perturbation expansion be of the form

$$p_s(R, Z, \theta) = p_0(R, Z, \theta) + \epsilon p_1(R, Z, \theta) + \epsilon^2 p_2(R, Z, \theta) + \dots \quad (51)$$

and the system of perturbation equation is

$$L_0[p_0] = 0$$

$$L_0[p_1] = L_1[p_0]$$

$$L_0[p_2] = L_1[p_1] + L_2[p_0]$$

...

$$L_0[p_n] = L_1[p_{n-1}] + L_2[p_{n-2}]. \quad (52)$$

It is convenient to let $p_n(R, Z, \theta) = p_s(R, Z) r_n(r, Z, \theta)$, where $p_s(R, Z)$ is defined in Eq. (46), so that the operator $L_0[p_n]$ takes the form

$$L_0[p_n] = L_0[p_s r_n] = \frac{\partial}{\partial R} \left[p_s \frac{\partial r_n}{\partial R} \right] + \frac{\partial}{\partial Z} \left[p_s \frac{\partial r_n}{\partial Z} \right], \quad (53)$$

which is a linear self-adjoint operator. Substituting into the FPE, Eq. (5) and collecting terms, the $O(\epsilon^0)$ equation is trivially satisfied with $p_0(R, Z, \theta) = p_s(R, Z) r_0(\theta)$, but unlike Example 3, $r_0(\theta)$ has yet to be defined. The $O(\epsilon^1)$ equation is

$$L_0[p_s r_1] = L_1[p_s r_0(\theta)] = 2kRZ p_s(R, Z) \frac{\partial}{\partial \theta} r_0(\theta) \cos 2\theta. \quad (54)$$

According to the solvability condition,

$$\int_0^{2\pi} \int_0^\infty \int_{-\infty}^\infty 2kRZ p_s(R, Z) \frac{\partial}{\partial \theta} r_0(\theta) \cos 2\theta \times p_s(R, Z) N(\theta) dZ dR d\theta = 0$$

where the term $p_s(R, Z) N(\theta)$ belongs to the kernel of L_0 . Since this has to hold for an arbitrary $N(\theta)$, it is required that

$$\int_0^{2\pi} \int_{-\infty}^\infty 2kRZ p_s^2(R, Z) dZ dR = 0. \quad (55)$$

As $p_s(R, Z)$ is symmetric in Z , this implies that Fredholm's alternative is satisfied and that a unique solution for r_1 can be found. Using the fact that L_0 is a linear operator, r_1 can then be expressed as the sum of a homogeneous and particular solution

$$r_1(R, Z, \theta) = H(\theta) + 2k \frac{\partial}{\partial \theta} r_0(\theta) \cos 2\theta P(R, Z), \quad (56)$$

where $H(\theta)$ is the homogeneous solution of $L_0[p_s H(\theta)] = 0$ and $P(R, Z)$ is a particular solution of $L_0[p_s P(R, Z)] = RZ p_s(R, Z)$. It remains now to solve for $P(R, Z)$. Using Galerkin's approximation, let $P = \sum C_{mn} R^m Z^n$ and take weight functions of the form $R^p Z^q$. Define

$$M(m, n) = \int_0^\infty \int_{-\infty}^\infty R^m Z^n p_s(R, Z) dZ dR. \quad (57)$$

A simple 3-mode expansion, $P(R, Z) = C_{20} R^2 + C_{11} RZ + C_{02} Z^2$, yields

$$P(R, Z) = -\frac{M(2, 2)}{M(0, 2) + M(2, 0)} RZ. \quad (58)$$

Now, at $O(\epsilon^2)$:

$$L_0[p_s r_2] = 2kRZ \frac{\partial}{\partial \theta} [r_1(R, Z, \theta) \cos 2\theta] + \frac{(\lambda - \mu)}{2} \frac{\partial}{\partial \theta} [r_0(\theta) \sin 2\theta]. \quad (59)$$

Substituting for $r_1(R, Z, \theta)$ and invoking Fredholm's alternative, $r_0(\theta)$ has to satisfy

$$\frac{\partial}{\partial \theta} \left\{ 2C r_0(\theta) \sin 2\theta + \cos 2\theta \frac{\partial}{\partial \theta} [r_0(\theta) \cos 2\theta] \right\} = 0, \quad (60)$$

with $C = (\lambda - \mu)/(16k^2 E[RZP(R, Z)])$, where the expectation is taken with respect to $p_s(R, Z)$. This equation may be rewritten as

$$-\frac{\partial}{\partial \theta} \left\{ -\left[C \sin 2\theta + \frac{1}{2} \sin 4\theta \right] r_0 \right\} + \frac{1}{2} \frac{\partial^2}{\partial \theta^2} [r_0 \cos^2 2\theta] = 0, \quad (61)$$

which takes the form of a steady-state Fokker-Planck equation with drift and diffusion defined, respectively, by

$$\Phi(\theta) = -\left[C \sin 2\theta + \frac{1}{2} \sin 4\theta \right] \text{ and } \Psi^2(\theta) = \cos^2 2\theta. \quad (62)$$

The process evolves on the half circle $\theta \in [0, \pi]$ with singularities at $\theta = \pi/4$ and $3\pi/4$. As $C \neq 0$, the drift at the singular points is not zero and thus the singular points can be classified as left and right shunts depending on the sign of the drift term. The boundary point classification is performed using the Feller classification scheme (1954). It is shown in Appendix B that the boundary points $\theta = 0, \pi$ are both perfectly reflecting regular points. Therefore, the θ process is ergodic and the Lyapunov exponent can be found using Eq. (24) to be

$$\Lambda = \frac{\lambda + \mu}{2} + \frac{\mu - \lambda}{2} E[\cos 2\theta] + k(E[R^2] + E[Z^2]). \quad (63)$$

Now consider the case $C > 0$, (similar results can be derived for $C < 0$). The singular points are given as left and right shunts for $\theta = \pi/4$ and $3\pi/4$, respectively. That a nontrivial normalizable solution for r_0 exists on the intervals, $(0, \pi/4)$ and $(3\pi/4, \pi)$ is shown in Appendix B. r_0 is given by:

$C > 0$.

$$r_0(\theta) = \begin{cases} \frac{N}{\exp(C/\cos 2\theta) \cos 2\theta} & 0 \leq \theta \leq \pi/4 \text{ or } 3\pi/4 \leq \theta \leq \pi \\ 0 & \text{else} \end{cases} \quad (64)$$

where N is a normalization constant. The Lyapunov exponent, Eq. (63), is plotted against ν (where $\lambda = \nu$ and $\mu = \nu + 1$) in Fig. 7 for $k = -1$. The deterministic system undergoes primary bifurcations at $\nu = 0$ and -1 . A secondary bifurcation occurs at $\nu = 0.5$. It can be seen that these features are robust (i.e., the Lyapunov exponent remains negative) and a decrease in robustness coincides with the occurrence of the first primary

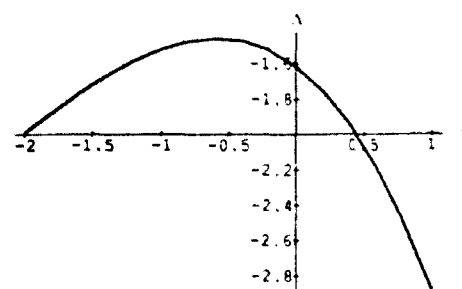


Fig. 7 Lyapunov exponent (Hopf-pitchfork bifurcation)

bifurcation. Once again, the Lyapunov exponent does not reflect the qualitative changes in the pdf but does indicate when nonlinear effects become significant.

Conclusion

The major conclusions of this investigation are as follows:
1 While the Lyapunov exponent provides a robustness measure for the combined effects of nonlinearities and noise, it is not a suitable bifurcation parameter for nonlinear stochastic systems in the sense that it does not reflect the qualitative changes in the steady-state probability density function. This occurs whenever $X = 0$ is not a solution of the nonlinear stochastic system. Examples of nonlinear systems under external (additive) random excitation and systems under parametric random excitation (multiplicative noise) with a nonzero reference input were shown to possess negative Lyapunov exponents.

2 The results of this investigation suggest that the extremum of the Lyapunov exponent (with respect to the bifurcation parameter for the deterministic system) provides an indication of when nonlinear effects become important. For the one and two-dimensional systems perturbed by external random excitation, it was observed that this extremum follows the occurrence of the first bifurcation in the corresponding deterministic system. It is left as a conjecture that this is a general characteristic of nonlinear systems perturbed by external random excitation.

Acknowledgment

This research was partially supported by the NSF through Grant 90-57437 PY1 which is monitored by Dr. Devendra Garg and AFOSR through Grant 91-0041 which is monitored by Dr. Spencer Wu.

References

- Andronov, A. A., Vitt, A. A., and Khaikin, S. E., 1966, *Theory of Oscillators*, Pergamon Press, London.
- Arnold, L., 1988, "Lyapunov Exponent of Nonlinear Stochastic Systems," *Nonlinear Stochastic Dynamic Engineering Systems*, F. Ziegler, and G. I. Schueller, eds., Springer-Verlag, New York.
- Arnold, L., Papanicolaou, G., and Wihstutz, V., 1986, "Asymptotic Analysis of the Lyapunov Exponent and Rotation Number of the Random Oscillator and Applications," *SIAM Journal of Applied Mathematics*, Vol. 46, No. 3, pp. 427-450.
- Arnold, V., 1983, *Geometrical Methods in the Theory of Ordinary Differential Equations*, Springer-Verlag, New York.
- Ariaratnam, S. T., and Xie, W. C., 1988a, "Stochastic Stability of Oscillatory Systems," *ASME JOURNAL OF APPLIED MECHANICS*, Vol. 55, pp. 458-488.
- Ariaratnam, S. T., and Xie, W. C., 1988b, "Dynamic Snap-Buckling of Structures under Stochastic Loads," *Stochastic Structural Dynamics: Progress in Theory and Applications*, S. T. Ariaratnam, G. I. Schueller, and J. Elishakoff, eds., Elsevier, New York.
- Barnish, B. R., 1988, "New Tools for Robustness Analysis," *IEEE Proceedings of the 27th Conference on Decision and Control*, pp. 1-6.
- Blankenship, G., and Papanicolaou, G. C., 1978, "Stability and Control of Stochastic Systems with Wide-Band Noise Disturbances: I," *SIAM Journal of Applied Mathematics*, Vol. 34, No. 3, pp. 437-476.
- Bylov, B. F., Vinograd, R. E., Grobman, D. M., and Nemytski, V. V., 1966, *Theory of Lyapunov Exponents*, NAUKA, Moscow.
- Caughy, T. K., and Gray, A. H., Jr., 1965, "On the Almost-Sure Stability of Linear Dynamics Systems with Stochastic Coefficients," *ASME JOURNAL OF APPLIED MECHANICS*, Vol. 32, pp. 365-372.
- Dorato, P., 1987, "A Historical Review of Robust Control," *IEEE Control Systems Magazine*, Apr., pp. 44-47.
- Feller, W., 1954, "Diffusion Process in One Dimension," *Trans. of Amer. Math. Society*, Vol. 97, pp. 1-31.
- Horsthemke, W., and Lefever, R., 1984, *Noise-Induced Transitions*, Springer-Verlag, New York.
- Infante, E. F., 1968, "On the Stability of Some Linear Nonautonomous Random Systems," *ASME JOURNAL OF APPLIED MECHANICS*, Vol. 35, pp. 7-12.
- Kozin, F., and Wu, C. M., 1973, "On the Stability of Linear Stochastic Differential Equations," *ASME JOURNAL OF APPLIED MECHANICS*, Vol. 40, pp. 87-92.
- Lin, Y. K., 1986, *Probabilistic Theory of Structural Dynamics*, R. Krieger, FL.

Nishioka, K., 1976, "On the Stability of Two-Dimensional Linear Stochastic Systems," *Kodai Mathematics Seminar Report*, Vol. 27, pp. 211-230.

Willems, J. C., and Blankenship, G. C., 1971, "Frequency Domain Stability Criteria for Stochastic Systems," *IEEE Transactions on Automatic Control*, Vol. 16, pp. 292-299.

Willems, J. C., and Willems, J. C., 1983, "Robust Stabilization of Uncertain Systems," *SIAM Journal of Control and Optimization*, Vol. 21, pp. 352-374.

Wonham, W. H., 1967, "Optimal Stationary Control of a Linear System with State Dependent Noise," *SIAM Journal of Control*, Vol. 5, pp. 486-500.

Yaz, E., 1988, "Deterministic and Stochastic Robustness Measures for Discrete Systems," *IEEE Transactions on Automatic Control*, Vol. 33, pp. 952-955.

Yaz, E., and Yildizbayrak, N., 1985, "Robustness of Feedback-Stabilized Systems in the Presence of Non-linear and Random Perturbations," *International Journal of Control*, Vol. 41, pp. 345-353.

APPENDIX A

The scaling employed is adapted from Horsthemke and Lefever (1984) and may be justified as follows:

1 The X and Y processes are assumed from the start to be stationary (ergodic) processes. This stationary state is achieved only in the limit $t \rightarrow \infty$. Hence, in the Itô representation of the X and Y processes, time is scaled as $t \rightarrow t/\epsilon^2$ so that the stationary state is reached in the limit $\epsilon \rightarrow 0$.

2 Now consider the effect of such a scaled process $Z(t) = X(t/\epsilon^2)$ in the θ equation. For example,

$$d\theta = f(\theta)dt + Z(t)g(\theta)dt. \quad (65)$$

The spectrum of $Z(t) = X(t/\epsilon^2)$ is given by

$$\begin{aligned} S_Z(\omega) &= \frac{1}{2\pi} \int_{-\infty}^{\infty} E[Z(t)Z(t+\tau)] \exp(-j\omega\tau) d\tau \\ &= \frac{1}{2\pi} \int_{-\infty}^{\infty} E[X(t/\epsilon^2)X(t/\epsilon^2 + \tau/\epsilon^2)] \exp(-j\omega\tau) d\tau \\ &= \frac{\epsilon^2}{2\pi} \int_{-\infty}^{\infty} E[X(t/\epsilon^2)X(t/\epsilon^2 + s)] \\ &\quad \times \exp(-j\epsilon^2\omega s) ds \quad (\text{let } s = \tau/\epsilon^2) \\ &= \epsilon^2 S_X(\epsilon^2\omega) \end{aligned} \quad (66)$$

which tends to zero as $\epsilon \rightarrow 0$. This implies that by simply scaling time alone, one will obtain a noiseless limit. Hence, the amplitude of the process $X(t/\epsilon^2)$ should be multiplied by a factor of $1/\epsilon$ to ensure that noise effects are not excluded in the limit.

APPENDIX B

The ergodic assumption is shown to be valid by considering the properties of the sample paths of the θ process on the unit half circle. The drift and diffusion are, respectively,

$$\Phi(\theta) = - \left[C \sin 2\theta + \frac{1}{2} \sin 4\theta \right] \quad \text{and} \quad \Psi^2(\theta) = \cos^2 2\theta. \quad (67)$$

Take $C > 0$, and by symmetry it is only necessary to study the process on $(0, \pi/4)$. The diffusion is singular at $\theta = \pi/4$ with $\Phi(\pi/4) = -C < 0$, yielding $\theta = \pi/4$ as a left shunt.

In order to complete the proof of ergodicity, the behavior at $\theta = 0$ must be known. To this end, we introduce scale and speed measures defined, respectively, as

$$S(\theta) = \int^{\theta} s(x)dx, \quad M(\theta) = \int^{\theta} m(x)dx \quad (68)$$

where

$$s(x) = \exp[-B(x)], \quad m(x) = \frac{1}{\Psi^2(x)s(x)}$$

$$B(x) = \int^x \frac{2\Phi(\eta)}{\Psi^2(\eta)} d\eta \quad (69)$$

$s(x)$ and $m(x)$ are called the scale and speed densities. The scale and speed measures are found to be

$$S(\theta) = \int_0^\theta \frac{\text{Exp}\left[\frac{C}{\cos 2\eta}\right]}{|\cos 2\eta|} d\eta, \quad M(\theta) = \int_\theta^\pi \frac{\text{Exp}\left[-\frac{C}{\cos 2\eta}\right]}{|\cos 2\eta|} d\eta. \quad (70)$$

Again, only consider $C > 0$ and $\theta \in [0, \pi/4)$. Both functions are bounded and continuous on $\theta \in [0, \pi/4)$ and as such the integrals on this region are also bounded. Thus, $\theta = 0$ is a regular point.

The property of pure reflection can be determined from a physical argument. It is clear that unless the coupling coefficients are both zero, it is not possible to have a solution with

$z(t) = 0$. Since $\theta = 0$ implies $z = 0$, there can be no accumulation of probability mass at the point.

As $\theta = 0$ is purely reflecting and $\theta = \pi/4$ is a left shunt, the region $(0, \pi/4)$ has the property of recurrence or ergodicity and a unique, normalizable stationary density exists on this interval. Similar conclusions may be made for the interval $(3\pi/4, \pi)$. Should θ start outside the intervals $(0, \pi/4)$ and $(3\pi/4, \pi)$, it can be shown (Nishoka, 1976) that the θ process moves into either one of the two intervals in finite time with probability one. The temporal average can then be replaced by the ensemble average computed with respect to

$$p(\theta) = Nm(\theta) = \frac{N}{\cos 2\theta \text{Exp}[C/\cos 2\theta]} \quad (71)$$

where N is a normalization constant. Similar results can be obtained for $C < 0$.